

Development of ISO Compliant Repeatability Procedures for Evaluating Collaborative Robots

A Major Qualifying Project Report

Submitted to the Faculty of

WORCESTER POLYTECHNIC INSTITUTE

in partial fulfillment of the requirements for the

Degree of Bachelor of Science

In

Mechanical Engineering

by

Joshua Baker

Timothy Kurisko

Haoran Li

David Poganski

James Worcester

April 24th, 2014

Approved:

Prof. Cosme Furlong, Major Advisor

Abstract

The goal of this project is to provide the sponsor with a test fixture and procedure to characterize positioning repeatability of collaborative robots as a function of payload and acceleration according to ISO 9283. Using the Universal Robot's model UR10 as a testing platform, the objective was accomplished by analyzing the current state of the art techniques for robot characterization; completing a vibrational analysis to select and implement suitable metrology equipment; designing, optimizing, and manufacturing a test fixture; developing a testing procedure and software; and applying the fixture and test procedures to characterize positioning repeatability. The outcomes prove the potential of the developed methods and equipment for expansion to additional projects of interest to the sponsor.

Acknowledgements

Our most sincere thanks to the sponsor of this project without whom our work would not have been possible. Thanks also to Chengjih Li and Loren Gjata for their guidance and early mornings spent together working on our developments. Our gratitude also goes out to our main advisor, Professor Cosme Furlong, who spent many long hours with us on the development of every aspect of this project and pushed our team not to settle for mediocre work. Thank you to Diana Lados, our co-advisor, who helped us to refine our presentations; our appreciation to Barbara Furhman for helping us with all of our purchasing needs; and thanks to Emmit Joyal for helping during the realization of the fixture hardware.

Executive Summary

This project involves the use of ISO 9283 to develop a method to evaluate the positional repeatability for collaborative robotic arms. By using the Universal Robots UR10 robotic arm as a platform, this project proved the potential for the method developed by the project team to evaluate collaborative robots against manufacturer's claims for varying applications.

The design process began with an investigation into current state-of-the-art metrology techniques. This project evaluated accepted methods versus techniques developed by the project team according to the sponsor's needs to select the optimal methodology for evaluating collaborative robots. The end result was the selection of the Direct Contact Method (DCM), which involves the measurement of tool tip displacement using a piston type contact sensor.

A dynamic analysis of the UR10 allowed the determination of the robot's natural frequencies of vibration, which led to the selection of an appropriate sensor type for the DCM based on sampling rate. Following initial sensor comparisons and evaluations for different manufacturers, two displacement transducers were purchased, set up, calibrated, and tested for linearity. An OMEGA Linear Variable Differential Transducer (LVDT) performed best, after which an appropriate fixture was designed, optimized, and fabricated such that the LVDT could be attached to the UR10 with varying payloads. An accompanying gauge block was designed and fabricated to provide a set of ISO 9283 compliant positions at which the UR10's repeatability could be tested.

Using a Polyscope script procedure, UR10's scripting language, and LabVIEW, software was developed to capture tool tip displacement data according to the DCM. Analysis of the recorded data using a MATLAB program proved that repeatability of the UR10 is influenced by

varying payload and acceleration only in the vertical axis, which provides the counter force to the payload.

The fulfillment of the project included delivery of the DCM as a package containing all necessary hardware, software, and user instructions in combination with the UR10 analysis to demonstrate the DCM's ability to characterize repeatability as well as the potential of the DCM for different projects of interest to the sponsor.

Table of Contents

Abstract	2
Acknowledgements	3
Executive Summary	4
Table of Figures	9
List of Tables	12
1. Introduction	13
2. Background	14
2.1 Universal Robots, UR10	14
2.2 International Standard 9283	15
2.2.2 ISO Technical Report 13309:1995	19
3. Generation and Comparison of Test Methods	22
3.1 Trilateration Methods	22
3.1.1 Cable Trilateration (CTM)	23
3.1.2 Ultrasonic Trilateration (UTM)	24
3.2 Inertial Measuring Unit (IMU)	25
3.3 Laser Tracking Camera System (LTCS)	25
3.4 MicroElectroMechanical Systems (MEMS) Mirrors	28
3.5 Direct Contact Method (DCM)	29
3.6 Selection of a Method	29
3.7 Implementation of the Direct Contact Method	30
4. Characterization of Natural Frequency	32
4.1 MEMS Accelerometers	34
4.2 Vibrations	35
4.3 Experimental Results	37
4.3.1 Interpretation	41
5. Realization of the Direct Contact Method	46
6. Selection of Sensor	48
6.1 Omega GP911-2.5-S LVDT and MicroStrain SG-DVRT	50
6.1.1 Calibration	51
7. Synthesis of Hardware	54

7.1 Design of Fixture.....	54
7.1.1 Attachment of LVDT.....	55
7.1.2 Modulation of Payload	56
7.1.3 Analysis	56
7.2 Gauge Block Design.....	58
7.3 Fabrication.....	60
7.4 Validation of Fixture Assembly	62
8. Testing Procedure Overview.....	63
9. Development of Software	67
9.1 LabVIEW and Polyscope Program	67
9.2 MATLAB Analysis	69
10. Collection of Data	70
10.1 Repeatability Parameters.....	71
10.1.1 Repeatability vs. Payload	71
10.1.2 Repeatability versus Acceleration	74
10.2 Statistical Analysis	75
11. Conclusions and Recommendations	77
11.1 Future Work	77
11.1.1. Refinement of Hardware	78
11.1.2. Refinement of Software.....	79
11.2 Vision for the Direct Contact Method.....	80
12. References	81
13. Appendices.....	82
Appendix A: Universal Robots, UR10 specifications.....	82
Appendix B: Repeatability Methods Detailed Descriptions	83
Appendix C: Method Evaluations Criteria and Equations	92
Appendix D: Accelerometer Specifications and LABVIEW Program.....	94
Appendix E: Sensor Evaluation Criteria	97
Appendix F: Student's t-Test for OMEGA and MicroStrain Transducer Verification.....	98
Appendix G: Mechanical Drawings	100
Appendix H: UR10 Repeatability Polyscope Program	105
Appendix I: Repeatability Analysis MATLAB Script.....	109

Appendix J: Denavit-Hartenberg Parameters..... 112

Transformations**Error! Bookmark not defined.**

Appendix K: Repeatability Data Tables..... 113

Appendix L: Instruction Manual for the DCM Repeatability Procedure..... 122

List of Figures

Fig. 1. The Universal Robots UR10 collaborative robot	14
Fig. 2. Calculation of point P using trilateration in 2D.....	20
Fig. 3. Inertial measurement unit attached to a robotic arm.	20
Fig. 4. Cable trilateration as presented in the International Standards Organization's technical report 13309.....	23
Fig. 5. Ultrasonic trilateration as presented in the International Standards Organization's technical report 13309.	24
Fig. 6. Use of Gaussian distribution to find the center of a laser beam.	26
Fig. 7. Close up view of the optical head and detector sub-system attached to the UR10.	27
Fig. 8. The UR10 outfitted with the optical head and two detector systems to evaluate repeatability at two points.	27
Fig. 9. Visualization of the MEMS Mirrors photo detector tracking method.....	28
Fig. 10. Conceptualization of a stepped gauge block to provide five contact points for the displacement sensor.....	29
Fig. 11. Spring, mass, dashpot diagram showing mass (m), stiffness (k), damping (c), and displacement (x).	32
Fig. 12. Plots of over, critically, and under damped systems.	33
Fig. 13. The accelerometer experiment set up showing the two accelerometers, coordinate system, and ABS fixture.....	35
Fig. 14. The UR10's tool tip displacement along the X axis for the vibration experiment.	36
Fig. 15. The UR10's tool tip velocity along the X axis for the vibration experiment.....	36
Fig. 16. The UR10's tool tip acceleration along the X axis for the vibration experiment.	37

Fig. 17. Time domain plot of the UR10's vibrations for X Axis motion.	38
Fig. 18. Fast Fourier Transform of accelerometer data for X motion with noise.	39
Fig. 19. Deconvolved vibration data showing frequency peaks at 30 and 125 Hz.	40
Fig. 20. Amplitude of vibration versus acceleration along the X axis.	42
Fig. 21. Amplitude of vibration versus acceleration along the Y axis.	42
Fig. 22. Amplitude of vibration versus acceleration along the Z-axis.	43
Fig. 23. Frequency of vibration versus acceleration along the X axis.	43
Fig. 24. Frequency of vibration versus acceleration along the Y axis.	44
Fig. 25. Frequency of vibration versus acceleration along the Z axis.	44
Fig. 26. Steps taken in the realization of the Direct Contact Method.	46
Fig. 27. OMEGA GP911 Linear Variable Differential Transducer (LVDT).	49
Fig. 28. LORD MicroStrain SG-DVRT displacement sensor.	49
Fig. 29. Top view of the OMEGA LVDT mounted to a Newport actuator and micro-stage for calibration.	51
Fig. 30. Side view of the OMEGA LVDT mounted to the Newport actuator and micro-stage for calibration.	52
Fig. 31. Sensor fixture design shown with representative sensor, payload, and locking nut.	55
Fig. 32. Back view of sensor fixture showing the five-pin plug on the flat face of the flange.	56
Fig. 33. Von Mises stresses in the sensor fixture.	57
Fig. 34. Vibrational analysis of the sensor fixture showing a max frequency of 1687 Hz.	58
Fig. 35. Gauge block assembled and mounted to an optical breadboard.	59
Fig. 36. Fixture with 10 kg payload mounted to the UR10.	61
Fig. 37. Flow chart for the Direct Contact Method testing procedure.	63

Fig. 38. Laboratory set-up for the Direct Contact Method.	64
Fig. 39. Alignment procedure for the gauge block and UR10.	65
Fig. 40. Process flow for data acquisition at each gauge location.	66
Fig. 41. Front panel of the recording program.	67
Fig. 42. Block diagram of the LVDT recording program.	68
Fig. 43. Gauge block with directional labels.	70
Fig. 44. Plot of Payload vs. Repeatability with acceleration constant at 0.2g.	73
Fig. 45. Repeatability as a function of acceleration in the X Direction.	75
Fig. 46: ISO technical report.	85

List of Tables

Table 1. Robot characteristics as defined in ISO 9283.....	16
Table 2. Decision matrix used for method selection.....	30
Table 3. Representative results of the vibration experiment, shown for the Z axis.....	40
Table 4. Sensor evaluation decision matrix.	50
Table 5. Calibration results and analysis of the OMEGA LVDT and MicroStrain SG-DVRT. ..	53
Table 6. Average repeatability for the UR10 for varying payloads with constant 0.2g acceleration.....	73

1. Introduction

Industrial robots used for assembly must be evaluated in order to ensure the accurate construction of products. Although manufacturers evaluate and report a robot's characteristics to potential customers, it is difficult for customers to compare robots against one another and across varying applications. Industrial standards allow the determination of robotic characteristics using standardized criteria and experimental procedures. State of the art techniques used to perform evaluations according to such standards are typically both costly and difficult to implement.

The sponsor of this project was interested in the development of a low cost and simple method to evaluate collaborative robots as a means of comparison before purchase. The Universal Robot's UR10 was used as a platform for the development and analysis of the project team's method. The method included all necessary hardware, software, and instructions, and was capable of analyzing the UR10's repeatability as functions of payload and acceleration as proof of the method's feasibility.

The goal of this project was accomplished by developing an ISO 9283 compliant method; selecting and implementing appropriate metrology equipment; designing and fabricating a sensor fixture; programming the UR10 and accompanying LabVIEW software; and developing a MATLAB script to analyze the data allowing for the evaluation of the UR10's repeatability.

2. Background

Robots have long been used to perform repetitive motions in assembly lines as a means to enhance production rates - such robots typically replace human workers in factories. The latest state-of-the-art collaborative robots are designed to be implemented in conjunction with humans in an effort to allow people and industrial robots to work in close proximity. One such robot, of particular interest to the sponsor of this project, is the Universal Robots UR10 (Fig. 1).



Fig. 1. The Universal Robots UR10 collaborative robot [Universal Robots, 2014].

2.1 Universal Robots, UR10

Universal Robots emphasizes the UR10's smooth motion, precision handling and safety features. The UR10 has 6 joints with 360 degrees of rotational freedom, a working radius of 1.3 meters, and can support up to 10 kilograms. Universal Robots provides a unique Polyscope software interface that allows the user to quickly and easily program multiple end points of the UR10 simply by manually moving the UR10 to a position and recording the position in its own global

coordinate system. The UR10 can then be easily programmed to move from point to point in succession, with a positional repeatability of 0.1 mm according to Universal Robots. For a complete list of the UR10's specifications, see Appendix A.

The repeatability as reported by the manufacturer must be calculated according to industrial standards. The International Standard Organization's (ISO) 9283 is of particular interest in that the standard specifies strict testing, environmental, and statistical standards to follow in the analysis of an industrial robot. The user of an industrial robot can determine repeatability characteristics and discover which variables affect the robot's dynamic characteristics by following ISO 9283 specifications.

2.2 International Standard 9283

ISO 9283 specifies guidelines for testing industrial robots [ISO 9283, 1998]. In order to be ISO 9283 compliant all tests must use the same paths, cycles, and environmental conditions. The robot must be set up according to the manufacturer's specifications with all necessary leveling operations, alignment procedures, and functional testing completed. The testing must be preceded by any appropriate warming up time, as dictated by the manufacturer.

Operational and environmental conditions must be normalized and repeated for each test. Normal operating conditions include requirements for electric, hydraulic and pneumatic power, power fluctuations and disturbances, and maximum safe operating limits. Environmental conditions include temperature, relative humidity, electromagnetic and electrostatic fields, radio frequency interference, atmospheric contaminants, and altitude limits.

All metrology equipment must be fully calibrated and the testing must account for any and all uncertainty with respect to the metrology equipment, systematic errors, and calculation

errors. The measurements taken in the testing must be with reference to the tool center point (TCP) inside the robot's workspace [ISO 9283, 1998].

Robot characterization may take place after all of the preceding requirements have been met.

Table 1 shows a list of applicable test characteristics, brief explanations, and statistical methods that could be applicable to the UR10 based on the project team's findings.

Table 1. Robot characteristics as defined in ISO 9283.

characteristics to test	explanation	method/equations
position stabilization time	how quickly a robot can stop at the attained pose	define the limit band (repeatability value or as specified by manufacturer); elapsed time from the instance of the initial crossing into the limit band until the instance when the robot remains within the limit band; using path "P1 → P5 → P4 → P3 → P2 → P1"; repeat this procedure three times, for each pose the mean value of t of three cycles is calculated
position overshoot	robot capability to make smooth and accurate stops at attained poses	maximum distance from the attained position after the instance of initial crossing into the limit band and when the robot goes outside the limit band again; overshoot, OV, = 0 if maximum value measured, D_{ij} , is smaller or equal to limit band; max $D_{ij} = \max \sqrt{(x_{ij} - x_j)^2 + (y_{ij} - y_j)^2 + (z_{ij} - z_j)^2}$; test

		<p>conditions: 100% rated load: 100%, 50% and 10% of rated velocity; 10% rated load (optional): 100%, 50% and 10% of rated velocity; all for one pose, 3 cycles same as position stabilization time; use maximum value of three times of measurement</p>
minimum posing time	<p>time between departure from and arrival at a stationary state when traversing a predetermined distance and/or sweeping through a predetermined angle under pose-to-pose control; including pose stabilization time</p>	<p>use 100% rated velocity and in addition test shall be performed with optimized velocities for each part of the cycle if applicable to achieve a shorter posing time.; 3 cycles; 100% and 10% rated load.</p>

static compliance	maximum amount of displacement per unit of applied load.	unit: mm/N with reference to the base coordinate. Forces used in the tests shall be applied in three directions, both positive and negative, parallel to the axes of the base coordinate system. Forces increase in steps of 10% of rated load up to 10% of rated load, one direction at a time; measure the corresponding displacement of each force and direction; with servos on and brakes off. repeat three times for each direction; with center of mechanical interface placed at P1 (defined in pose section)
pose repeatability (position only)	closeness of agreement between the attained poses after n repeat visits to the same command pose in the same direction	for position: $RP_l = \bar{l} + 3S_l$; $\bar{l} = \frac{1}{n} \cdot \sum l_j$ (with j from 1 to n); $l_j = \sqrt{(x_j - \bar{x})^2 + (y_j - \bar{y})^2 + (z_j - \bar{z})^2}$; x_j, y_j, z_j and $\bar{x}, \bar{y}, \bar{z}$ as in pose accuracy. $S_l = \sqrt{\frac{\sum (l_j - \bar{l})^2}{n-1}}$. For orientation: $RP_a = \pm 3\sqrt{\frac{\sum (a_j - \bar{a})^2}{n-1}}$. (same for angle b and c) Cycles: path 1 → P1, path 2 → P1, path 3 → P1; path 1 → P2, path 2 → P2, path 3 → P2; path 1 → P4, path 2 → P4, path 3 → P4; repeat 30 cycles
drift of pose repeatability (position only)	variation of pose repeatability over a	$dRP_p = RP_{t=1} - RP_{t=T} $ for position. Same for orientation. Other requirements same as drift of pose accuracy

	specified time, T	
--	----------------------	--

Of the methods found in

Table 1, the sponsor indicated interest in pose repeatability in reference to position only, which corresponded to the ability of the UR10 to return to a set of coordinates in three dimensional space. Note that as such, of the six potential degrees of freedom of the UR10, the repeatability analysis accounts for the coordinate tool position and not the angular position that would determine the UR10's tool face orientation.

2.2.2 ISO Technical Report 13309:1995

As an addendum to ISO 9283, the International Standards Organization published a technical report outlining methods by which one could analyze industrial robots according to the guidelines written in ISO 9283. The report describes eight types of performance measuring methods and includes potential limitations of each method [ISO13309, 1995]. The two types of methods deemed most useful to the sponsor's interests were:

- Trilateration Methods – the measurement of distances from a single point, P at the robot's tool tip, to two observation locations allows the calculation of point P, Fig. 2
- Inertial Measuring Methods – the attachment of accelerometers and gyroscopes to the tool tip allows characterization of the robot's pose and path provided the initial position is known, Fig. 3

These methods were extrapolated to fit the UR10 and evaluated alongside methods developed by the project team.

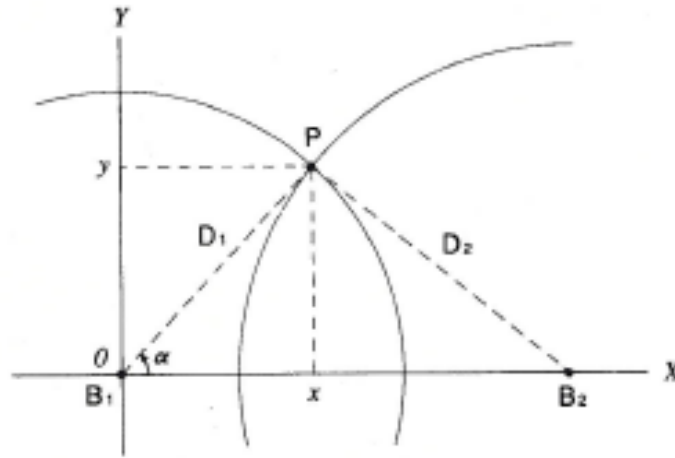


Fig. 2. Calculation of point P using trilateration in 2D [Thomas and Ros, 2005].

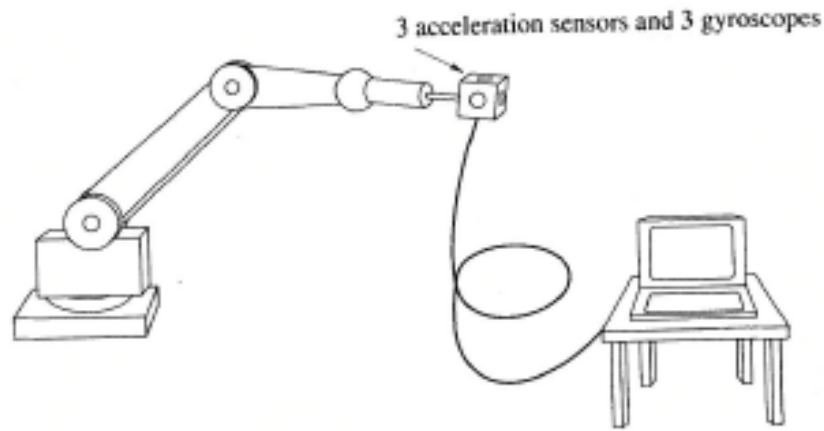


Fig. 3. Inertial measurement unit attached to a robotic arm [ISO 13309, 1995].

Please note that Fig. 2 shows a two dimensional representation of the Trilateration method, in which the (x, y) coordinate position of P can be found using the distances $\overline{B_1P}$ and $\overline{B_2P}$ as radii of circles, where the point P lies on the intersection of the two circles [3]. The method used in calculating a robot's tool tip position requires three dimensions, and thus the simultaneous

solution of three quadratic equations. This topic is further developed in the section titled “3.1 Trilateration Methods”.

3. Generation and Comparison of Test Methods

Based on the sponsor's interests and ISO 9283, the methods chosen for evaluation had to meet the following constraints:

- Minimum resolution of 0.01 mm
- Total cost no greater than \$5000
- Capability to apply 10%, 50%, and 100% of maximum payload (1, 5, and 10 kg respectively)
- Measurement of 3 Degrees of Freedom (X, Y, Z)
- Measure five positions, thirty times each

Five methods were chosen for evaluation using the above constraints. These five methods were composed of two trilateration methods, an Inertial Measuring Unit (IMU), a laser and optics based tracking system, Micro Electromechanical Sensor (MEMS) mirrors, and a contact method using a displacement sensor. The following sections briefly describe each method including potential positive and negative factors associated with each method. For full explanations of the considered test methods, including implementation and data processing, see Appendix B.

3.1 Trilateration Methods

Trilateration techniques involve the use of algebra in conjunction with three length measurements to a point of interest, P, to find the Cartesian coordinates of point P (Fig. 2). The ISO technical report provided two suggested methods for trilateration location of a robot tool tip: cable trilateration and sonic trilateration [ISO 13309, 1995].

3.1.1 Cable Trilateration (CTM)

Cable Trilateration uses a system of three optical encoders attached to pulleys to measure a length of cable originating from each pulley. The pulleys are placed at three observation points, with known Cartesian coordinates, in the robot's work space with the ends of the cables attached to the robot's tool tip. The lengths of the cables can be used to calculate the tool point location.

Fig. 4 shows an example of cable trilateration as demonstrated in ISO/TR 13309.

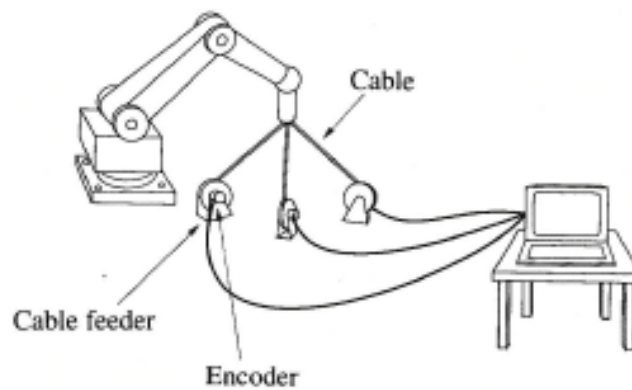


Fig. 4. Cable trilateration as presented in the International Standards Organization's technical report [ISO 13309, 1995].

Drawbacks of this method include restriction of the applied loads on the robot's tool tip, restricted motion paths to avoid tangling the cables, and acceleration limits to prevent cable slip on the pulleys.

3.1.2 Ultrasonic Trilateration (UTM)

Ultrasonic trilateration uses three ultrasonic microphones placed at known observation points in combination with an ultrasonic sound generator attached to the robot's tool tip [ISO 13309, 1995]. The microphones measure pulses from the generator and the time between receiving each pulse can be used to calculate the length from the microphone to the generator. The three lengths allow tool tip calculation using the trilateration method. Fig. 5 shows an example of Ultrasonic Trilateration. Drawbacks include fluctuations in ultrasonic intensity due to absorption effects at high levels of humidity and potential interference to other equipment exposed to ultrasonic pulses.

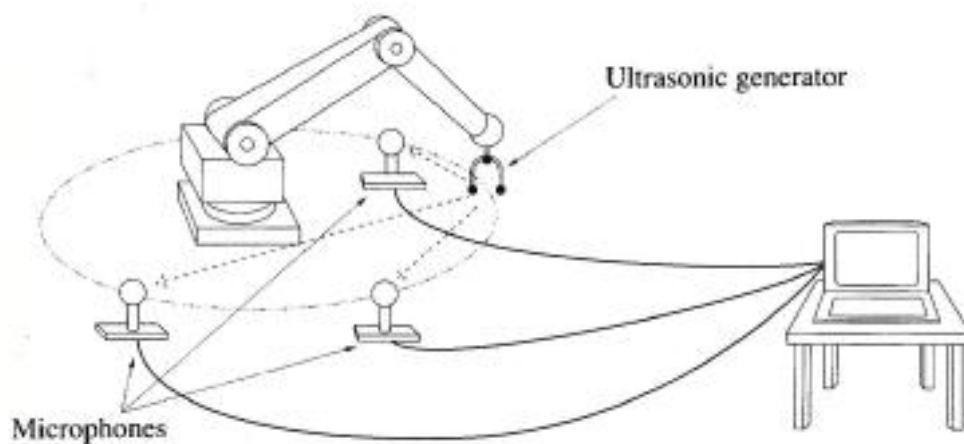


Fig. 5. Ultrasonic trilateration as presented in the International Standards Organization's technical report [ISO 13309, 1995].

3.2 Inertial Measuring Unit (IMU)

The inertial measurement unit (Fig. 3) is a package of three accelerometers and three gyroscopes that can be attached to the robot's tool tip [ISO 13309, 1995]. When the initial position of the UR10 is known, the accelerations and angles read by the sensors can be used in combination with differential equations to calculate the final position of the UR10.

The IMU method suffers from compounding error in that the known acceleration must be integrated twice to find position – any errors in the acceleration will be magnified in the final position. Furthermore, as the robot's tool tip continues to move, the superposition of error in the acceleration causes extreme compounding of inaccuracies unless calibration is performed at each position.

3.3 Laser Tracking Camera System (LTCS)

The LTCS is a new method designed by the project team to operate using the detectability of the center of a beam of light based on the Gaussian distribution of light intensity from a laser beam. Fig. 6 illustrates how the center of a laser beam could be found using light intensity distribution across camera pixels based on the Gaussian distribution. The highest intensity of light is found at the center of the beam, with a normal (Gaussian) distribution of the intensity along the X and Y axes. The respective maximum intensities on the X and Y axes yield a coordinate location of the beam center on the XY plane. Cameras would be used as photo-detectors to find the center of laser beams in the LTCS method.

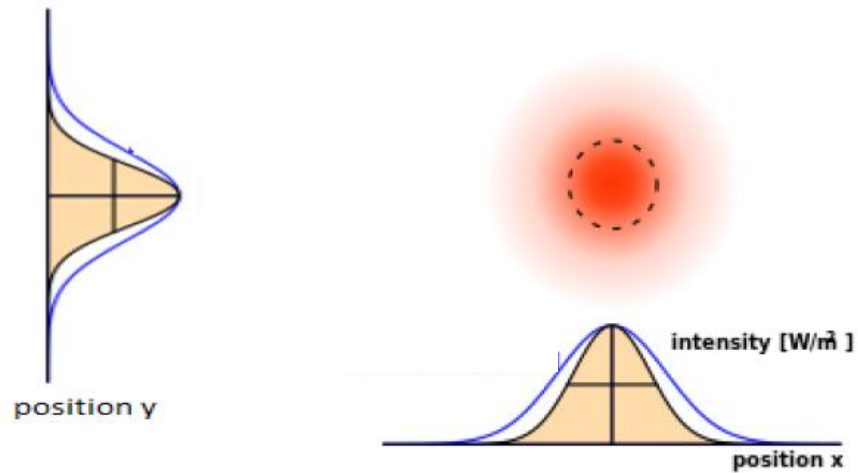


Fig. 6. Use of Gaussian distribution to find the center of a laser beam.

Three cameras positioned orthogonally to each other point towards a single location in space, which would be the UR10's final position. The UR10 carries an "Optical Head," composed of a laser and two beam splitters to generate three orthogonal laser beams. The beams are calibrated to point to the center of the camera positioned along the laser's axis when the UR10 is at its position of interest, after which the UR10 moves to another position and back to its calibrated position. Based on any displacement in the three centers of the laser beams at the calibrated position, the system is able to measure and report the repeatability of the robot in three dimensions. Camera systems, or "Detector Sub-systems," can be placed at any position of interest to determine the UR10's repeatability at that point. Fig. 7 and Fig. 8 show a close up of the UR10 outfitted with the system and the LTCS in place to measure repeatability at two points, respectively.

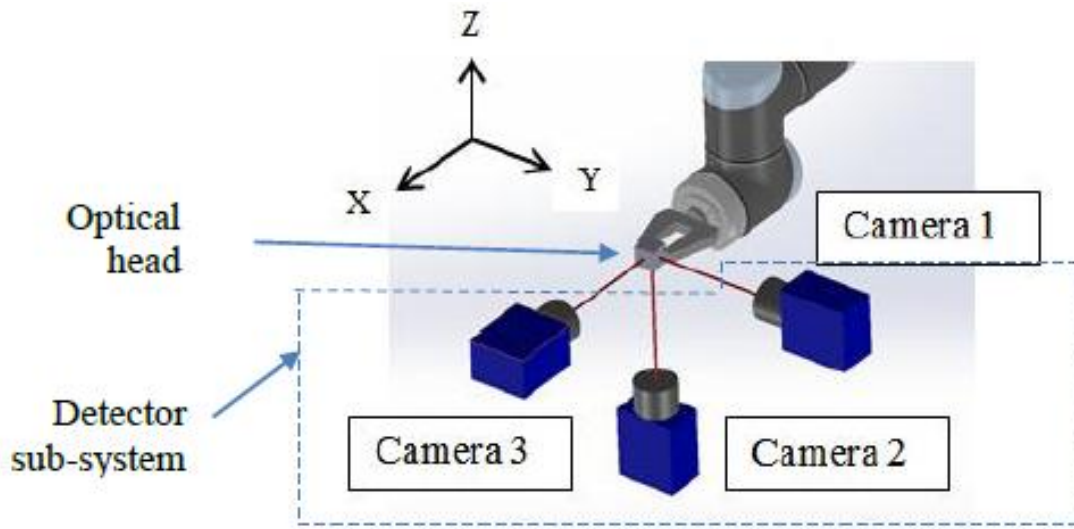


Fig. 7. Close up view of the optical head and detector sub-system attached to the UR10.

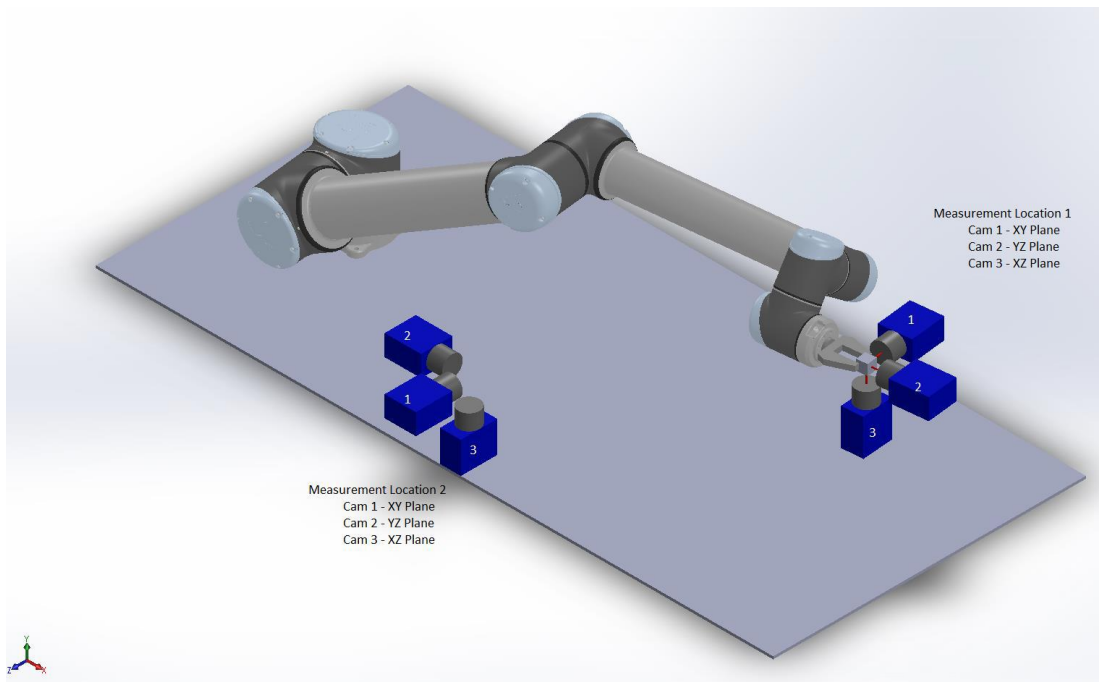


Fig. 8. The UR10 outfitted with the optical head and two detector systems to evaluate repeatability at two points.

The LTCS is unique in its ability to provide sub-micron level resolution and the potential for six degree of freedom measurements without any additional modifications. These features come with an increased cost of several thousand dollars per measurement position.

3.4 MicroElectroMechanical Systems (MEMS) Mirrors

The MEMS mirrors system is comprised of two gimbal-less dual-axis micro-mirror scanners with integrated mirrors, which are used to reflect a laser beam into space [Mirrorcletech, 2014]. The mirrors are activated alternatively to move the laser in a spiral pattern, which is detected by a photo-detector. When the photo-detector senses the laser, the angles of both mirrors are recorded and used to calculate the position of the photo detector. Fig. 9 shows the MEMS mirrors set up tracing the path of a photo detector at (b).

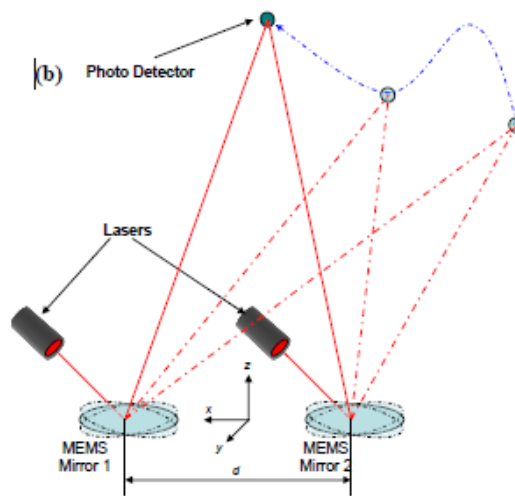


Fig. 9. Visualization of the MEMS Mirrors photo detector, tracking method [Mirrorcletech, 2014].

3.5 Direct Contact Method (DCM)

The direct contact method uses a displacement sensor attached to the tool tip of the UR10 to record the displacement of the sensor tip as the UR10 touches several measurement positions along an axis. Fig. 10 shows an example of using a stepped gauge block to provide five contact positions along a single axis. By performing statistical analyses on the displacements across a sample of contacts for each axis, the repeatability of the UR10 could be determined for all three coordinate axes.

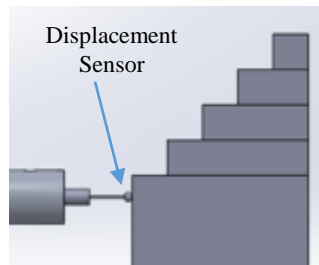


Fig. 10. Conceptualization of a stepped gauge block to provide five contact points for the displacement sensor.

3.6 Selection of a Method

A decision matrix was developed as a comparison metric between the six methods described above. These systems were evaluated according to their cost, resolution, accuracy, mobility, set-up time, number of measureable degrees of freedom, and necessity for software programming. For an explanation of the weighting system and equations used in the matrix, see Appendix C. Table 2 shows the method evaluation with the DCM proving to be the optimal system.

Table 2. Decision matrix used for method selection.

<u>System</u>	<u>Cost</u> (20%)	<u>Resolution</u> (20%)	<u>Repeatability</u> (20%)	<u>Accuracy</u> (10%)	<u>Mobility</u> (10%)	<u>Start-Up</u> (5%)	<u>DOF</u> (5%)	<u>Software</u> (10%)	<u>Total</u> (100)%
LTCS	80	100	100	100	100	100	100	15	87.5
UTM	100	0	0	0	100	50	100	75	45
CTM	100	100	50	0	100	67	50	0	65.8
MEMS Mirror	60	100	100	100	70	50	67	35	78.35
IMU	100	100	0	70	100	60	100	35	68.5
Direct Contact	100	100	100	100	100	90	50	85	95.5

3.7 Implementation of the Direct Contact Method

The DCM characterizes a robot's repeatability by recording the robot's ability to return to a point on a uniaxial displacement sensor's measuring range. In practice, the method involves teaching the robot five positions on each of the X, Y, and Z axes. Each position corresponds to a face on a gauge block such that the displacement sensor will contact the block and read a displacement for the axis perpendicular to the gauge block face. A more repeatable robot will achieve the same displacement more often than a less repeatable one – the repeatability is calculated according to the equations established in ISO 9283.

The full development of the DCM involves the selection of an appropriate sensor; calibration of the sensor; implementation and attachment of the sensor fixture; design of an appropriate gauge block; fabrication of necessary fixture and purchase of the gauge block; verification of fabricated materials; development of a data collection procedure and accompanying software; data collection; and presentation of the data results.

In an effort to choose an appropriate sensor, the project team performed a dynamic analysis of the UR10 to find the natural frequency of oscillation for the tool tip. The result of this analysis was a minimum sampling rate, which led to the selection of the displacement sensor.

4. Characterization of Natural Frequency

In the case of sampling a continuous function, such as the position of the UR10's tool tip, a certain sampling rate must be achieved such that the function is band limited to one half of the sampling rate. This sampling frequency is known as the Nyquist frequency [Nyquist Frequency, 2002].

The continuous function for the UR10's tool tip position is a function of the stiffness, mass, and damping characteristics of the arm. Fig. 11 shows a mass-spring-dashpot analogy in which the UR10 can be represented by the mass, while the motors at each joint represent both the springs and dashpots.

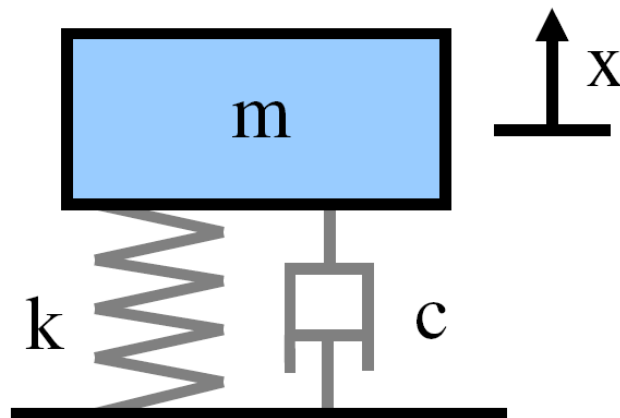


Fig. 11. Spring, mass, dashpot diagram showing mass (m), stiffness (k), damping (c), and displacement (x) [Khanlou, 2014].

Using Newton's second law one can derive the differential equation solving for the position of the mass according to Equation 4.1.

$$\ddot{x} + \frac{c}{m}\dot{x} + \frac{k}{m}x = 0 \quad (4.1)$$

Where x is the position of the mass, c is the damping ratio, m is the mass, and k is the stiffness.

Fig. 12 shows a plot of the underdamped UR10 motion, which is the result of the robot oscillating as it approaches a position based on its attempts to correct itself. The underdamped motion is compared to both over damped and critically damped systems.

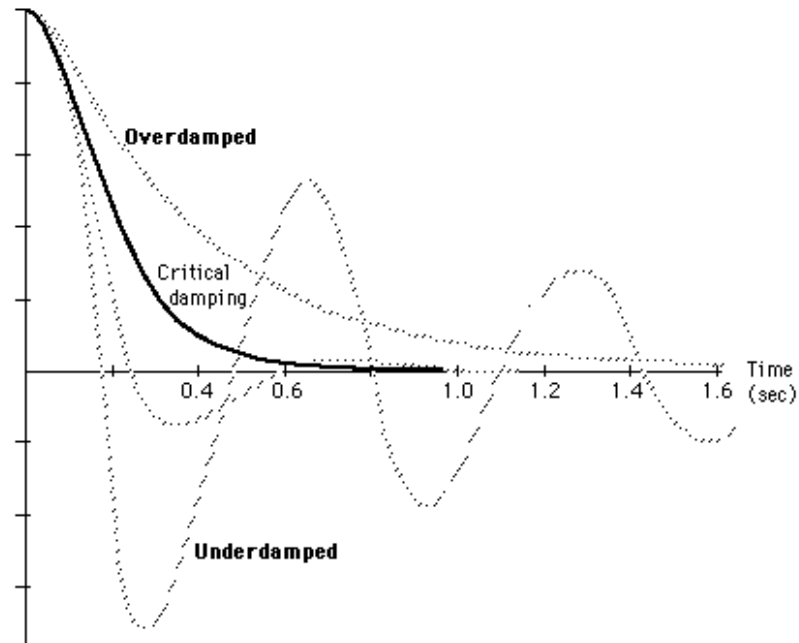


Fig. 12. Plots of over, critically, and under damped systems [The Student Room, 2014].

The rate at which the robot oscillates in its correction is the natural frequency of vibration. Any sensor used to measure the positional characteristics of the UR10 must have a sampling rate at least equal to two times the natural frequency of oscillation of the UR10 according to the Nyquist Criterion [Nyquist Frequency, 2002]. With the use of MEMS

accelerometers, an analysis of the vibrational characteristics of the UR10 allowed the selection of an appropriate sensor.

4.1 MEMS Accelerometers

MEMS accelerometers use internal cantilever beams with masses and magnets attached to measure the acceleration experienced by the accelerometer according to changing capacitance [Analog Devices, 2014]. In the case of the UR10, the attachment of accelerometers to the tool tip allowed for measurement and recording of changing accelerations as the UR10 moved from position to position. These accelerations correspond to the dynamic characteristics of the UR10, namely, the natural frequencies of vibration of the robot.

Two dual-axis 35g MEMS accelerometers were attached to the UR10 tool tip using a fixture fabricated using a Dimensional Rapid Prototype Machine such that the UR10's tool tip mass was minimally affected by the fixture. Each accelerometer was capable of measuring up to 35g's (343 m/s^2) of acceleration at 55 mV/g and can be seen mounted to the accelerometer fixture along with their respective measuring axis in

Fig. 13.

Once the accelerometers were attached to the UR10 a LABVIEW program was run in conjunction with the UR10's motion to acquire vibration data. For more information regarding the specifications of the accelerometers and the LABVIEW program see Appendix D.

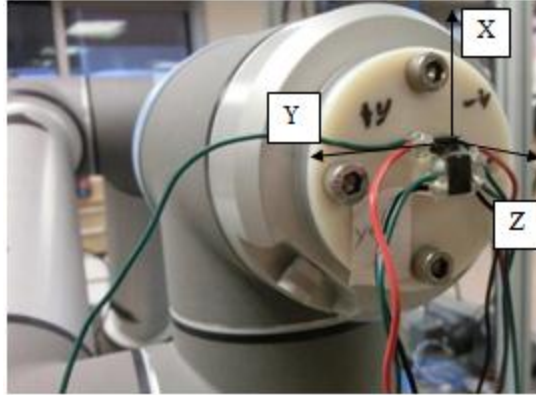


Fig. 13. The accelerometer experiment set up showing the two accelerometers, coordinate system, and ABS fixture.

4.2 Vibrations

The purpose of the vibrations testing was to determine the natural frequency of vibration for the UR10 in regards to the three principal axes: X, Y, and Z. The experiment aimed to collect data from the accelerometers using motion along each of the three axes of interest at different accelerations.

The UR10 was taught two positions along a single axis – an initial position (position 1) at which the robot started the data acquisition and a final position (position 2) where the robot stopped its motion. The UR10 was programmed to send a DC voltage to trigger acquisition at position 1, after which the robot moved to position 2 along the axis. After reaching position 2 the UR10 stopped and the LABVIEW program continued to collect data for 5 seconds. Fig. 14, Fig. 15, and Fig. 16 show representations of the UR10's displacement, velocity, and acceleration for the vibration experiment. All three of these figures correspond to measurements along the X-Axis.

The procedure was run along each of the three principal axes (X, Y, and Z), for five trials each at accelerations of 0.2g, 0.4g, 0.6g, 0.8g, and 1g.

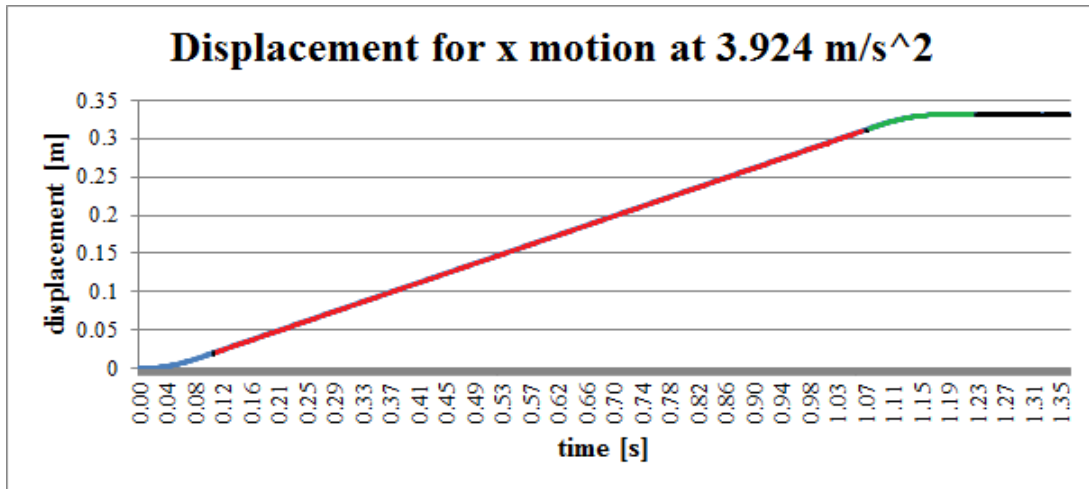


Fig. 14. The UR10's tool tip displacement along the X axis for the vibration experiment.

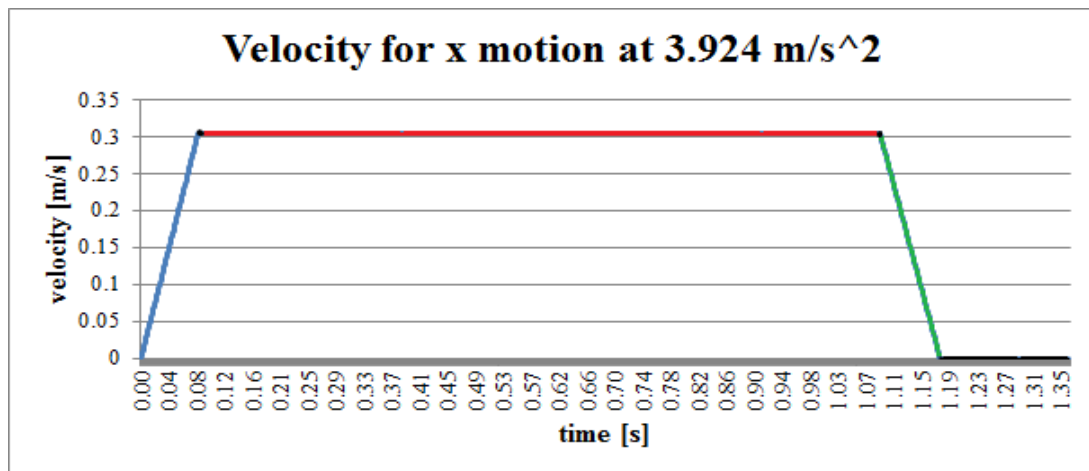


Fig. 15. The UR10's tool tip velocity along the X axis for the vibration experiment.

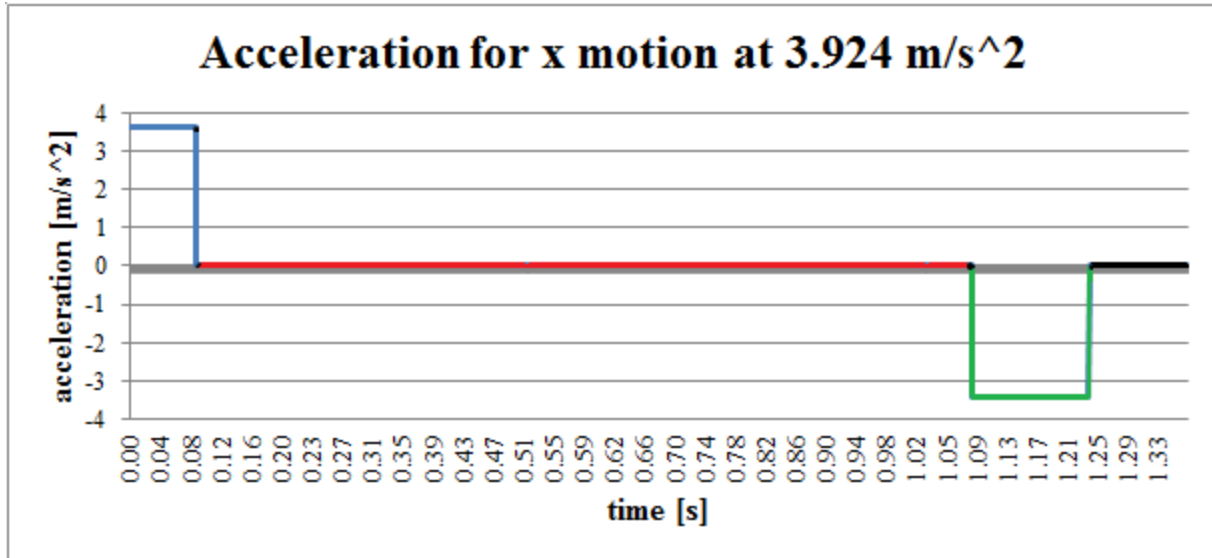


Fig. 16. The UR10's tool tip acceleration along the X axis for the vibration experiment.

The UR10 was also subject to several Impact Tests in which the UR10 was positioned and left stationary to simulate a cantilever beam based on the fixed base and free tool tip – in this way, the UR10 was most similar to the mass-spring-dashpot analogy described above. The robot was then lightly struck with a white rubber mallet, a dark mallet, a hand on the second to last link, and hand on the tool tip. The table that the UR10 was mounted to was also struck with a hammer.

4.3 Experimental Results

The data collected during the vibrations experiments were first plotted in the time domain in an effort to confirm the expected acceleration trends of acceleration from zero to constant velocity; maintenance of constant velocity; and deceleration from constant to zero velocity as exhibited in Fig. 16. A representative graph can be seen in Fig. 17– all motion plots followed the pattern seen

in this graph. Following the confirmation of the expected accelerations pattern, a Fast Fourier Transform (FFT) was used to convert the data into the frequency domain (Fig. 18).

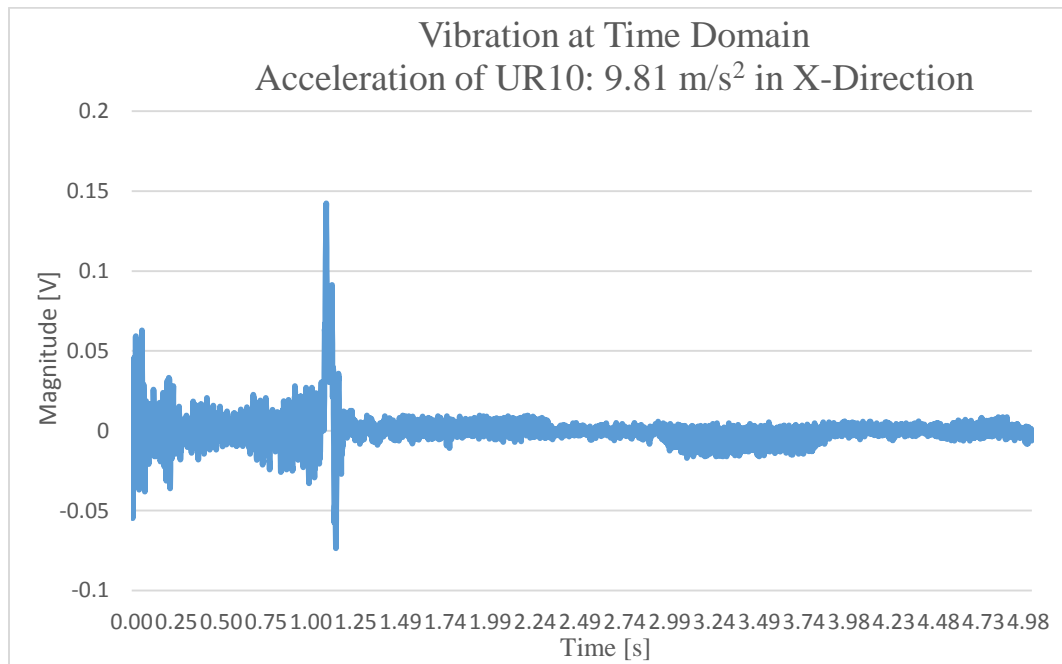


Fig. 17. Time domain plot of the UR10's vibrations for X Axis motion.

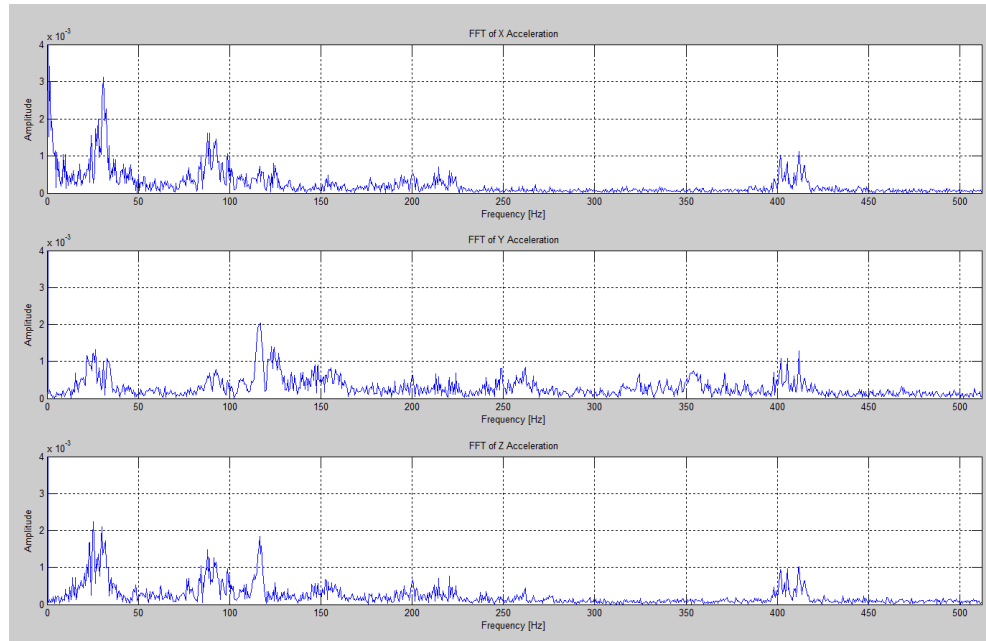


Fig. 18. Fast Fourier Transform of accelerometer data for X motion with noise.

After de-convolving the noise out of the data, two peaks emerged in the frequency data for the motion tests at roughly 30 and 125 Hz as represented by Fig. 19. These peaks were seen in the vibrations along all three test axes (X, Y, and Z). The Impact Tests produced a peak at 125 Hz as well.

Table 3 shows the results of the vibrational analyses in which the frequency peaks along each axis were averaged to find the natural frequency of that axis.

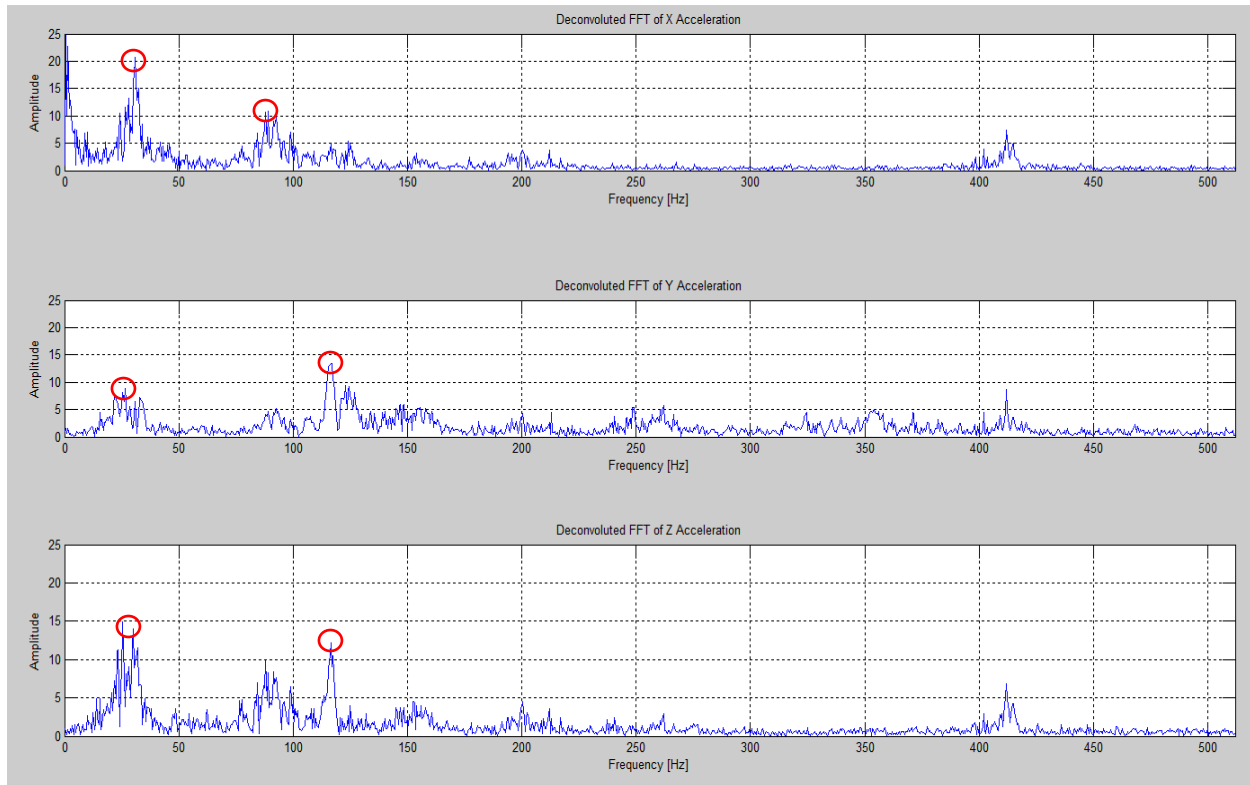


Fig. 19. Deconvolved vibration data showing frequency peaks at 30 and 125 Hz.

Table 3. Representative results of the vibration experiment, shown for the Z axis.

Z Accelerometer	0-44 Hz	45-89 Hz	90-134 Hz	135-179hz	180-224 Hz	225-269Hz	270-314Hz	315-359 Hz	360-404Hz	405-450Hz
Trial A Acceleration	17		124					345		
Trial A noise	11							334, 345		
Trial B Acceleration	13		128					346		
Trial B noise	12							334, 346		
Trial C Acceleration	20		124					346		
Trial C noise								333, 346		
Trial D Acceleration	18		124					346		
Trial D noise								333, 346		
Trial E Acceleration	17		126					346		
Trial E noise	16							331, 347		
Average Natural Frequency		19	125.2							
Standard Deviation		1.414213562	1.7888544							

4.3.1 Interpretation

The data from the accelerometer experiment resulted in three findings:

- Amplitude of vibration increases with increased tool tip acceleration
- Frequency of vibration is not related to acceleration
- The natural frequency of the robot is 125 Hz

Fig. 20, Fig. 21, and Fig. 22 show plots of the amplitude of the vibration at 125 Hz versus tool tip acceleration. The amplitude of the vibration increases with the acceleration along all three axes, as expected based on the increase in forces required to create larger accelerations at the tool tip.

Fig. 23,

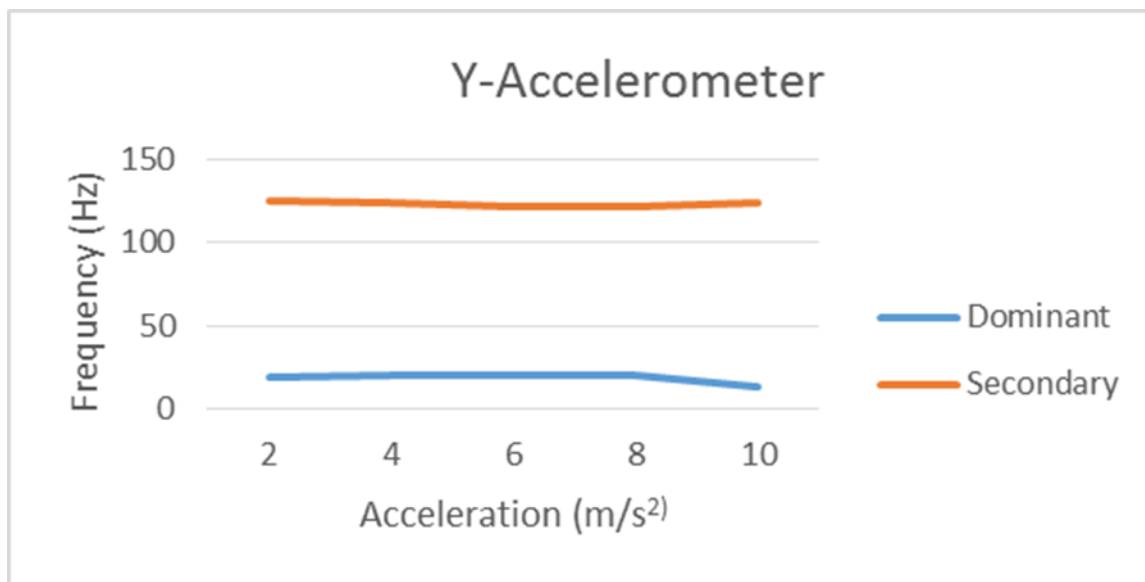


Fig. 24, and Fig. 25 show the relationship between the natural frequency of vibration and increased tool tip acceleration. As expected of the natural frequency, the UR10 oscillates at the same rate independently from the acceleration. The presence of this relationship further reinforces the next claim – that the natural frequency of the robot is 125 Hz.

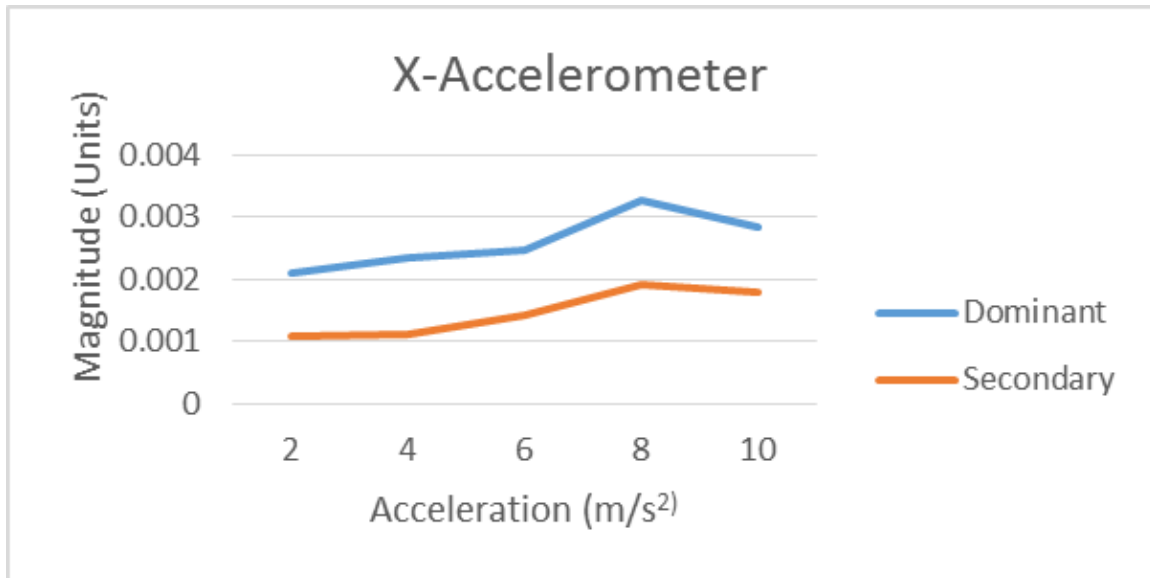


Fig. 20. Amplitude of vibration versus acceleration along the X axis.

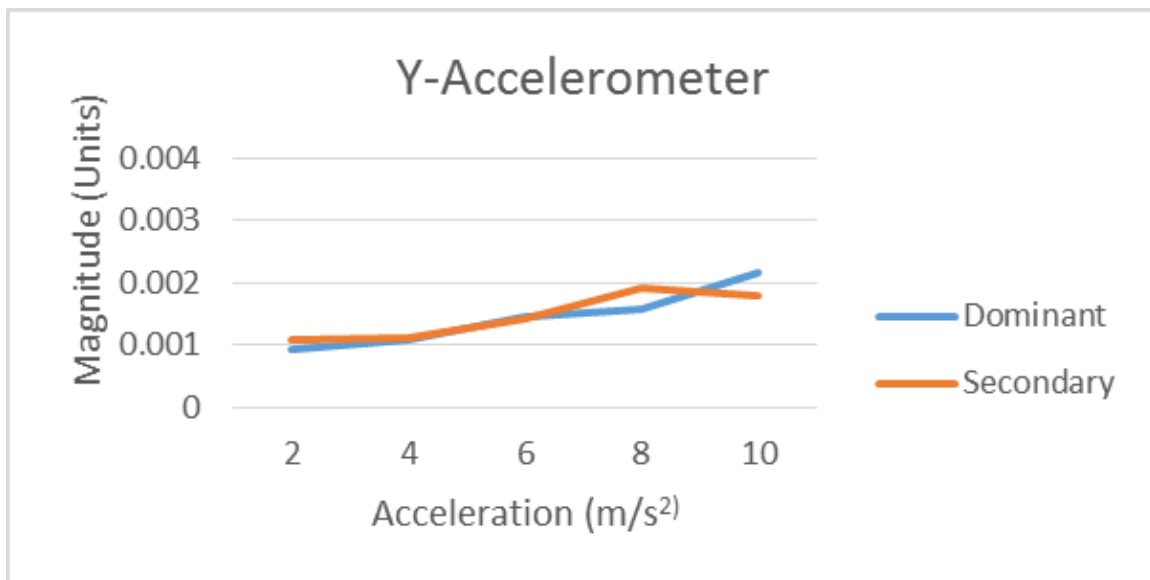


Fig. 21. Amplitude of vibration versus acceleration along the Y axis.

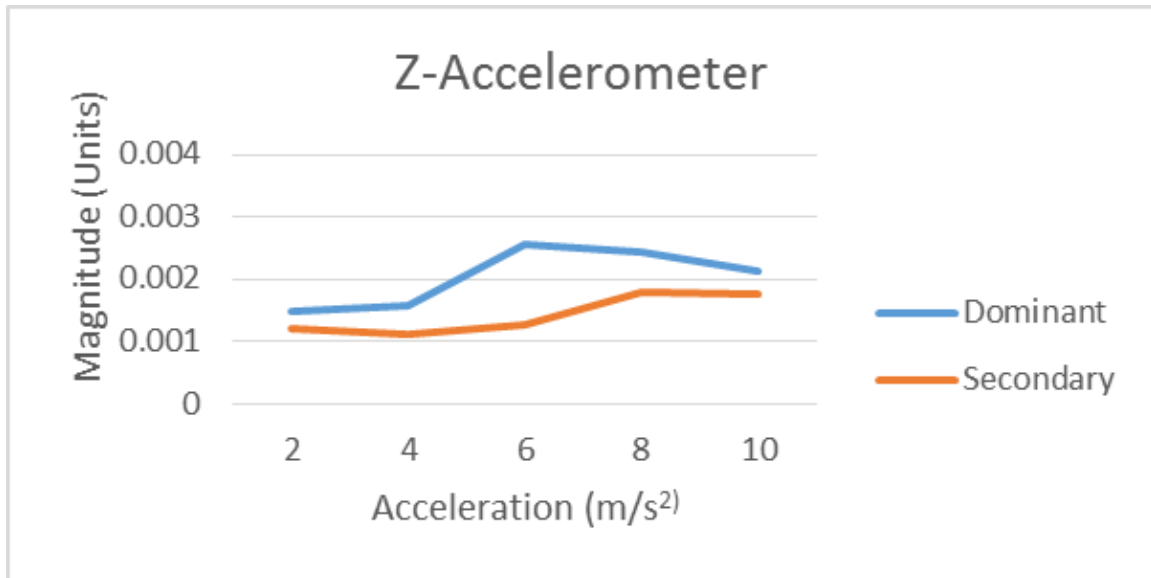


Fig. 22. Amplitude of vibration versus acceleration along the Z-axis.

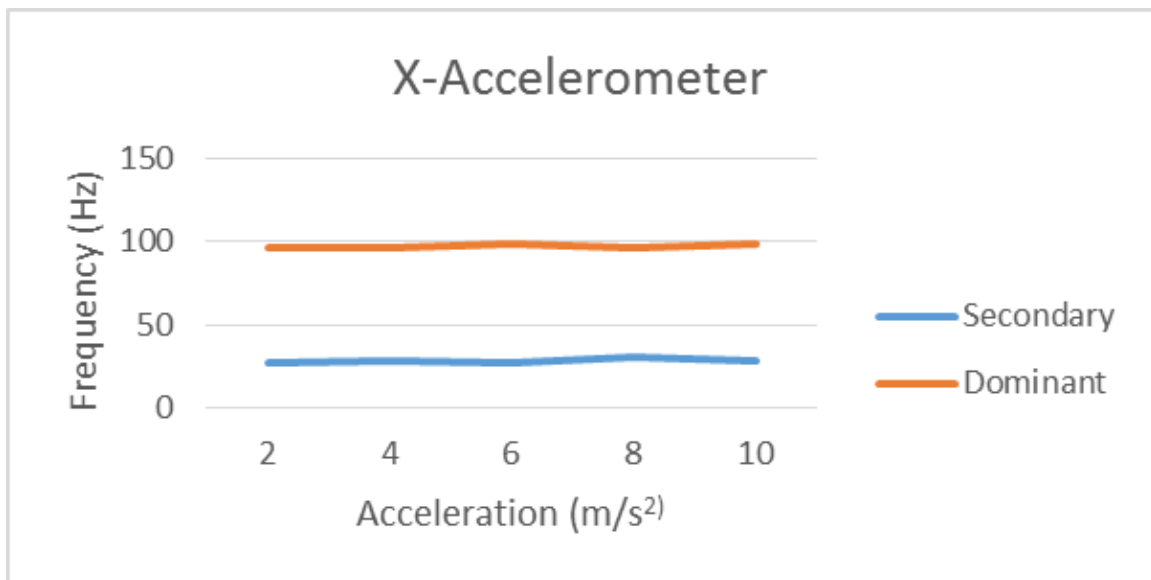


Fig. 23. Frequency of vibration versus acceleration along the X axis.

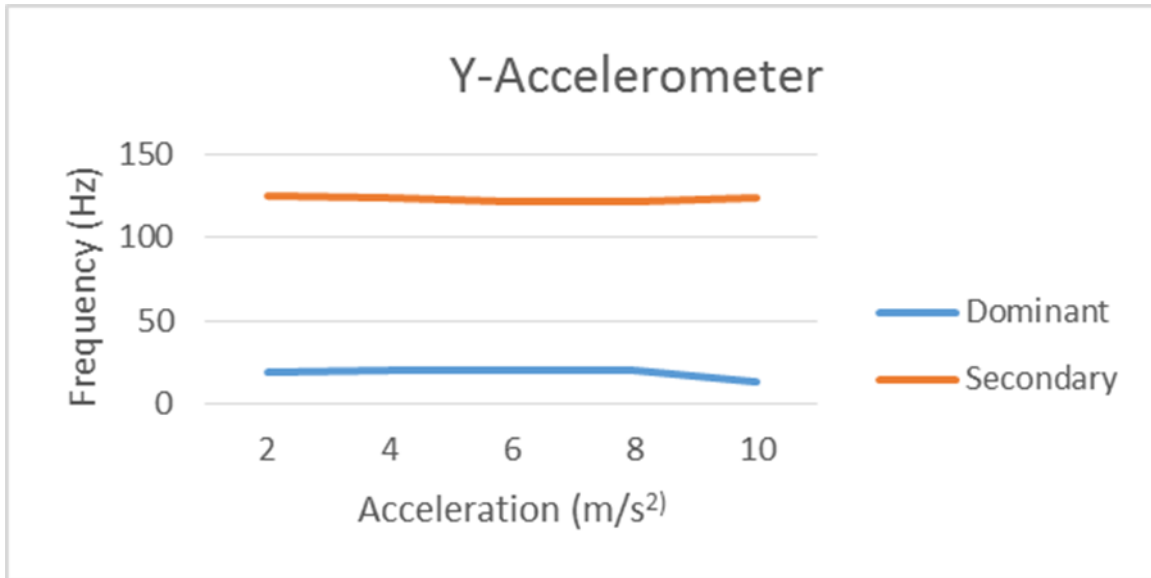


Fig. 24. Frequency of vibration versus acceleration along the Y axis.

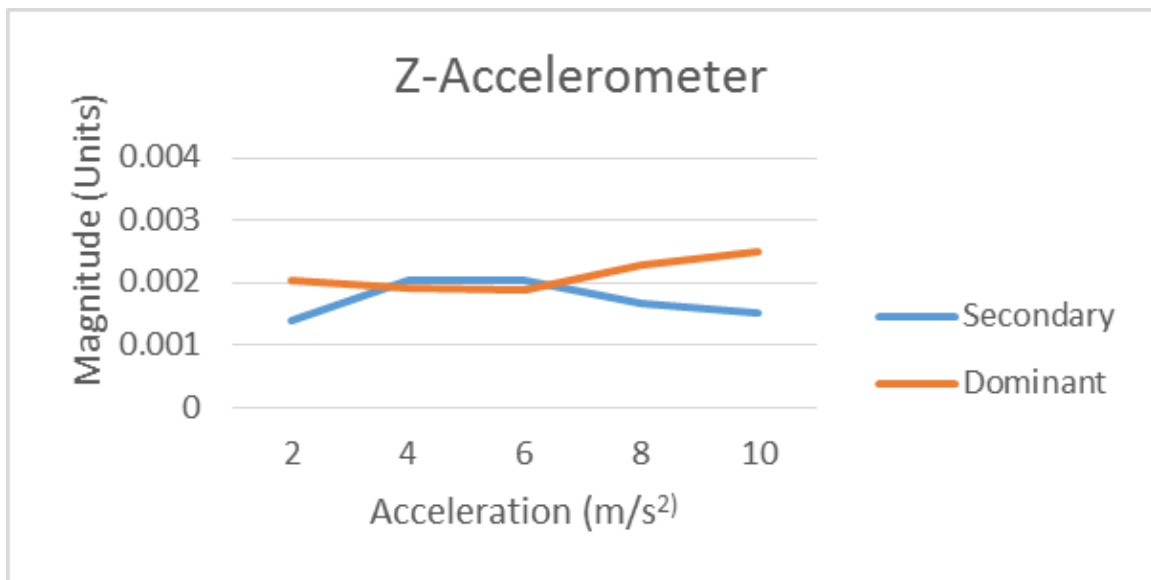


Fig. 25. Frequency of vibration versus acceleration along the Z axis.

Based on the presence of a 125 Hz frequency in both the dynamic and impact vibration tests, the team concluded that the natural frequency of the UR10 was 125 Hz. Such a claim is

validated through the concept of the natural frequency, which is an inherent characteristic of a system that will always appear when the system is stimulated, regardless of the stimulus type.

Using the natural frequency of 125 Hz and the concept of the Nyquist frequency, the team determined that any sensor used to measure the position of the UR10 must have a sampling frequency of at least 250 Hz.

5. Realization of the Direct Contact Method

The development of the Direct Contact Method was accomplished according to the flow chart shown in Fig. 26.

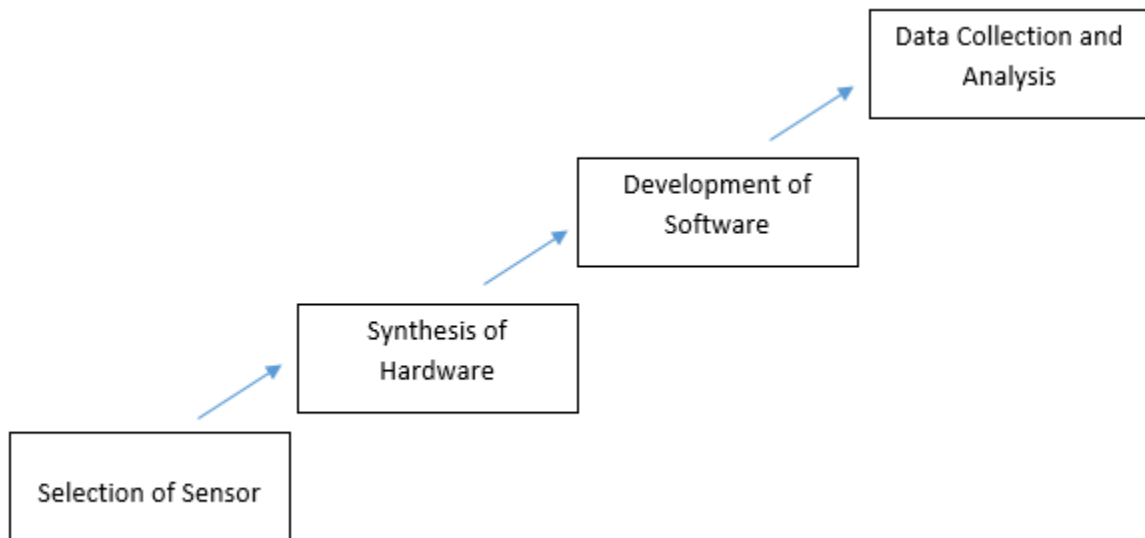


Fig. 26. Steps taken in the realization of the Direct Contact Method.

The selection of sensor involved the identification and evaluation of displacement sensors according to the project's needs. The two most appropriate sensors were ordered and tested to see which performed better in practice.

The synthesis of hardware involved the design of a fixture to mount the selected sensor to the UR10. The fixture was optimized, then fabricated. A gauge block was also designed and fabricated to provide the contact positions for the repeatability procedure.

For the DCM to function properly, a LABVIEW program was needed to collect data from the displacement sensor. This LABVIEW program was written to communicate with the UR10's Polyscope program for accurate data acquisition.

A MATLAB script was written to process and output the results of the repeatability procedure according to the equations given in ISO 9283.

6. Selection of Sensor

The Direct Contact Method, required a sensor with a sampling rate of at least 250 Hz. The selection of a suitable sensor involved the research and comparison of linear potentiometers. Four distinct models were selected and compared based on: cost, resolution, repeatability, measurement range, signal conditioning, signal output, signal to noise ratio, shipping time, and mounting type. For an explanation of the aforementioned criteria and equations used to evaluate the sensors, see Appendix E.

The most suitable sensors were the Omega GP911 Linear Variable Differential Transducer (LVDT, Fig. 27), LORD MicroStrain Sub-miniature DVRT (Fig. 28) Honeywell LVDT, and Mitutoyo electronic displacement indicator.

Table 4 shows the evaluation of the sensors. Based on the results of the decision matrix, the Omega GP911 and MicroStrain SG-DVRT were ordered for testing purposes. Note that the Mitutoyo indicator was ruled out because the sensor was only able to measure a maximum and minimum deflection, which would not work with the goals of the DCM.

After arrival, the Omega and MicroStrain displacement transducers were set up in Worcester Polytechnic Institute's (WPI) Center for Holographic Studies and Laser micro-mechaTronics according to the manufacturer's instructions. Both sensors were then calibrated and evaluated using a linear actuator and micro-stage to validate the manufacturer's claims for repeatability and linearity.



Fig. 27. OMEGA GP911 Linear Variable Differential Transducer (LVDT) [Omega, 2014].



Fig. 28. LORD MicroStrain SG-DVRT displacement sensor [Microstrain, 2014].

Table 4. Sensor evaluation decision matrix.

<u>Category</u>	<u>Category</u> <u>Value</u>	<u>Lord</u> <u>MicroStrain</u>	<u>LVDT</u> <u>Omega</u>	<u>Mitutoyo</u>	<u>Honeywell</u>
<u>Cost</u>	10 points	84%	94%	-	86%
<u>Resolution</u>	5 points	95%	95%	-	99%
<u>Repeatability</u>	10 points	99%	87%	-	80%
<u>Measurement</u> <u>Range</u>	10 points	100%	100%	-	100%
<u>Signal</u> <u>Conditioning</u>	15 points	85%	100%	-	85%
<u>Signal Output</u>	10 points	100%	100%	-	100%
<u>Signal to Noise</u> <u>Ratio</u>	15 points	98%	90%	-	Not Provided
<u>Shipping Time</u>	20 points	80%	100%	-	20%
<u>Mount Type</u>	5 points	100%	75%	-	100%
<u>Total Score</u>	100 points	91%	95%	-	63.26%

6.1 Omega GP911-2.5-S LVDT and MicroStrain SG-DVRT

The Omega and MicroStrain sensors were evaluated to determine which of the two would be most effective in the DCM. The two sensors were set-up and calibrated using a Newport LTA-

HS actuator and micro-stage, which had 0.5 micron repeatability, in order to determine which sensor performed better in practice.

6.1.1 Calibration

Fig. 29 and Fig. 30 show the Omega displacement transducer mounted to the actuator stage. The MicroStrain DVRT was mounted and tested in the same way.

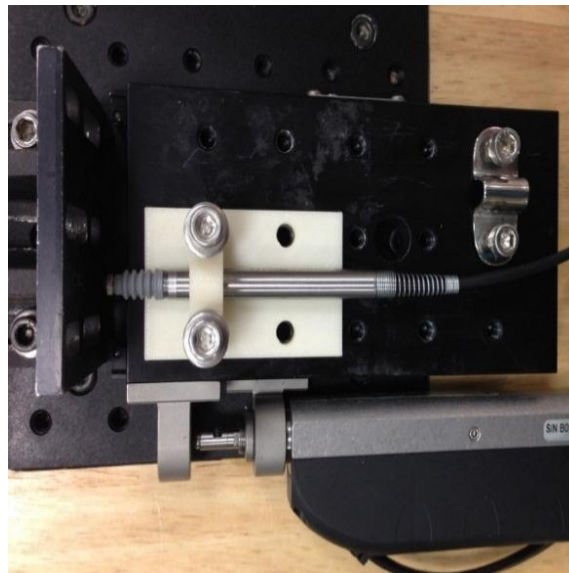


Fig. 29. Top view of the OMEGA LVDT mounted to a Newport actuator and micro-stage for calibration.

A LabVIEW program was used to control the stage, which moved in 0.5 mm increments across the measuring range of each sensor. Ten iterations were performed at each position and the resulting data was processed in MATLAB. A Student's t-test was used to determine that a linear fit of displacement to each sensor's voltage would give sufficient accuracy (Appendix F).

The calibration resulted in calculated repeatability, accuracy, and linearity for each of the two sensors. Table 5 shows the results of the calibration procedures - the Omega LVDT outperformed the MicroStrain SG-DVRT.

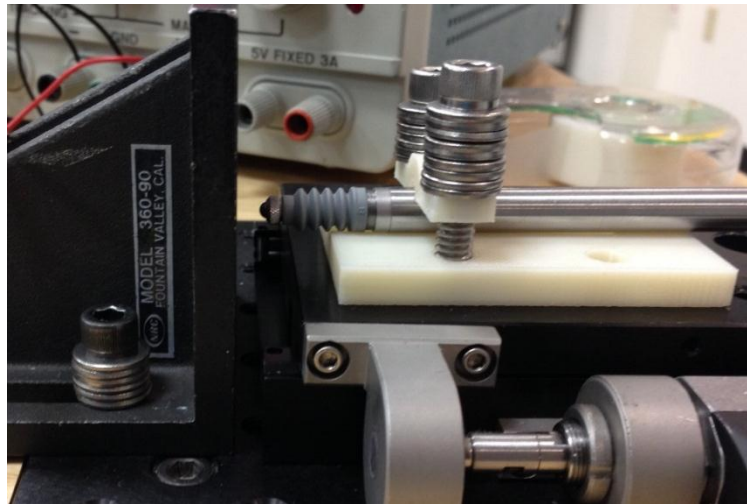


Fig. 30. Side view of the OMEGA LVDT mounted to the Newport actuator and micro-stage for calibration.

Note that the MicroStrain sensor proved to be extremely susceptible to magnetic fields, which caused the sensor to perform poorly. In addition to being outperformed by the Omega LVDT, the MicroStrain DVRT would not be an acceptable sensor without the addition of magnetic shielding.

Table 5. Calibration results and analysis of the OMEGA LVDT and MicroStrain SG-DVRT.

Manufacturer	Micro Strain (0.45 mm to 10.45 mm as full range)					Omega (0.0 mm to 6.0 mm as full range)						
	repeatability	accuracy	Hysteresis	Upper limit fitting equations lower limit	linearity	norm of residual	repeatability	accuracy	Hysteresis	Upper limit fitting equations lower limit	linearity	norm of residual
Manufacturer specifications	± 1 μm	± 1.0 % using linear; ± 0.1 % using polynomial	± 1 μm	NA	NA	NA	± 0.15 μm	NA	NA	NA	0.5% rdg or 0.1% FS	NA
Test results (full range, at Optical Lab for Micro Strain and at HL031 for Omega)	± 300 μm	± 288 μm		2.0091 * V + 0.7610 1.9692 * V + 0.6520 1.9293 * V + 0.5430	0.9712	0.029	± 3.3 μm	± 4.3 μm		0.2690 * V + 2.8372 0.2487 * V + 2.6968 0.2283 * V + 2.5564	0.9276	0.079
Test results with reversed wire (full range, at HL031)	NA	NA	not needed since moving in one direction	NA	NA	NA	± 3.8 μm	± 6.0 μm	not needed since moving in one direction	0.4546 * V + 2.9717 0.4542 * V + 2.9701 0.4538 * V + 2.9686	0.9990	0.0011
Test results (0.5 to 5.5 mm at Optical Lab for Micro Strain, 2.45 to 8.45 mm at HL031 for Omega)	± 120 μm	± 59 μm		2.0897 * V + 0.4723 2.0701 * V + 0.4241 2.0505 * V + 0.3760	0.9902	0.024	NA	± 1.3 μm		2nd order fitting used	NA	0.026
Test results with reversed wire (0.5 to 5.5 mm, at HL031)	NA	NA		NA	NA	NA	± 2.0 μm	± 2.0 μm		0.4541 * V + 2.9702 0.4539 * V + 2.9694 0.4536 * V + 2.9685	0.9996	0.00098
Test results with reversed wire (0.5 to 5.5 mm, at Optical Lab for Omega)	NA	NA		NA	NA	NA	± 2.7 μm	± 2.1 μm		0.4546 * V + 2.9706 0.4542 * V + 2.9696 0.4538 * V + 2.9686	0.9995	0.00041

* repeatability and accuracy determined on 95% confidence for microstrain, 98% confidence for Omega; if repeatability worse than $30 \mu\text{m}$ (one third of sponsor desired limit, 0.1 mm), it is considered disqualified and highlighted in red.

7. Synthesis of Hardware

The DCM required the ability to mount the Omega LVDT to the UR10 while meeting the following basic requirements

- Modular payload of 10%, 50%, and 100% of UR10's capability
- Minimum length to keep loading closest to true center of UR10 tool tip
- Non-interfering natural frequency of vibration
- Integrated wire port for plug and play capability

Furthermore, the DCM required a gauge block to provide five contact points for each axis – see section “7.2 Gauge Block Design.” Mechanical drawings for all of the hardware components can be found in Appendix G.

7.1 Design of Fixture

A fixture was designed to house the LVDT and wiring internally, with the outside of the fixture serving as an attachment point for increased payloads. Fig. 31 shows the preliminary design in an exploded view featuring: a flange with matching pilot and bolt circle to the UR10; a hollow shaft to house the LVDT body and wiring internally; and the outside diameter of the shaft serving as a mount for increased payloads in the form of oversized washers.

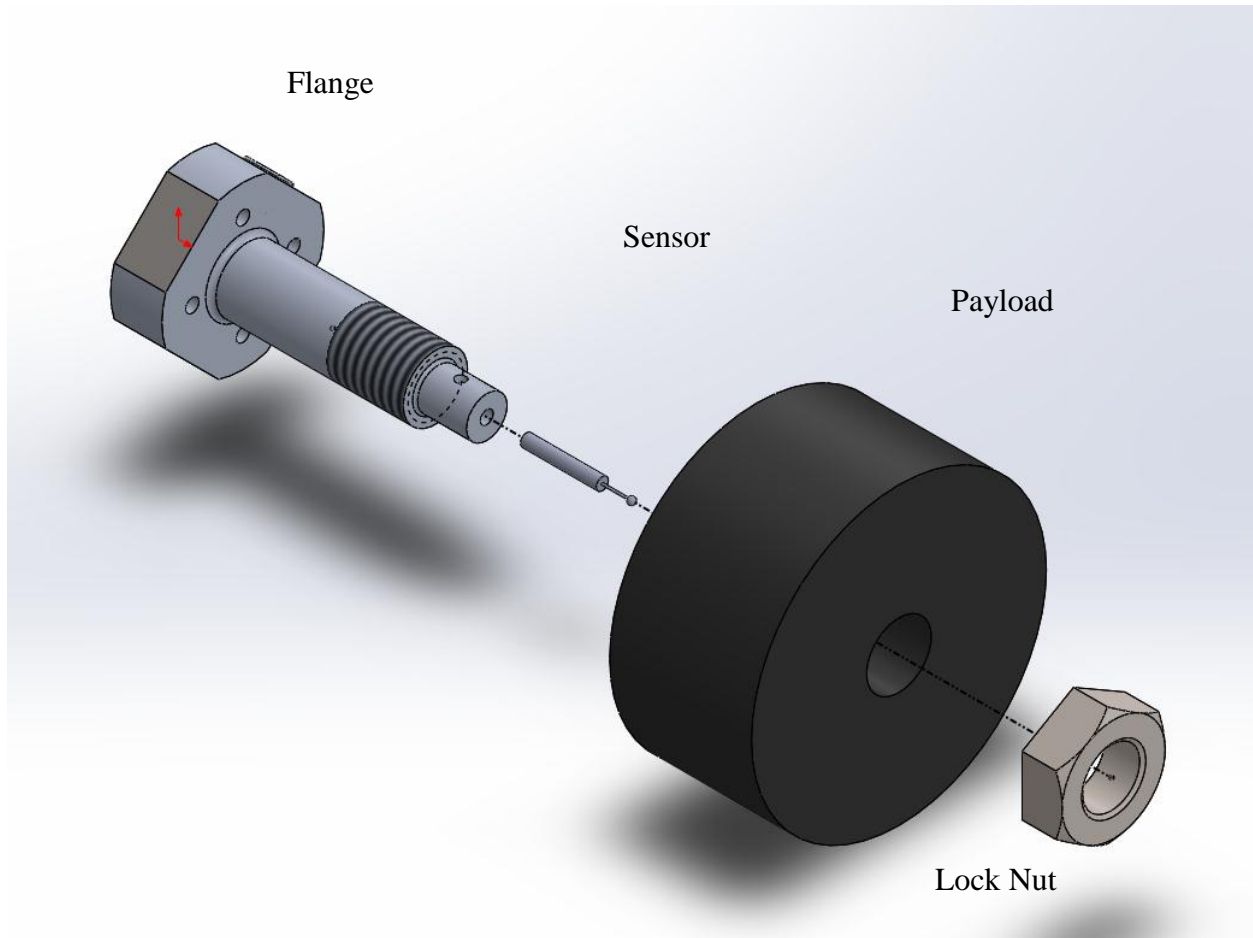


Fig. 31. Sensor fixture design shown with representative sensor, payload, and locking nut.

7.1.1 Attachment of LVDT

As shown in Fig. 31, the LVDT can slip through the front of the fixture through a hole bored into the shaft. The wire runs through the center of the shaft and out through a hole drilled through the mounting flange. Once in place, the LVDT wire must be soldered to a five pin plug (Fig. 32) and the LVDT body is held in place using a nylon tipped M5x0.8 set screw torqued to 0.8 Newton-meters as specified by the GP911 User Manual.

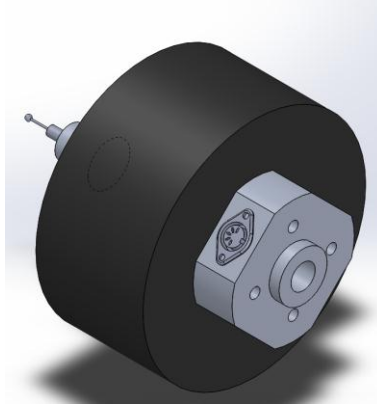


Fig. 32. Back view of sensor fixture showing the five-pin plug on the flat face of the flange.

7.1.2 Modulation of Payload

The washers were made from cast iron due to its high density, allowing for minimal washer dimensions for the required payloads of 50% and 100% of the maximum payload. The washers slide over the outside of the fixture's shaft and are designed to maintain a center of gravity along the UR10 tool tip's central axis. The first 1.5" of the outer shaft is threaded with 1.25"X 7 UNC threads such that the washer can be locked in place using two 1.25" jam nuts. The washers have four clearance holes to allow the heads of the M6 bolts (used to mount the fixture to the UR10) to sit within the washers – aiding in alignment and prevention of vibrations in the washers.

7.1.3 Analysis

The fixture was optimized using Finite Element Analysis (FEA), run through the ANSYS client within SolidWorks 2013. The goal of this optimization was to:

- Minimize cantilever length of the shaft
- Maintain fixture mass of 1 kg

- Minimize washer dimensions
- Minimize cost of materials
- Natural frequency at least ten times that of the UR10 with max payload

7.1.1.1 Assumptions and Results

The fixture material chosen for the analysis was Series 304 Stainless Steel, which was chosen to minimize any potential magnetic interference. The fixture was fixed about the back of the flange where it connects to the UR10 and a force of 1000 N was applied to the shaft to simulate the worst case loading on the fixture. The results, shown in Fig. 33, demonstrate the maximum Von Mises stress on the shaft after optimization.

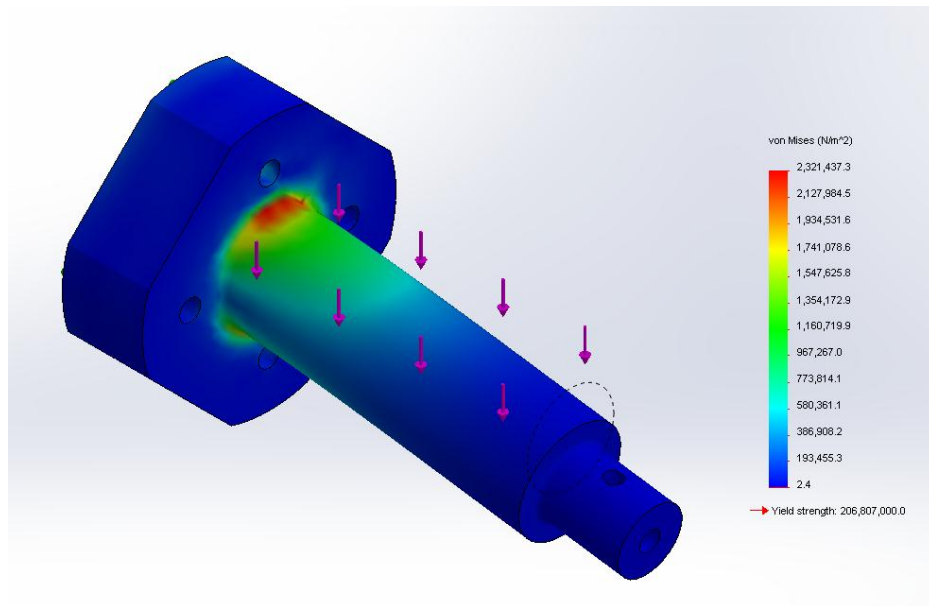


Fig. 33. Von Mises stresses in the sensor fixture.

At the base of the cantilever, the stress is 2.3 MPa giving a minimum safety factor of 89.

This safety factor shows that the dimensional needs relating to securing the LVDT and

decreasing the outer diameter of the payload were more critical to the design than the stresses caused by the applied loads.

The natural frequency of vibration with the 10kg payload is 1687 Hz as seen in Fig. 34. This frequency is the lowest frequency of the fixture as evidenced by Equation (6.1).

$$\omega_n = \sqrt{\frac{k}{m}} \quad (6.1)$$

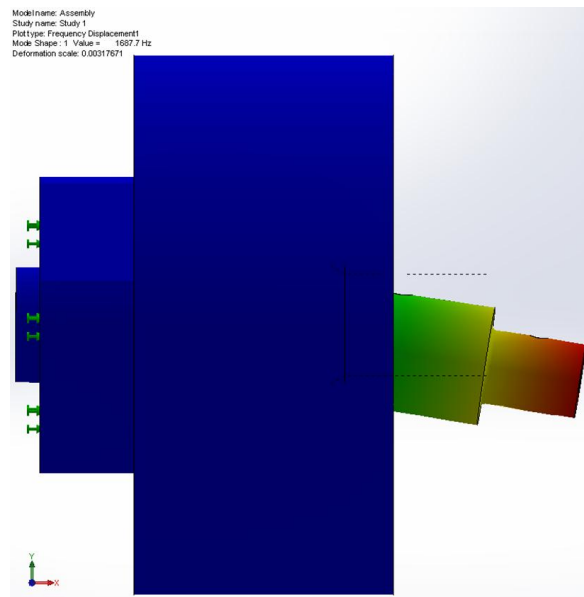


Fig. 34. Vibrational analysis of the sensor fixture showing a max frequency of 1687 Hz.

7.2 Gauge Block Design

The gauge block was designed to provide five measurement positions for the UR10 based on ISO 9283 guidelines. Based on the ability for the LVDT to measure repeatability for a single axis at a time, the gauge was designed with three faces each having five positions to allow appropriate measurements for all three principal axes. The gauge block was designed to take into

account both the surface roughness of the gauge as well as thermo mechanical expansions to ensure dimensional accuracy during testing.

A checkered pattern of pockets was designed to accomplish the above while simultaneously keeping the volume minimal for sensor clearance and preventing the largest washer from contacting the test table. Fig. 35, shows the realization of this goal.

The checkered pockets were designed to be large enough to account for the diameter of the sensor and any possible error in an effort to reduce chances of a damaging collision. The overall size of the block was chosen such that the range of payloads would not collide with the mounting table and in order to prevent a collision between the fixture and the block.

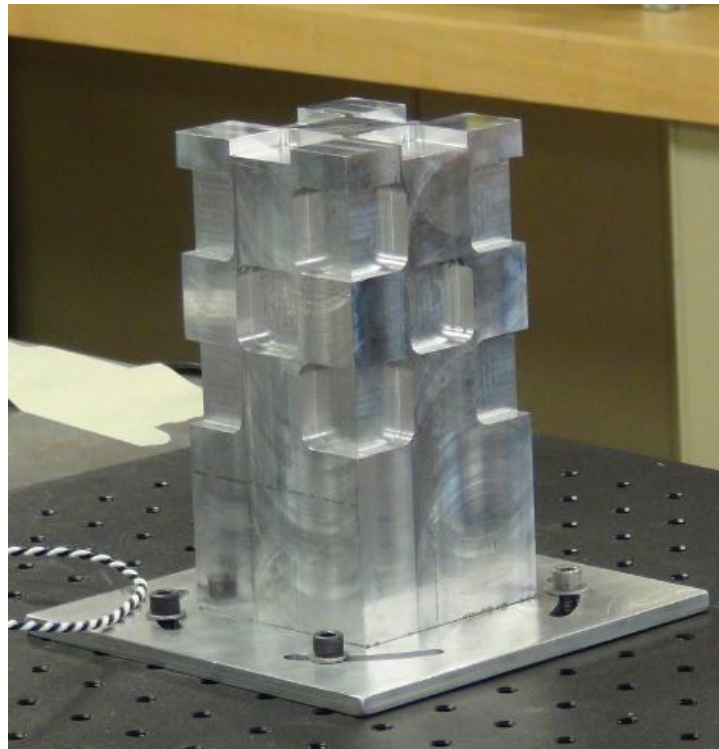


Fig. 35. Gauge block assembled and mounted to an optical breadboard.

Aluminum 7075 was selected as the manufacturing material in an effort to minimize micron level errors caused by temperature fluctuations. Low head M5 bolts were chosen to mount the gauge block to the plate, while 1/4-20 UNC bolts were necessary to mount the plate to the sponsor's optical breadboard table. Four slots for the 1/4-20 bolts allowed alignment of the gauge such that the UR10 tool face and front gauge face were parallel.

7.3 Fabrication

The manufacturing of the fixture components was completed using the machine shop in Washburn/Higgins Labs in addition to a lathe at Reich USA (Mahwah, NJ) capable of turning cast iron with a diameter of 6".

The washers were fabricated using 6" Diameter cylindrical bar stock ordered from McMaster Carr. The stock was cut to the rough size of the washers using a band saw, then faced to 2.75" in length on a manual lathe. The 50% payload washer was turned down to 4" outer diameter, then both washers were bored to the fixture shaft's diameter with a sliding tolerance. The M6 bolt head counter bores were done with a Haas MiniMill.

The fixture was made using 3.5" diameter Series 304 Stainless Steel. The front shaft and sensor holding profile were turned down on a Haas T1 lathe, then bored to fit the LVDT. The back pilot was turned on the same lathe and bored to allow the LVDT wires to run through. A Haas MiniMill was used to create the flange profile and M6 bolt circle, while a drill press was used for the set screw and plug holes. Fig. 36 shows the finished fixture mounted to the UR10 with the largest payload attached.

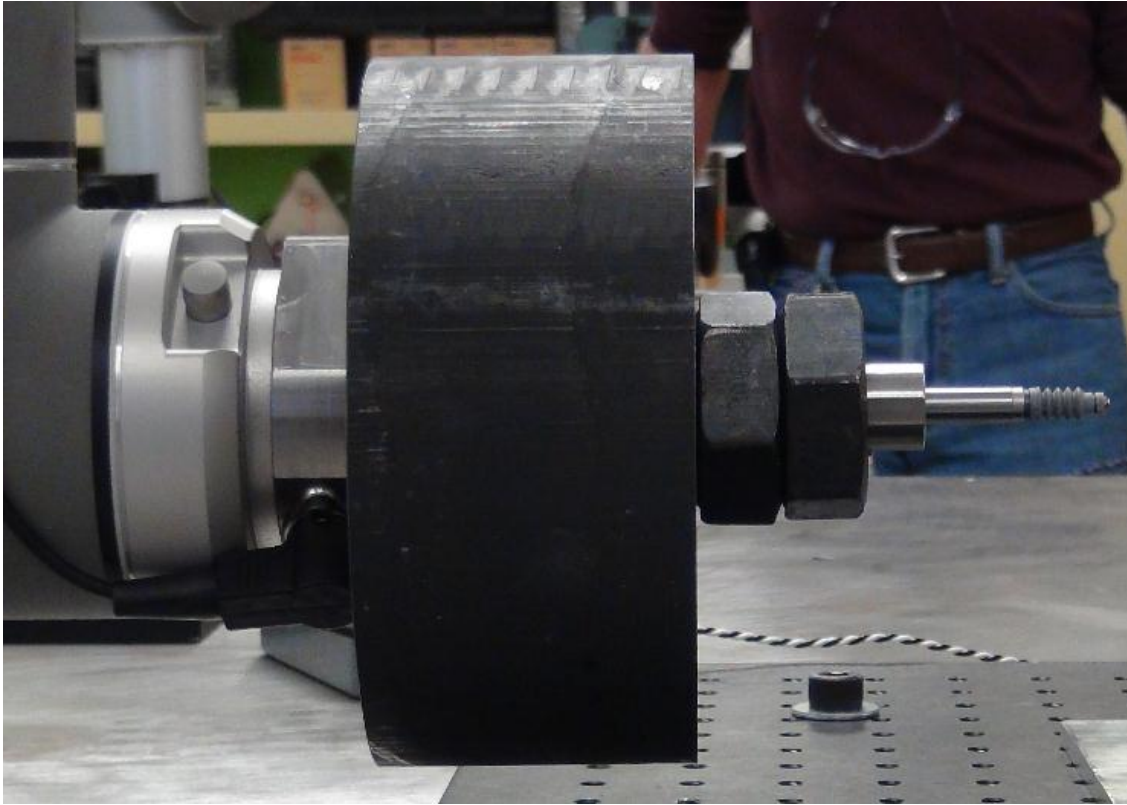


Fig. 36. Fixture with 10 kg payload mounted to the UR10.

The team chose to manufacture the gauge block in Washburn Shop rather than purchase a certified block from a third-party based on the need for a customized block with five measurement positions on three faces. The customized gauge blocks that were researched required a minimum 6-week lead time for manufacturing at a third-party machine shop and an addition of several weeks for certification. Although dimensional tolerances for the gauge block were important, the DCM procedure does not actually measure position, but displacement, and as such tolerances beyond the 0.02 mm achievable in WPI's Washburn Shop were not necessary – leading to the selection of a Haas MiniMill for the pocketing operation on the gauge block. Fig. 36 shows the completed assembly.

7.4 Validation of Fixture Assembly

Every component was inspected and verified post-fabrication. The LVDT was pushed through the front bore, soldered to the five pin plug and mounted within the fixture, then tested using the sensor calibration procedure originally used for sensor evaluation.

8. Testing Procedure Overview

The testing procedure was developed to follow the flow chart shown in Fig. 37. The full Direct Contact Method instruction manual can be found in Appendix L.

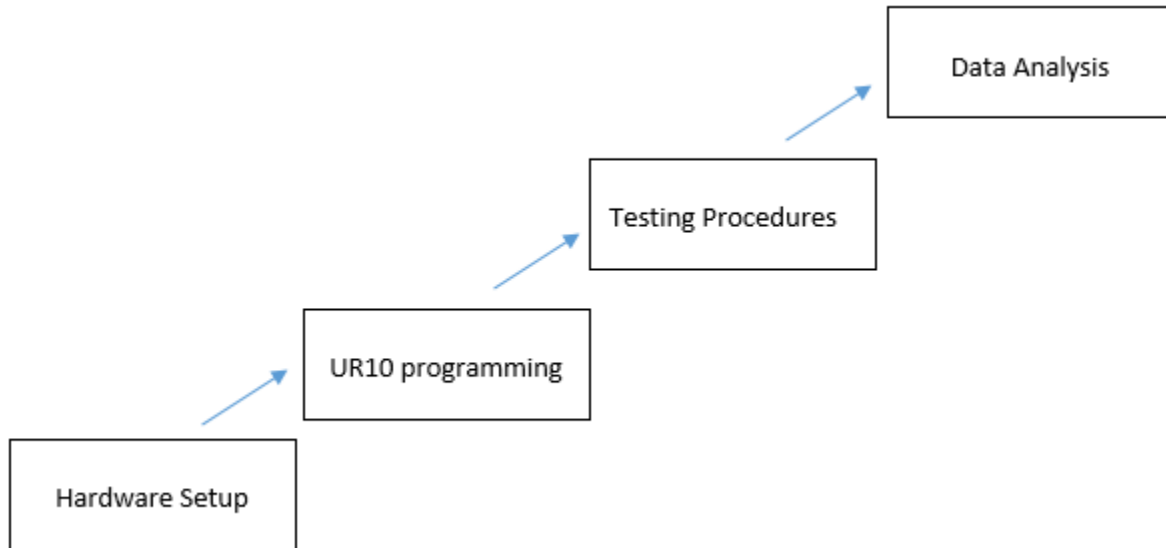


Fig. 37. Flow chart for the Direct Contact Method testing procedure.

The hardware set-up involves mounting the sensor fixture to the UR10; mounting the gauge block to the table; connecting wires from the UR10 to the LDX signal conditioner; connecting the sensor to the LDX; and connecting the signal conditioner to the Data Acquisition (DAQ) box, which transfers data to a computer. Fig. 38 shows the laboratory set-up. The UR10 provides power to the signal conditioner, which powers the LVDT and filters out the sensor's noise before passing the signal to the DAQ box and laptop.

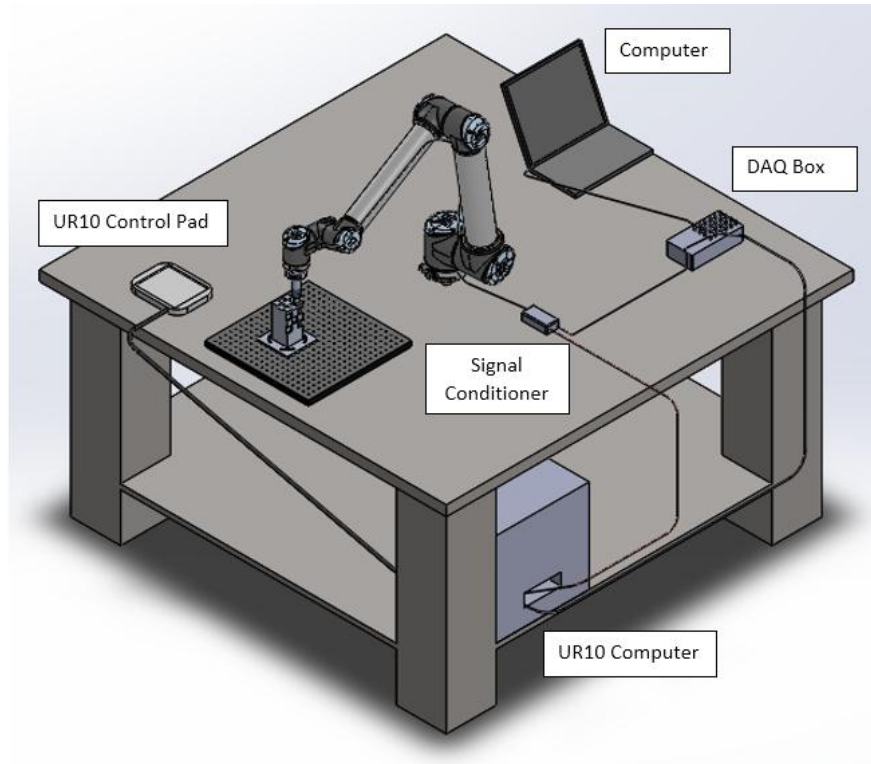


Fig. 38. Laboratory set-up for the Direct Contact Method.

After hardware set-up, the UR10 must be taught all of the necessary contact positions along the gauge block. This step involves aligning the gauge block to the UR10 (Fig. 39) and manually teaching the robot to touch five positions on each face. These positions correspond to the five pockets on the vertical faces of the gauge and four pockets plus the raised middle surface on the top face.

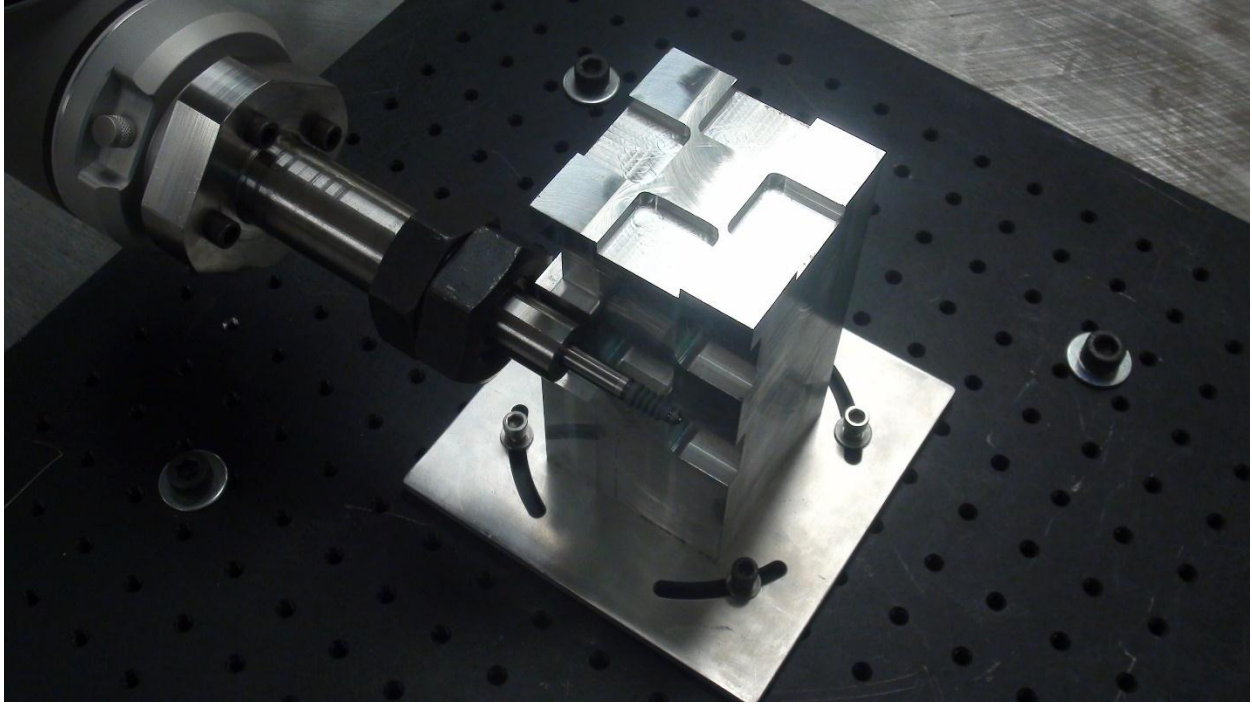


Fig. 39. Alignment procedure for the gauge block and UR10.

The data acquisition at each position follows the sequence shown in Fig. 40: the UR10 moves to touch a gauge face; the UR10 sends a signal to start data acquisition; the UR10 waits 2 seconds; the UR10 moves to the next position and the process repeats. A single full testing procedure involves the robot touching each of the fifteen gauge block positions 30 times each. Each test can be modified to allow repeatability testing with modified payload and acceleration: payload can be changed by attaching/removing the oversized washers and acceleration can be modified using the UR10 control pad. The project team ran tests with payloads of 1, 5, and 10 kg and accelerations of 0.2, 0.5, and 1.0g.



Fig. 40. Process flow for data acquisition at each gauge location.

Software programs were developed to collect and analyze the data as described in the following section titled “Development of Software.”

9. Development of Software

A LabVIEW program and UR10 Polyscope Program were developed for recording repeatability data. A MATLAB script was written to process the data and output repeatability according to ISO 9283.

9.1 LabVIEW and Polyscope Program

The LabVIEW program was written to receive two separate AC voltages from the UR10 and LVDT. Whenever the UR10's voltage signal was above 3V the program recorded the LVDT's voltage for two seconds and wrote the data to an excel sheet. The program was able to record as many points as necessary until the user stopped LabVIEW, due to a nested while loop. Fig. 41 and Fig. 42 show the front panel and block diagram from the LabVIEW program.

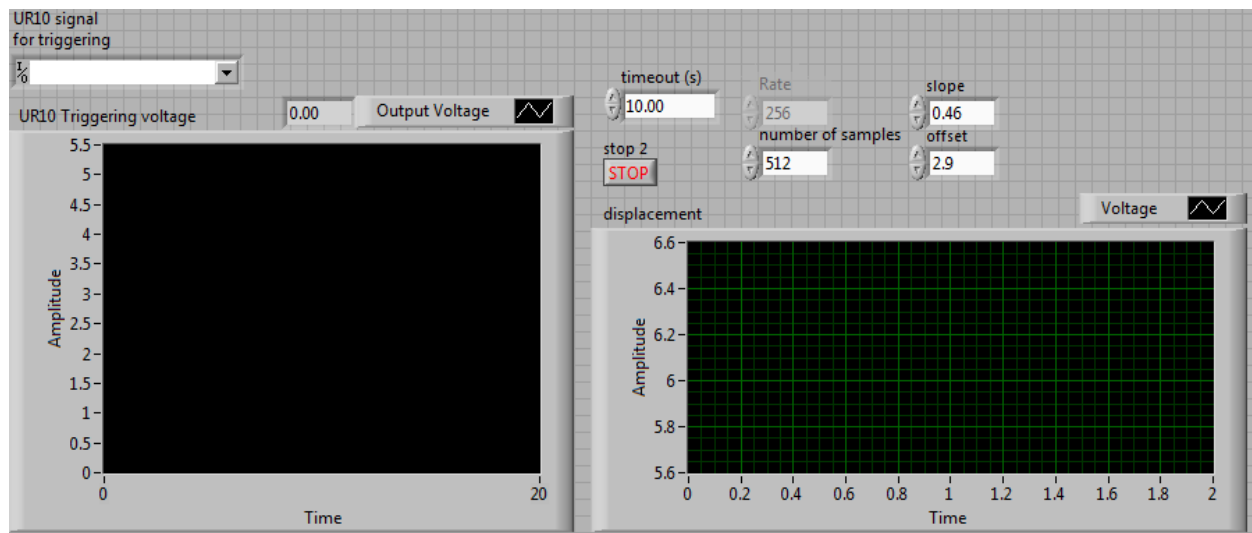


Fig. 41. Front panel of the recording program.

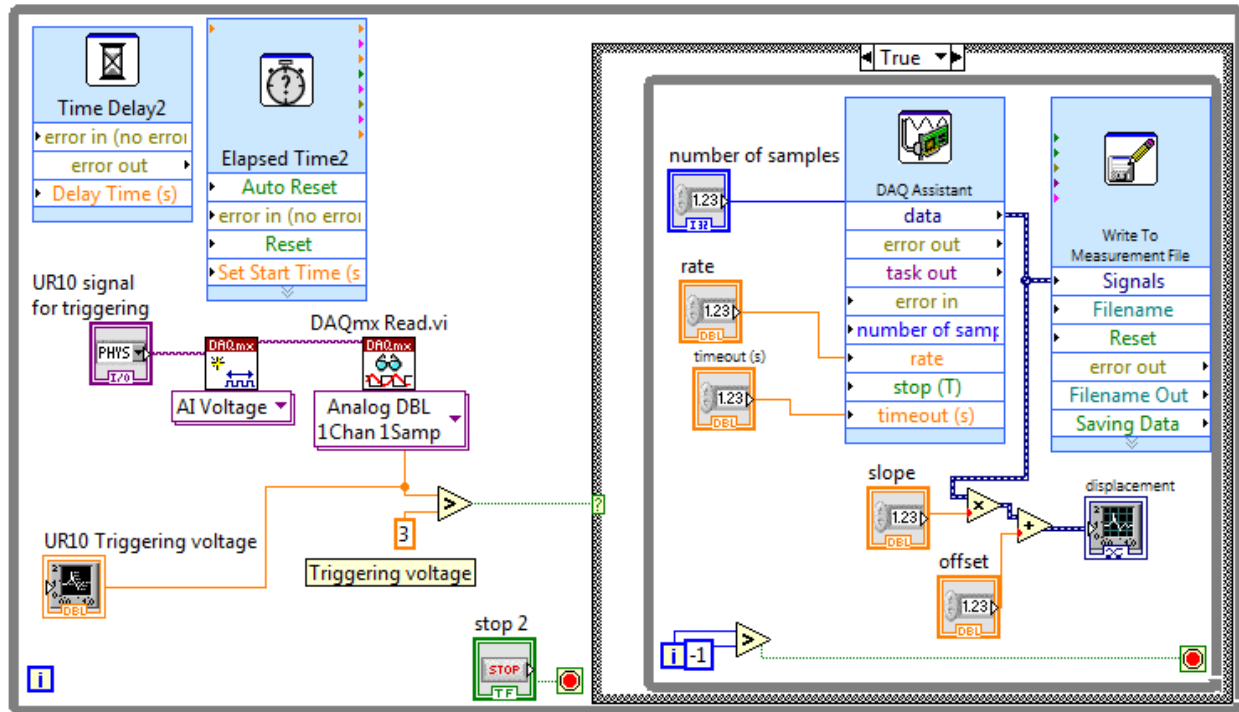


Fig. 42. Block diagram of the LVDT recording program.

The UR10's program was written by manually teaching the robot contact positions on the Gauge block. For the horizontal X and Y axis measurements the UR10 was taught to touch the five pockets and for the vertical Z axis the robot touched four pockets plus the raised middle portion of the top face. At each position the robot was calibrated to displace the sensor 1.25 mm for the largest possible measuring range in either direction. The UR10 was also programmed to wait for two seconds at each displaced position to prevent vibrations in the LVDT piston from interfering with the LVDT's measurements. The full Polyscope program as outputted by the UR10 is included in Appendix H.

9.2 MATLAB Analysis

The MATLAB script was written to process all of the voltage files recorded from LabVIEW.

The script prompts a user to input several parameters including the sampling rate, sampling duration, iterations per position, positions tested per test, number of axes (directions) tested, number of payloads tested, and number of payloads tested. Based on the user's inputs the script will output repeatability values for each test. The full MATLAB script is included in Appendix I.

10. Collection of Data

The UR10 was programmed to touch the five pockets on the two vertical faces of the gauge block to characterize X and Y repeatability, in addition to four pockets and the middle surface of the top plane of the block to characterize Z repeatability (Fig. 43).

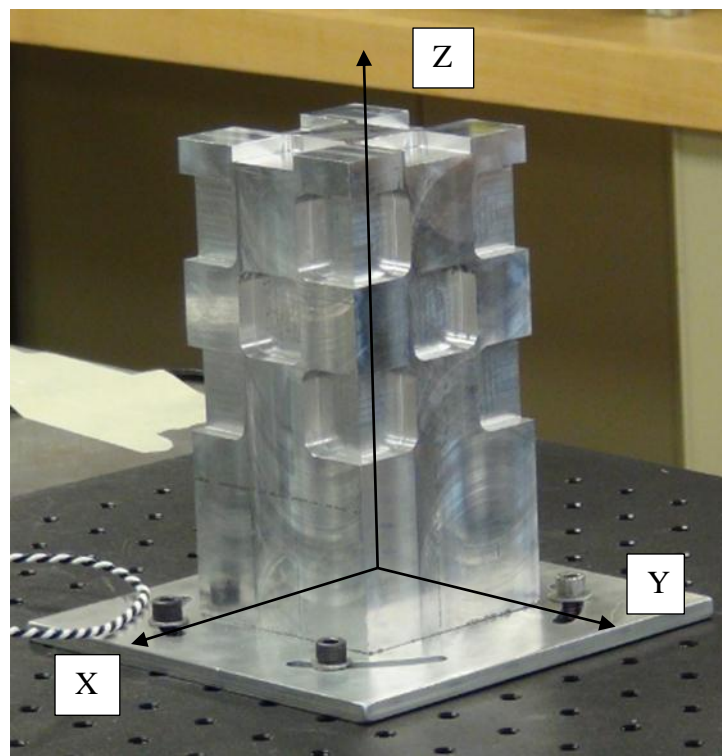


Fig. 43. Gauge block with directional labels.

The UR10 sent a 5V DC signal to start the collection of data from the LVDT when the UR10 was at its final position for each measurement position. The UR10 then waited for 2 seconds, sent out a 1V signal to turn off data collection, and moved to the next position along the same face. The five measurement points on each axis were touched thirty times each before the UR10

moved to the next axis. In a single procedure the UR10 performed X, Y, and Z repeatability measurements in that order. Each repeatability procedure took approximately 45 minutes over a total of 9 tests.

10.1 Repeatability Parameters

The goal of the DCM was to characterize the repeatability of a collaborative robot as functions of payload and acceleration. According to ISO 9283 the payload was tested at 10, 50, and 100% of the UR10's maximum capabilities, while the acceleration was 0.2, 0.5, and 1 g. The data collection resulted in data files containing the LVDT's displacement as it touched each of the fifteen gauge block positions 30 times for the payloads and accelerations described above.

For the following analysis and explanation, increasing repeatability indicates that the repeatability value became larger. For all cases, a smaller value for repeatability indicates higher robot precision, which is more desirable.

10.1.1 Repeatability vs. Payload

ISO 9283 dictates that a robot should be evaluated at 10%, 50%, and 100% of its maximum payload. To that end the repeatability procedure was run for all three payloads by attaching only the fixture (1 kg); the 4" diameter washer and fixture (5 kg); and the 6" diameter washer and fixture (10 kg); respectively.

The analysis showed that the repeatability of the UR10 is independent of payload for the X and Y directions. The average repeatability for X and Y is 0.05 and 0.04 mm respectively, well within Universal Robots specification of 0.1mm.

For the Z direction repeatability deteriorates as payload increases. The UR10's repeatability increases from within manufacturer's tolerances (0.06 mm at 1 kg) to outside the tolerance (0.236 mm at 10 kg). The loss of repeatability is far less between 1 and 5 kg, than between 5 and 10 kg – a change of 0.006 and 0.169 mm respectively. These results indicate a threshold payload between 5 and 10 kg, after which the UR10 rapidly loses repeatability. The overall increase in repeatability for the Z Direction can be explained by the loading of the UR10 – the load acts in the Z direction, indicating that for larger loads the arm will have to exert a larger force in the Z direction, leading to larger amplitudes of oscillation and decreases in repeatability. Additional statistical analysis is necessary to prove the accuracy of this claim, see section “9.2 Statistical Analysis.”

Table 6 shows the average repeatability for each direction at the three different payloads. Note that for these tests the acceleration was a constant 0.2g; a data table containing all of the individual data points collected during the 9 tests can be found in Appendix K. Fig. 44 shows a plot of Payload versus Repeatability as presented in Table 6.

Table 6. Average repeatability for the UR10 for varying payloads with constant 0.2g acceleration.

Axis	Payload (kg)	Avg. Repeatability (mm)
X	1	0.055
	5	0.051
	10	0.053
Y	1	0.041
	5	0.029
	10	0.044
Z	1	0.061
	5	0.067
	10	0.236

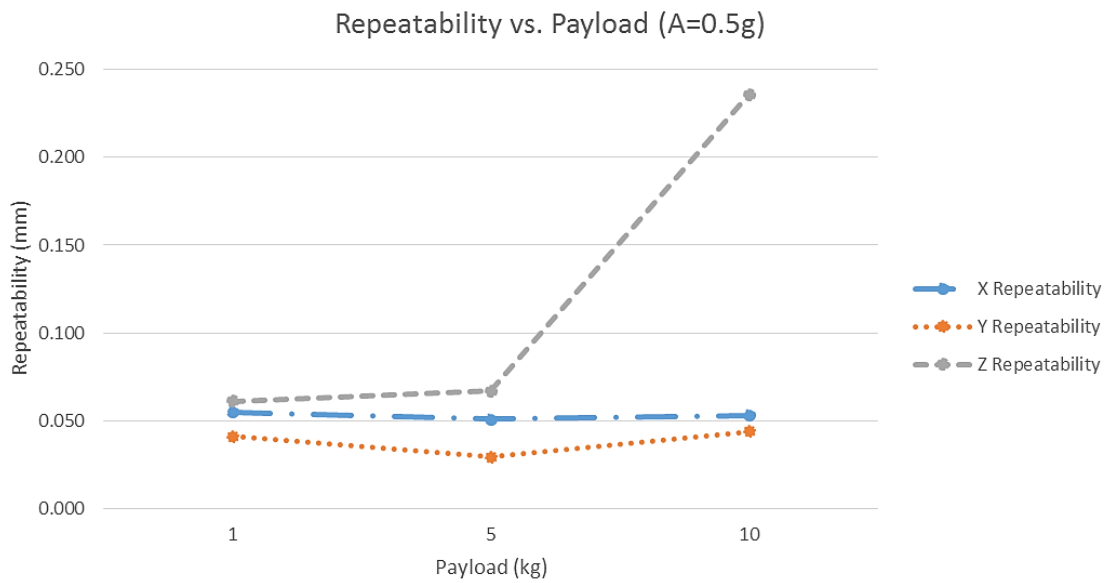


Fig. 44. Plot of Payload vs. Repeatability with acceleration constant at 0.2g.

10.1.2 Repeatability versus Acceleration

The UR10 has a safety feature that automatically stops the arm from moving when any link in the arm experiences a force of 150 Newtons. Based on this feature, the tool tip could reach a maximum acceleration of 1.0g before the tool's inertia caused a force in excess of 150 N (with max payload). Therefore the repeatability of the UR10 was calculated as a function of 0.2, 0.5, and 1.0g.

The data shows that repeatability deteriorates as acceleration increases for all directions. With a payload of 1 kg, the X direction repeatability increased from 0.055 to 0.201 mm; the Y direction repeatability increased from 0.041 to 0.063 mm; and the Z direction increased from 0.061 to 0.162 mm when the acceleration was increased from 0.2 to 1.0 g. These results show that only Y direction repeatability remains within the UR10's specifications at maximum acceleration. The worst case repeatability was 0.285 mm for the Z Direction with maximum payload and acceleration.

Fig. 45 shows a plot of the UR10's repeatability as a function of acceleration for the X direction, showing the trend of increasing repeatability with increasing acceleration.

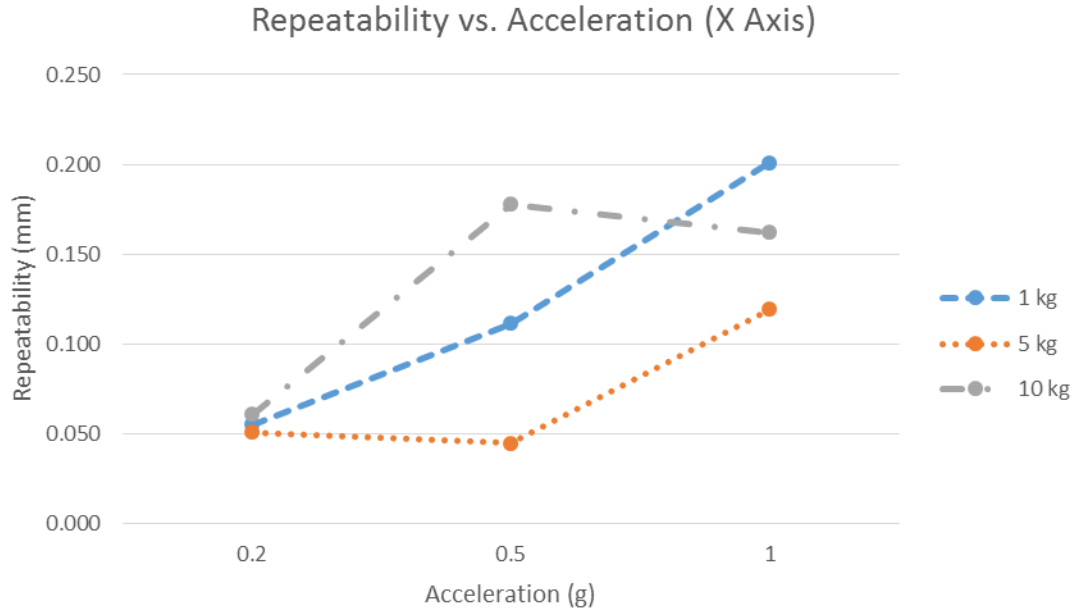


Fig. 45. Repeatability as a function of acceleration in the X Direction.

10.2 Statistical Analysis

The UR10 performs as indicated by Universal Robots for payloads below 5 kg and accelerations below 0.5g. These results indicate that for procedures in agreement with manufacturer's recommended speeds for the UR10, the UR10 will perform with a repeatability better than 0.1 mm.

A full statistical analysis is necessary to support the results found in the preliminary analysis of the UR10. The number of necessary tests requires assumptions for the risk of rejecting a true value and the risk of accepting a false null value during each test [Petrucelli et. al., 1999]. To establish a 95% confidence level in the relationships established in section "8.1 Repeatability Parameters," Eq. 10.1 should be used.

$$\delta = \frac{\sigma}{\sqrt{N}} * Z_{95\%} \quad (10.1)$$

The number of samples, N, then depends on the mean of the samples, standard deviation of the samples, and critical value from the normal distribution (z). For a 95% confidence interval, we have Eq. 10.2 and 10.3, which respectively calculate the critical value from the normal distribution and the number of samples required.

$$1 - \frac{\alpha}{2} = 0.975, z = 1.96 \quad (10.2)$$

$$N \geq \left(\frac{1.96}{\delta}\right)^2 * \sigma^2 \quad (10.3)$$

Based on the calculation of Eq. (10.2) and (10.3) using the mean and standard deviation from the preliminary tests, each test should be run two more times, for a total of 24 more tests. Based on the relationships described in “8.1 Repeatability Parameters,” two more tests would yield a 95% confidence level of any single data point being within one standard deviation of the mean repeatability values shown in Table 6.

11. Conclusions and Recommendations

The development of the Direct Contact Method was able to prove that collaborative robotic repeatability can be measured using a uniaxial displacement sensor. The uses of MEMS accelerometers allowed the selection of an appropriate sampling rate to accurately characterize the position of the UR10 using the fixture and gauge block designed by the project team.

The accompanying LabVIEW and MATLAB software accurately collected and analyzed data, leading to characterization of the UR10's repeatability as functions of payload and acceleration. Based on the results in "8.1 Repeatability Parameters," the UR10 meets the manufacturer's tolerances for all cases with accelerations below 10 kg for the X and Y directions, but does not meet manufacturer's tolerances in the Z direction when the payload is above 5 kg and/or when the acceleration is set above 0.5g.

The project team's recommendations would be to use the UR10 for high precision applications only when the UR10's acceleration is below 0.5g to avoid the loss of repeatability in the Z direction. Furthermore, the payload of such applications should remain below 5 kg if possible.

The next step in the development of the Direct Contact Method is to refine the method such that it can be used to evaluate other robots.

11.1 Future Work

The bulk of this project was focused on the development and verification of the Direct Contact Method for evaluating the repeatability of collaborative robots. The results of the UR10's analysis prove the feasibility of the DCM, but the method requires further development before it

can be applied to other robots. Improvements to the DCM could be broken into refinements to the hardware used in the method and the actual measurement process itself.

11.1.1 Refinement of Hardware

The fixture is designed specifically to mount to the UR10 as a single unit - a universal sensor housing should be developed. Such a housing would be able to mount to an adapter plate that contains the bolt housing bolt pattern/pilot on one side, and the required mounting configuration of the robot to be tested on the other side. Other methods such as a housing that only needs to be held by a robot's gripper could also be investigated.

The gauge block could be improved if a suitable third party block with appropriate surface finish and dimensional certification were found. Such a block would allow the testing of multiple locations within the robot's work space without the need to machine and measure surface finish in house.

Alternatively to the improvements described above, two cantilever displacement measuring systems could be added to the sensing fixture to reduce testing time. The LVDT would remain along the robot tool's Z axis, with the two cantilever sensors measuring displacement along the X and Y axes, respectively. Such a system would allow the testing of all three axes simultaneously, cutting testing time by 67%. If this development were implemented, the gauge block would have to be redesigned to provide contact points for all three sensors simultaneously. Furthermore, the Data Acquisition system would need two additional analog input channels for processing the three voltages.

11.1.2. Refinement of Software

The method itself could be improved with a robot program that incorporates the geometry of the gauge block such that the robot only needs to be taught the first position – the program would include offsets for all other motions based on the preliminary coordinates. The measurement method could also be combined with the robot in question's characteristic Denavit-Hartenberg parameters [Spong, 1989] as well as MEMS accelerometers to develop a full theoretical and experimental dynamic model.

11.1.2.1 Analysis of Measurements vs. Denavit-Hartenberg (DH) Parameters

The DH parameters are a standardized method for evaluating the coordinate transformation from the base to the tool tip of a multi-jointed (multiple degrees of freedom) robot. Such a method allows the determination of the tool tip coordinates in the base (global) coordinate system using the angles of each of the joints in the robotic arm. The DH parameters also allow the characterization of dynamic properties by incorporating inertia, momentum, and forces/torques applied to the robot [Spong, 1989].

The DH parameter calculations performed by the project team were not successful in determining the forward kinematics of the UR10's tool tip nor was the method successful in calculating the inverse kinematics. The further development and troubleshooting of the DH parameters would allow the combination of theoretical and measured repeatability to form a more accurate model for the UR10. The DH parameters and matrix transformation for the forward kinematics of the UR10 can be found in Appendix J.

11.1.2.2. Addition of Vibration Measurements

The addition of MEMS accelerometers to the LVDT fixture would allow the characterization of vibrations that occurred during repeatability measurements. These vibrations could be used to diagnose any potential changes in repeatability that occurred within a test or at certain positions within a robot's workspace.

11.2 Vision for the Direct Contact Method

This report described the development of the Direct Contact Method as a means for measuring collaborative robotic arm repeatability. The design process involved the comparison of state of the art methods for evaluating positional repeatability; selecting appropriate methods and metrology equipment; calibrating and implementing the LVDT; designing, optimizing, and fabricating the necessary fixture and gauge block; developing accompanying LabVIEW and MATLAB programs; implementation and testing of the DCM using the UR10; and analyzing the repeatability data to confirm the manufacturer's specifications for the UR10.

The final deliverables to the sponsor were the full DCM method package- including hardware, software, and a User Manual; a characterization of the UR10's repeatability as functions of payload and acceleration; and further recommendations for development of the DCM such that other robots can be evaluated before purchase.

The use of the UR10 allowed a demonstration of the Direct Contact Method's feasibility for evaluating collaborative robot repeatability. It is the project team's hope that the method developed in this report will be of use to the sponsor and that further development of the DCM will lead to increased implementation of low cost repeatability measuring solutions.

12. References

- [1] Universal Robots. <http://www.universal-robots.com>, Last Accessed April 2014.
- [2] ISO 9283. International Organization for Standardization, 1998.
- [3] ISO 13309. International Organization for Standardization, 1995.
- [4] Thomas, F. and Ros, L., “Revisiting Trilateration for Robot Localization,” *IEEE Trans. Robotics*, 21(1): 93-101, 2005.
- [5] Mirrorcle Technologies. <http://www.mirrorcletech.com>, Last Accessed April 2014.
- [6] Nyquist Frequency. *Cambridge Dictionary of Statistics*, Cambridge University Press, UK 2002.
- [7] Khanlou. <http://www.khanlou.com>, Last Accessed April 2014.
- [8] The Student Room. <http://www.thestudentroom.co.uk>, Last Accessed April 2014.
- [9] Analog Devices. <http://www.analog.com>, Last Accessed April 2014.
- [10] Omega. GP911-2.5s LVDT, <http://www.omega.com>, Last Accessed April 2014.
- [11] Microstrain. SG-DVRT-8mm, <http://www.microstrain.com>, Last Accessed April 2014.
- [12] Petrucci, J., Nandram, B., Chen, M., *Applied Statistics for Engineers and Scientists*, Pearson, 1999.
- [13] Spong, M.W., *Robot Dynamics and Control*, Ch. 3-4, John Wiley and Sons, 1989.
- [14] Digikey. <http://www.digikey.com>, Last Accessed April 2014.
- [15] IMU. <http://www.wikimedia.org>, Last Accessed April 2014.

Appendix B: Repeatability Methods Detailed Descriptions

MEMS Mirrors in 3D tracking application

How are we going to build it?

The MEMS mirrors system is comprised of two gimbal-less dual-axis micro-mirror scanners with integrated mirrors, a NI USB DAQ-version 4-channel high voltage amplifier, a 5mW red laser, a field programmable gate array (FPGA) board, 2 wide angle lenses, a photo-detector, tracking software, and a laptop.

How are we going to integrate it into different positions?

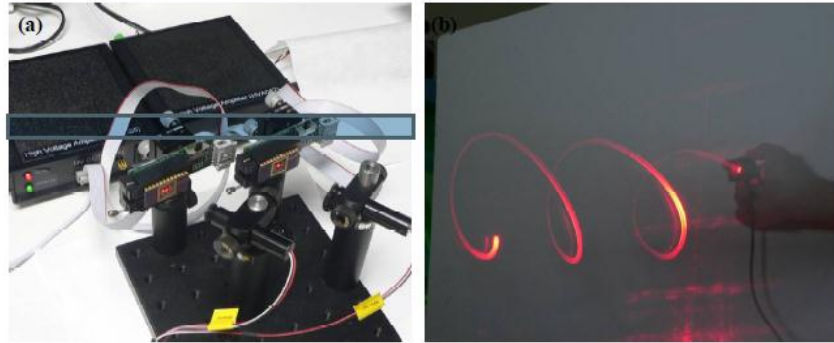
The MEMS mirror tracking system tracks a photo-detector in a specified field of view, on one plane. An end effector containing multiple (3-4) photo-detectors perpendicular to each other could be incorporated to allow for tracking of the robot when it is facing different planes. Additionally, the system is a mobile system and can be picked up and moved to different positions with ease.

How are we going to calibrate it?

First the lasers must be modulated to continuously alternate. This calibration can be done through programming software which accompanies the laser and the FPGA board.

The next step is to calibrate the photo-detector. The photo-detector is a 4-quadrant detector which means it has 4 quadrants which provide additional information such as the position of the laser on the detector. The detector and mirrors can then be programmed and calibrated using a LabVIEW code to signal the system when the laser is centered on the target.

How are we going to use it?



The system works by reflecting a laser off each micro-mirror through a wide angle lens into a common volume. Through the use of tracking software, both mirrors search in a spiral pattern from their origin (0 degree tilt) to maximum angles (up to 45 degrees when incorporating a wide angle lens). When a 4 quadrant photo-detector comes into the field of view it relays a signal to the FPGA board when it detects a laser. Since the photo-detector can only detect one laser at a time the system is time-multiplexed by laser modulation. This means that the lasers are continuously alternating.

Once the photo-detector has relayed a signal to the FPGA board, the system instantaneously records the angle of the device's x and y-axis in open-loop output values O_{X1} and O_{Y1} through the use of the high voltage amplifiers. Since the system is time-multiplexed, the second device then provides an additional set of open loop angles O_{X2} and O_{Y2} . These angles are then used to calculate a Z position.

How are we going to analyze the data it produces?

Using the output angles from the system and the following equations we can find the position of the photo detector with

$$Z = \frac{d \cdot K}{\tan(\theta_{\max})} \cdot \frac{1}{(O_{x1} - O_{x2})}$$

With Z known, X and Y are found from known parameters and by averaging from two devices' readings:

$$X = (O_{x2} + O_{x1}) \cdot Z \cdot \tan(\theta_{\max}) / (2K) = \frac{d}{2} \frac{(O_{x2} + O_{x1})}{(O_{x1} - O_{x2})}$$

$$Y = (O_{y2} + O_{y1}) \cdot Z \cdot \tan(\theta_{\max}) / (2K) = \frac{d}{2} \frac{(O_{y2} + O_{y1})}{(O_{y1} - O_{y2})}$$

These equations can be integrated into the system to continuously calculate the position of the end effector.

Cable Trilateration Method (CTM)

General Overview: The cable trilateration method uses the lengths of various cords attached to the tool tip of a robot (End Effector) to determine the tool tips location in 3D space.

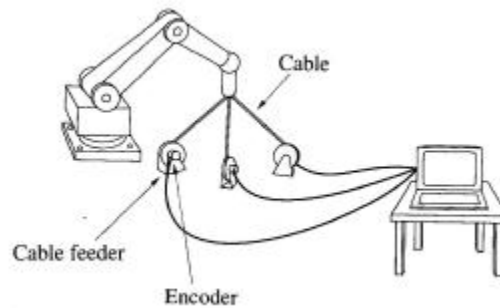


Fig. 46: ISO technical report [ISO 13309, 1995].

How are we going to build it?

The cable trilateration method typically uses a three or four pulley systems with optical encoders attached to measure the length of cables originating from each pulley. To build the system we would have to construct the pulleys with minimized cable slippage and minimized constant tension on each cable as to not add undue load on the robot's tool tip. Providing we could

achieve these characteristics, the pulleys are relatively simple in that they need only be free to rotate around a vertical axis (in addition to the pulley's own horizontal axis rotation) to track the robot without becoming entangled. Furthermore, each pulley must have an optical encoder attached to it by means of a shaft that rotates with the pulley such that the rotational position of the pulley is always known. The length of the cord is equal to the radius of the pulley multiplied by the number of revolutions of the pulley.

How are we going to integrate it into different positions?

The cable trilateration method can measure any number of points and is capable of recording path of motion as well as assessing positional repeatability. To integrate the CTM to record multiple positions we would simply have to teach/program the robot to go to multiple positions, the cable system does not require any extra effort to measure additional points as it constantly measures and plots the tool tip's position in space.

How are we going to calibrate it?

The typical calibration method requires two steps:

- 1) Calibrating the encoders – the pulleys must be placed in an approximately equilateral triangle in the robot's workspace. The cord of each pulley must be pulled to the adjacent pulley in order to measure and record the distance between each of the pulleys.
- 2) Robot Calibration – the cords must be attached to the robot's tool tip, then the robot must move through many (~50) points in its workspace while the CTM system measures position. The system then compares the robot's measured position to the CTM true position to establish a filter to account for any kinematic inaccuracies of the robot

How are we going to use it?

We would use a CTM system to characterize the repeatability of the robot according to ISO9283. The CTM method is capable of performing all of the tests in ISO9283, but we would only need to perform the pose repeatability tests. Typically, these involve measuring the repeatability at 5 unique positions approached from 3-directions, which could easily be accomplished using a CTM system.

How are we going to analyze the data it produces?

Commercial software is capable of directly outputting the results of tests such as those described in ISO9283. Furthermore, typical software shows a plot of the robot's position and 3-D coordinates in the form of (x,y,z) in real time. To that end, whether we design or purchase software for a CTM system, we would be able to output position and repeatability as well as path of motion.

Ultrasonic Trilateration Method

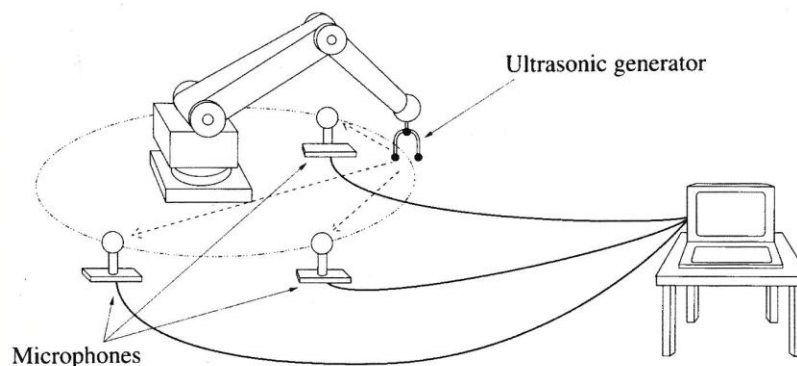


Fig. 47. Ultrasonic Trilateration Method as described in ISO 13309 [ISO 13309, 1995].

Above is the schematic sketch of Ultrasonic Trilateration Method. The position in 3D can be calculated with distance data from 3 stationary ultrasonic microphones which receive ultrasonic pulse trains from a sound source mounted on the robot.

If the orientation of robot needs to be measured, 3 independent sound sources are needed and each microphone can detect pulse trains from all 3 sources.

How are we going to build it?

Ultrasonic microphones and ultrasonic sound sources are going to be purchased from vendors.

Microphone mounts and tool tip that mounts ultrasonic generators will be manufactured

How are we going to integrate it into different positions?

The ultrasonic sound source will be mounted to the robot tool tip, and 3 microphones are stationary. They are capable to measure the pulse trains from the workspace. (Non-modular)

How are we going to calibrate it?

The system requires the calibration of both the sound source and the microphone. The results of distance value received by microphone from the source on same location need to be repeatable.

Results between different microphones and different sound sources also need to be repeatable.

The microphones are Directional, and diffraction becomes important when a physical object is about $\frac{1}{4}$ wavelength in size or larger. For 20 kHz, $\frac{1}{4}$ wavelength is about 4 mm, so the workspace needs to remain same condition. Sound intensity decreases by 6 dB with each doubling of distance from a point source. Ultrasound also loses energy quickly due to absorption effects, with absorption increasing along with frequency and humidity. For higher humidity, losses can reach over 3 dB/m at frequencies of 80 kHz [Digikey, 2014]. An ordinary tweeter component may be adequate for measurements up to 50 kHz.

How are we going to use it?

Such system can measure all required characteristics with a resolution: 0.05 – 1 mm, repeatability: 0.2 – 1 mm, Accuracy: 0.4 – 3 mm, and dynamic measuring sampling rate: 100 – 1000 ms/point. After building and calibrating such system, measurements need to be done in the same environment conditions and microphone configurations.

How are we going to analyze the data it produces?

Following the ISO9283 standard, the position (and orientation) data will be used directly into the equations provided by ISO9283, finding the required characteristics on the required points.

Inertial Measurement Unit (IMU)

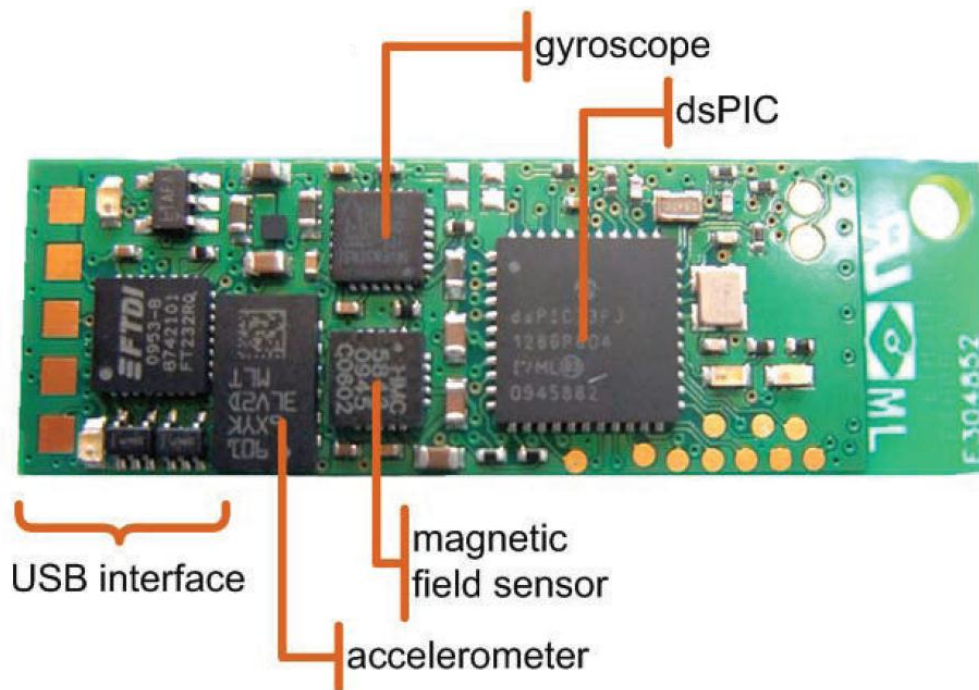


Fig. 48. Typical IMU system [Wikimedia, 2014].

How are we going to build it?

With the inertial measurement unit (IMU) we would only have to build our own if the ones on the market are not accurate enough for our price range.

In order to build an IMU multiple accelerometers and gyroscopes are needed. In order to track the position you need to measure the robot in the X, Y, and Z position as well as the roll, pitch, and yaw. All of these components would then be attached to a circuit board and which would go in a protective case.

How are we going to integrate into different positions?

The robot will be able to pick up this case and where ever it moves it will be tracked continuously. The only problem with this is there will be drift involved through the integrations from acceleration to position.

How are we going to calibrate it?

Calibration would be as simple as picking a position knowing where the robot thinks it is and setting the IMU to zero.

How are we going to use it?

From here the robot will be tracked and the IMU will output a position which can be related to where the robot thinks it is. From our calculations the repeatability is within 10 microns with an accuracy of 30 microns.

How are we going to analyze the data?

This data will be stored on a micro SD card on the circuit board which can be removed and put into a computer. This data can be uploaded to MATLAB, LabVIEW, or Microsoft Excel. After the data gathered on the SD card is uploaded the only thing left to input is the original coordinates of the robot that was used in calibration. The program will be able to relate the robots calibrated coordinates to the zero position of the IMU. The tracking of the IMU can then

be related back to where the robot thought it was. This will then tell us the accuracy and repeatability of the robot.

Appendix C: Method Evaluations Criteria and Equations

Evaluation Criteria

- **Cost:** If the cost is \$0 - \$5,000 award a score of 100.
 - If the cost is greater than \$5,000 use the following equation:

$$Score = 100 - \left[10 * \frac{Estimated\ Cost - 5000}{1000} \right]$$

- **Resolution:** If the resolution is less than or equal to 10µm award a score of 100.
 - If resolution is less than 10µm use the following equation:

$$Score = 100 - [5 * (Estimated\ Resolution - 10)]$$

- **Repeatability:** If the repeatability is less than or equal to 10µm award a score of 100.
 - If repeatability is less than 10µm use the following equation:

$$Score = 100 - [5 * (Estimated\ Repeatability - 10)]$$

- **Accuracy:** If the accuracy is less than or equal to 10µm award a score of 100.
 - If accuracy is less than 10µm use the following equation:

$$Score = 100 - [5 * (Estimated\ Accuracy - 10)]$$

- **Mobility:**
 - Score of 100 = Quick and easy to move, requires one person
 - Score of 50 = Moderately easy to move, may require more than 1 person
 - Score of 0 = Not mobile, fixed, requires more than one person to move
- **Start-up:** The following criteria was evaluated and assigned a score based on our perceived and projected difficulty of each task:
 - Number of calibrations needed to ready device (0,1,2...10)
 - Amount of training required
 - Required set up time is less than 1 hour or greater 1 hour
- **Degrees of Freedom (DOF):** $Score = \frac{Number\ of\ Degrees\ of\ Freedom}{6} * 100$
- **Software:** The following criteria was evaluated and any score landing in between the following values was evaluated by our perceived difficulty:
 - Score of 100 = Sensor/System comes with fully operational, out of box software
 - Score of 50 = Sensor/System comes with graphical user interface or equivalent software but requires programming or calibration in LabVIEW/MATLAB etc.
 - Score of 0 = No software is provided and the system requires extensive coding/programming

The following table lists the characteristics of each of the methods that were evaluated.

System	Cost	Resolution	Repeatability	Accuracy	Mobility	Start-Up Process	DOF	Software
LTCs	\$7,000 *see note at bottom*	\leq pixel size	\leq pixel size	\leq pixel size	Easy to pick up and move, consists of stationary cameras, an end effector, and laptop/computer	Calibrate cameras, align lasers calibrate accelerometer	6	No software besides camera GUI, will have to program our own software using LabVIEW/Matlab
UTM	$< \$1000$	0.05 – 1 mm	0.2 – 1 mm	0.4 – 3 mm	Easy to move around: 3 microphones, laptop, generator on tool tip	Set up microphones, laptop, and generator on manufactured tool tip; calibration of system measurement	3 – 6	Software to convert microphone signal to distance; then Matlab to position
CTM	\$1,500	10 μ m	20 μ m	300 μ m	Three pulleys, which must be mounted to the floor/test bed and a computer	Place pulleys in work space, calibrate encoders, attach to robot, calibrate to robot	3	Commercially available. Our own would use trilateration method extrapolated from encoder voltages and pulley geometry
MEMS Mirrors	\$9,000	$\leq 20\mu$ m	$\leq 20\mu$ m	$\leq 20\mu$ m	Light compact, two mirrors mounted to a board and an end effector that's attached to the robot	Align to field of view, align and measure distance between mirrors calibrate mirrors using photo-detectors, begin search pattern, activate photo-detector	4	Comes with a GUI and additional programmable software, can be calibrated and programmed when manufactured
IMU	\$1,000	3 μ m	-	4 μ m	Easy to pick up and move, Consists of one unit that is picked up by the robot	Requires calibration of the IMU (Accelerometers and Gyroscopes)	6	Software available compatible with matlab, LabVIEW, Microsoft Excel
Direct Contact	$< \$5,000$	$< 10\mu$ m	Same as resolution	Same as resolution	Easy to pick up and move, consists of stationary contact sensors, an end effector, and laptop/computer	Align contact sensors at end position and calibrate with zeroed deformation	3	Nearly complete software available compatible with external programs

*The cost of the LTCs system is our projected worst case scenario based upon recent research and quotes.

Appendix D: Accelerometer Specifications and LABVIEW Program

Two ADXL276 dual-axes accelerometers were used for the accelerometer experiment. Fig. 49 and Fig. 50 show the axes layout of the accelerometers and corresponding specifications. Fig. 51 and Fig. 52 show the front panel and block diagram of the LabVIEW program developed to characterize vibrations of the UR10.

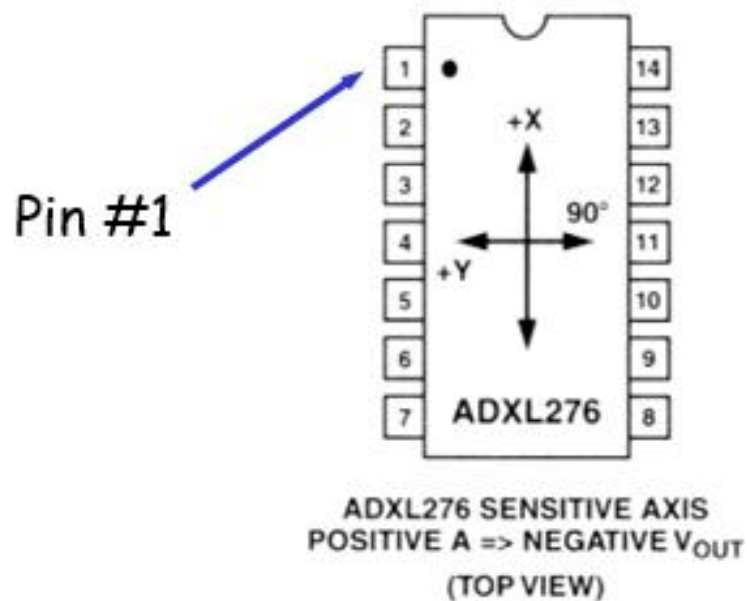


Fig. 49. Accelerometer diagram [Analog Devices, 2014].

ADXL76, ADXL269, ADXL276—SPECIFICATIONS

(@ $T_A = -40^{\circ}\text{C}$ to $+85^{\circ}\text{C}$, $V_S = 5\text{ V} \pm 5\%$, Acceleration = 0 g ; unless otherwise noted)

Parameter	Conditions	ADXL76Qs 18 ¹			ADXL269Qs 38 ²			ADXL276Qs 55 ³			Unit
		Min	Typ	Max	Min	Typ	Max	Min	Typ	Max	
SENSOR	Guaranteed Full-Scale Range	ADXL76 Only, Offset Adjusted ⁷ ADXL76 Only, Offset Adjusted									g g g g g
		± 115 ± 105			± 50 ± 45			± 35 ± 30			
	Nonlinearity				0.2						%
	Package Alignment Error ⁴				± 1						Degrees
	Sensor-to-Sensor Alignment Error Transverse Sensitivity ⁵	ADXL276, ADXL269			0.1 ± 2						Degrees %
SENSITIVITY	Sensitivity	18			38			55			mV/g
	Sensitivity Tolerance ^{5,6}	Ratiometric			-8 +8						%
	Temperature Drift	From 25°C to T_{MIN} to T_{MAX}			± 0.5						%
ZERO-g OFFSET LEVEL Output Zero-g Voltage ^{6,7} Temperature Drift	Offset from $V_S/2$ From 25°C to T_{MIN} to T_{MAX}	-198 3.6 +198			-418 7.6 +418			-605 11 +605			mV mV
ZERO-g ADJUSTMENT Voltage Gain Input Resistance Input Resistor Network Ratio %:1	$\Delta V_{\text{OUT}}/(\Delta V_{\text{ADJ}})_{\text{PIN}}$				0.45 0.5 0.55						V/V
					20 30 40						k Ω
					± 0.1						%
NOISE PERFORMANCE	Noise Density	10 Hz to Nominal Bandwidth			4 12			1 3			$\text{mg}/\sqrt{\text{Hz}}$
	Clock Noise	See Figure 18			5			1 3			mV p-p
FREQUENCY RESPONSE -3 dB Frequency ⁸ Bandwidth Temperature Drift Sensor Resonant Frequency	Bandwidth Options: See Ordering Guide				-10 +10						% Hz kHz
	Q = 5				20 24						
SELF-TEST ⁹ Output Change Logic "1" Voltage Logic "0" Voltage Input Resistance	@ 5 V	135 180 270			285 380 570			413 550 825			mV V V k Ω
					3.5 1.0						
	To GND				30 50						
OUTPUT AMPLIFIER Output Voltage Swing Capacitive Load Drive	$I_{\text{OUT}} = +100\text{ }\mu\text{A}$ $I_{\text{OUT}} = -100\text{ }\mu\text{A}$				$V_S - 0.25$ 0.25						V V pF
					1000						
POWER SUPPLY (V_S) Operating Voltage Range Functional Voltage Range Quiescent Supply Current					4.75 4.0 5.25						V V mA mA
					18 3 3.5 5						
TEMPERATURE RANGE ¹⁰					-40 +85						$^{\circ}\text{C}$

NOTES

¹For example, ADXL76Qs18 describes devices with a nominal sensitivity of 18 mV/g. See Ordering Guide for full part number.

²Trimmed at the factory to user specifications. May require 0-g adjust circuitry. Reference section on Zero-g Adjustment and Dynamic Range.

³Alignment error is specified as the angle between the true axis of sensitivity and the edge of the package.

⁴Transverse sensitivity is measured with an applied acceleration that is 90 degrees from the indicated axis of sensitivity.

⁵Ratiometric: $V_{\text{OUT}}(\text{accel}, V_S) = [V_S/2 \pm (a V_S/5\text{ V})] + [(a \text{ accel})(b V_S + c V_S^2)(1 \pm 0.08)]$ where a = offset range in volts. For a 38 mV/g sensor: $b = 5.725 \times 10^{-3}$ 1/g, $c = 0.375 \times 10^{-3}$ 1/g². (For a 55 mV/g sensor: $b = 8.284 \times 10^{-3}$ 1/g, $c = 0.542 \times 10^{-3}$ 1/g². See Figures 5 and 13. Spec includes temperature drift, life drift, and nonlinearity. Test conditions: 100 Hz, $\pm 50\text{ g}$ for the 38 mV/g and 18 mV/g sensor; 100 Hz $\pm 35\text{ g}$ for the 55 mV/g sensor.

⁶Error included in full-scale range specification.

⁷Proportional to $V_S/2$. See Figures 6 and 19.

⁸Includes Temperature Drift.

⁹ST pin from Logic "0" to "1." For the ADXL76: V_{OUT} change = $(V_{\text{OUT}}$ change @ 5 V) $\times (V_S/5\text{ V})$. For the ADXL269 and the ADXL276: V_{OUT} change = $(V_{\text{OUT}}$ change @ 5 V) $\times (V_S/5\text{ V})^2$.

¹⁰A higher temperature range available.

Specifications subject to change without notice.

Fig. 50. Accelerometer specifications table [Analog Devices, 2014].

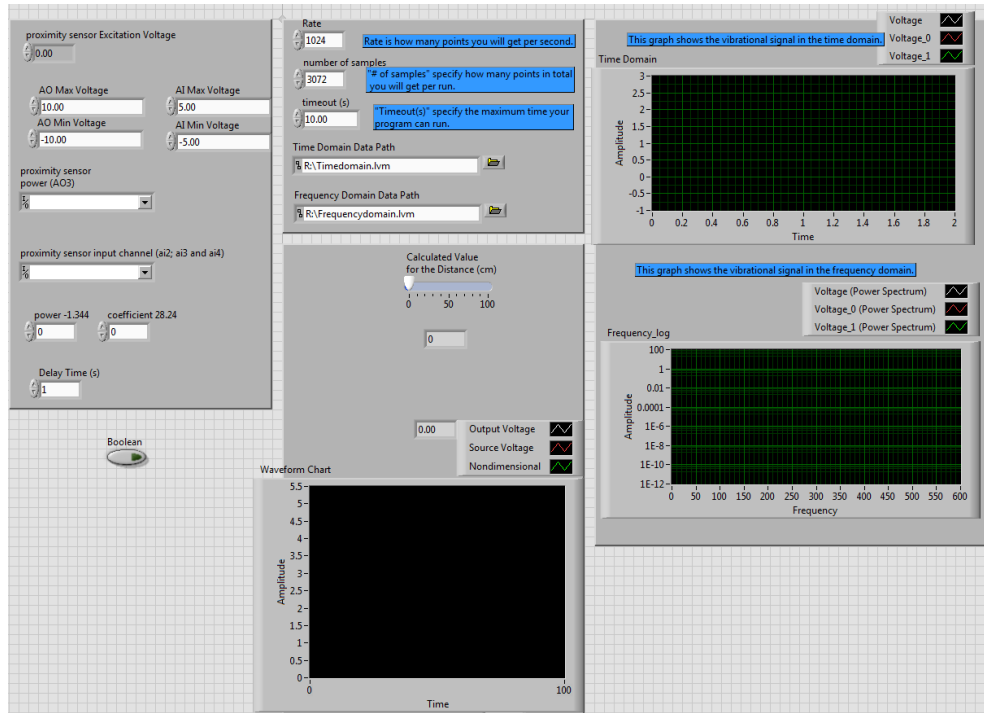


Fig. 51. Front panel of the LabVIEW program that was developed to characterize vibrations of the UR10.

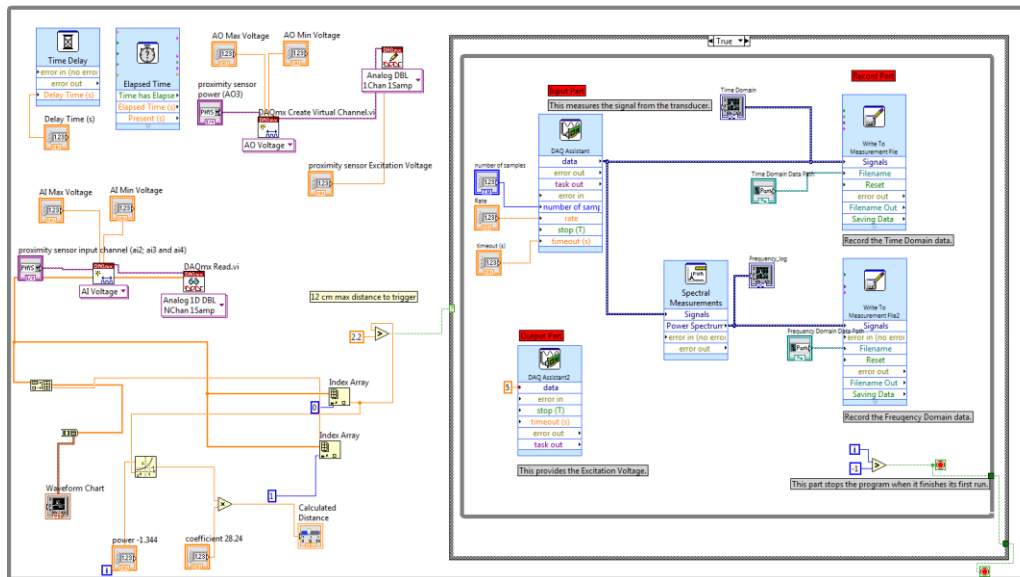


Fig. 52. Block diagram of the LabVIEW program that was developed to characterize vibrations of the UR10.

Appendix E: Sensor Evaluation Criteria

Criteria for Displacement Transducer Evaluation:

- Cost (10)
- Resolution (5)
- Repeatability (10)
- Measurement Range (10)
- Signal Conditioning (15)
- Signal Output (10)
- Signal to Noise ratio (15)
- Shipping Time (20)
- Mount Type (5)

Formulas for each criteria:

- Cost $\rightarrow 100 - 10 * (\text{Estimated Cost} / \$500)$
- Resolution $\rightarrow 100 - 5 * (\text{Resolution in microns})$
- Repeatability $\rightarrow 100 - (\text{Repeatability in microns})$
- Measurement Range $\rightarrow 50 * (\text{Range} / 2\text{mm})$ must be less than or equal to 100
- Signal Conditioning \rightarrow Internal=100; external=85; separate=50; none=0
- Signal Output \rightarrow signal directly to DAQ=100; need interface=50
- SNR $\rightarrow 100 - (1/\text{SNR}) * 1000$, not less than 0
- Shipping Time $\rightarrow 100 - 10 * (\text{each week of delivery time})$
- Mount Type \rightarrow Threaded=100; Clamp = 75

Appendix F: Student's t-Test for OMEGA and MicroStrain Transducer Verification

Use of t-Student's test to determine the significance of a quadratic term in a least-squares fitting. *Do we really need a quadratic term? Is a linear fit sufficient?*

Generate least squares matrices:

$$M := X^T \cdot X \quad M_i := M^{-1} \quad U := M_i \cdot (X^T \cdot Y)$$

Solution (coefficients):

$$U = \begin{bmatrix} 1 \\ 0.0001 \\ 0.0001 \end{bmatrix}$$

Model is: $y(z) := U_0 + U_1 \cdot z + U_2 \cdot z^2$

t-Test:

Sum of the square of the errors, determined from least squares equations:

$$SCE := Y^T \cdot Y - U^T \cdot X^T \cdot Y = 0.457$$

Degrees of freedom (DOF) for t-distribution:

$$n := 5 \quad (\text{Five data points})$$

$$\nu := 3 \quad (\text{Number of coefficients in the model})$$

$$DOF := n - \nu = 2$$

Estimated standard deviation:

$$s := \sqrt{\frac{SCE}{DOF}} = 0.478$$

Example plot of Determination of +/- ranges for slope and dc offset using probability approach (Student T-Test). Red and blue dashed lines, seen in Fig. 53, denote upper and lower limit for a confidence of 95%. The solid black line denotes the actual linear fitting.

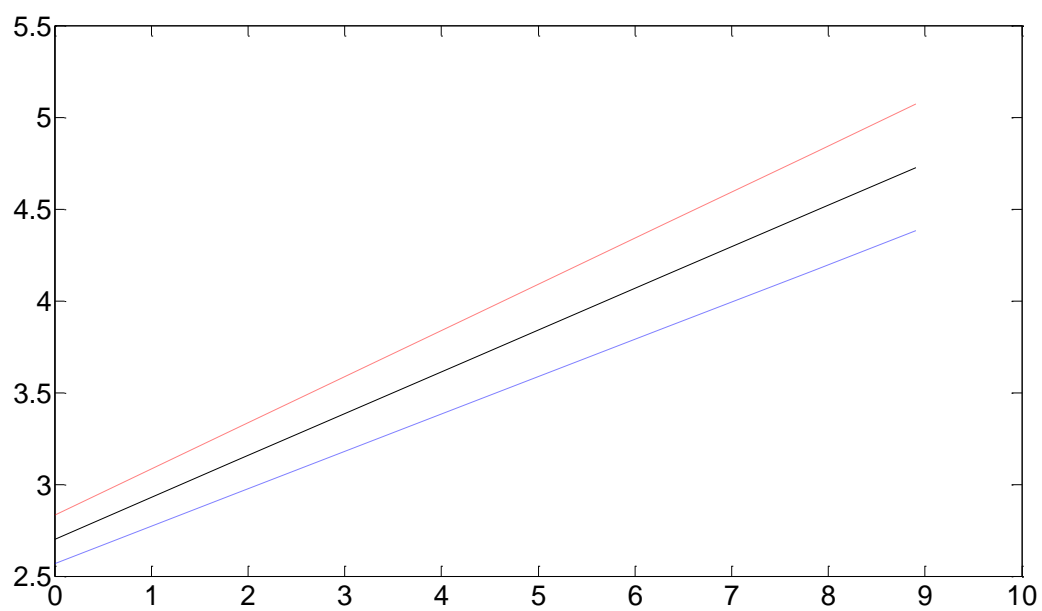
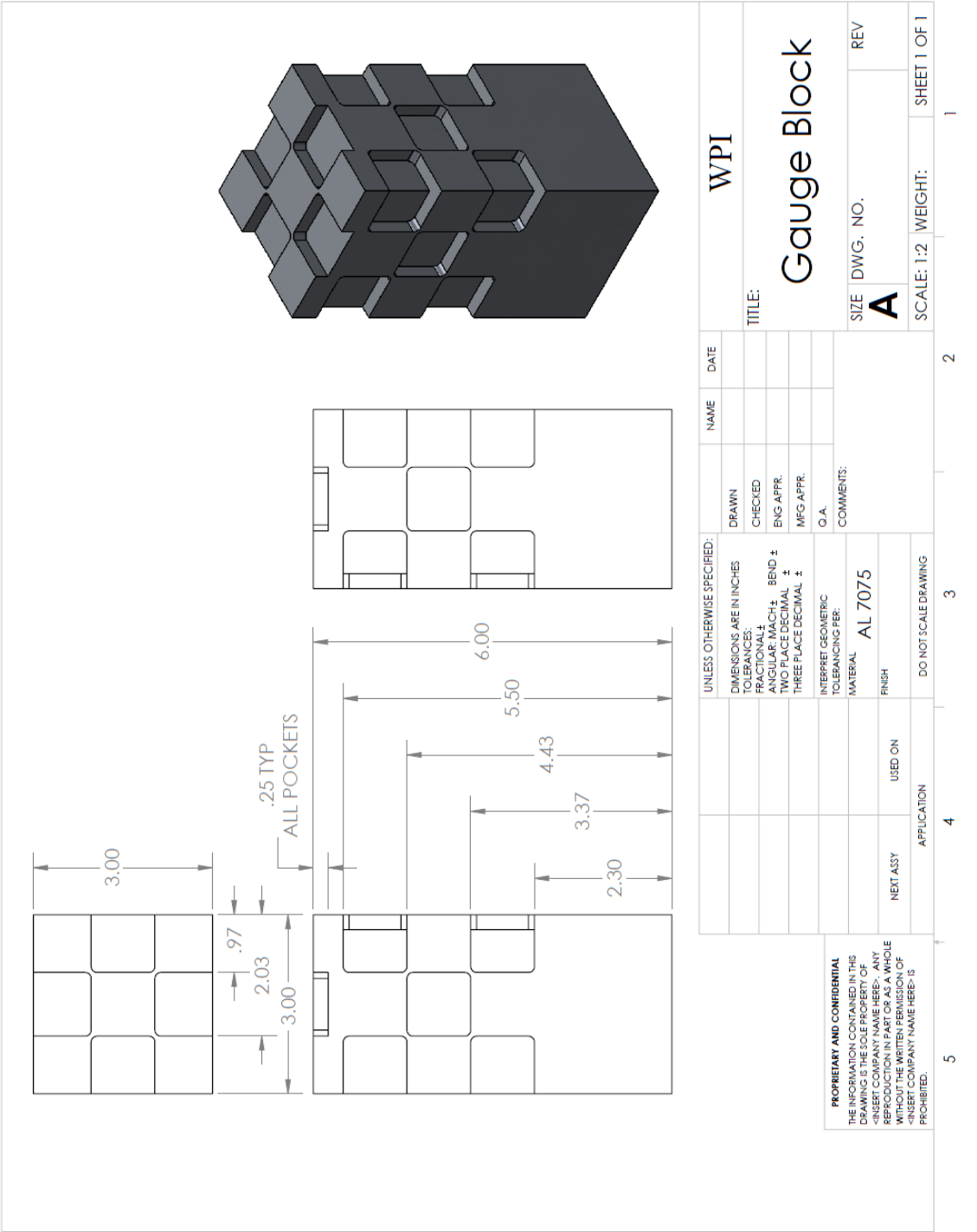
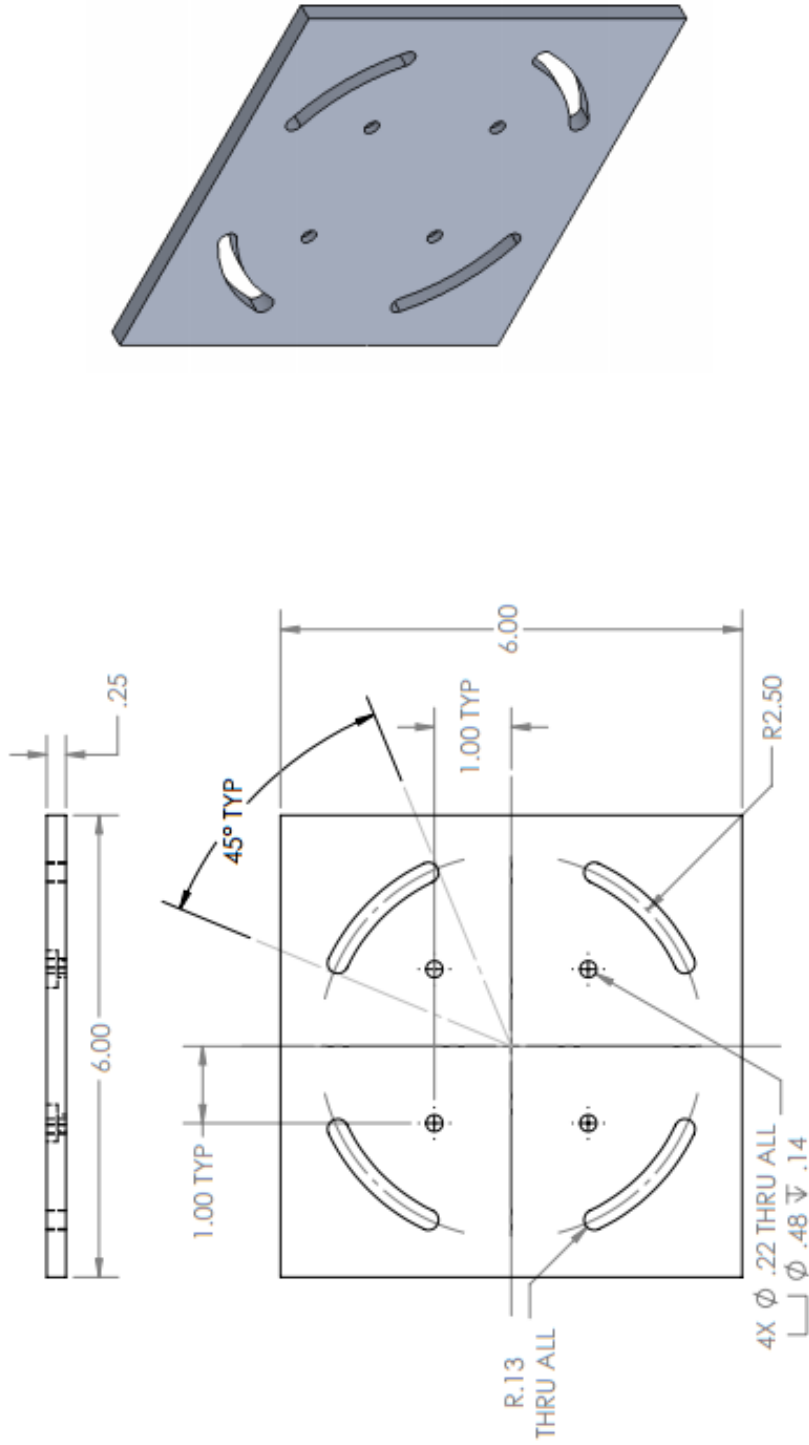


Fig. 53. Example of 95% confidence intervals for linear fitting.

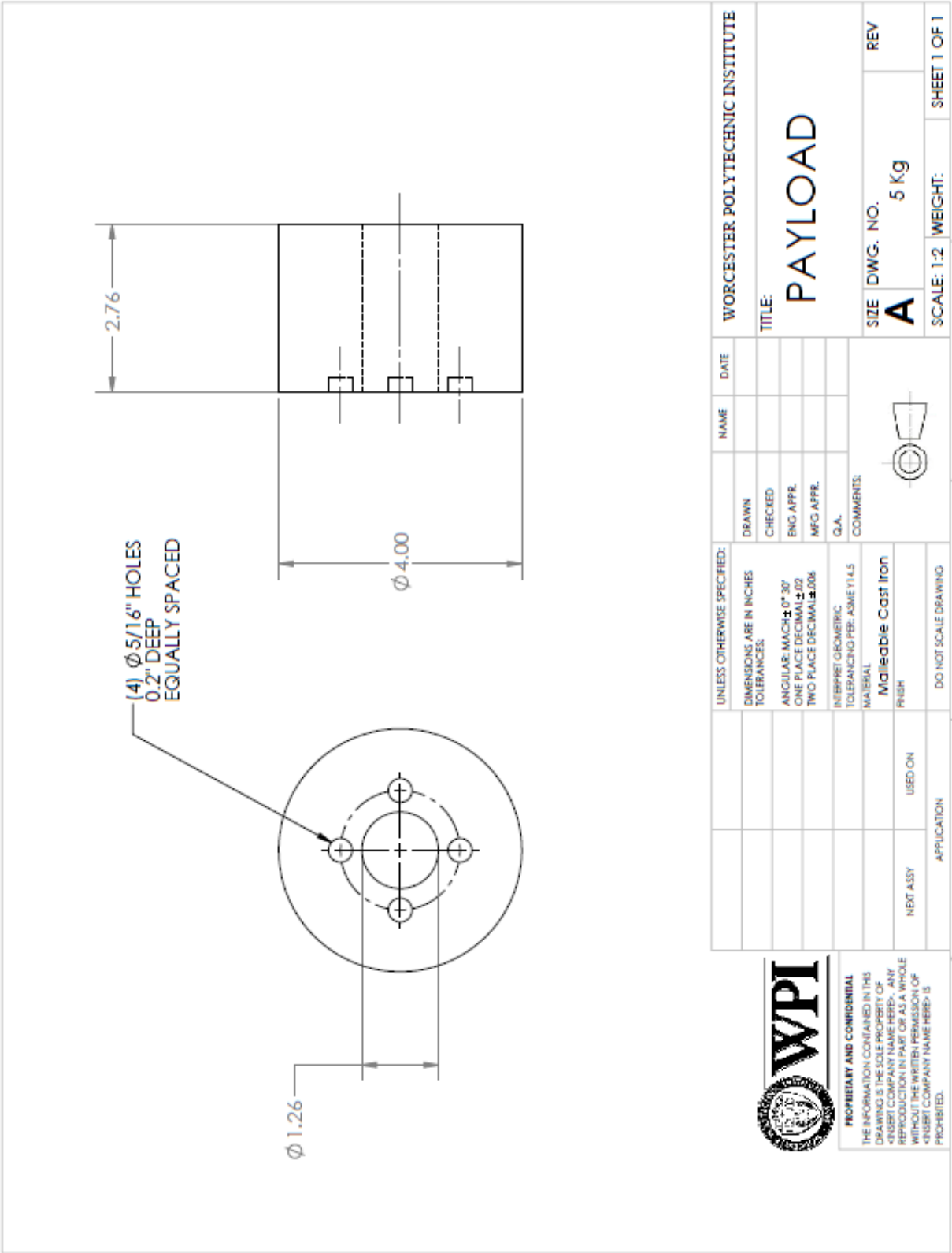
Appendix G: Mechanical Drawings

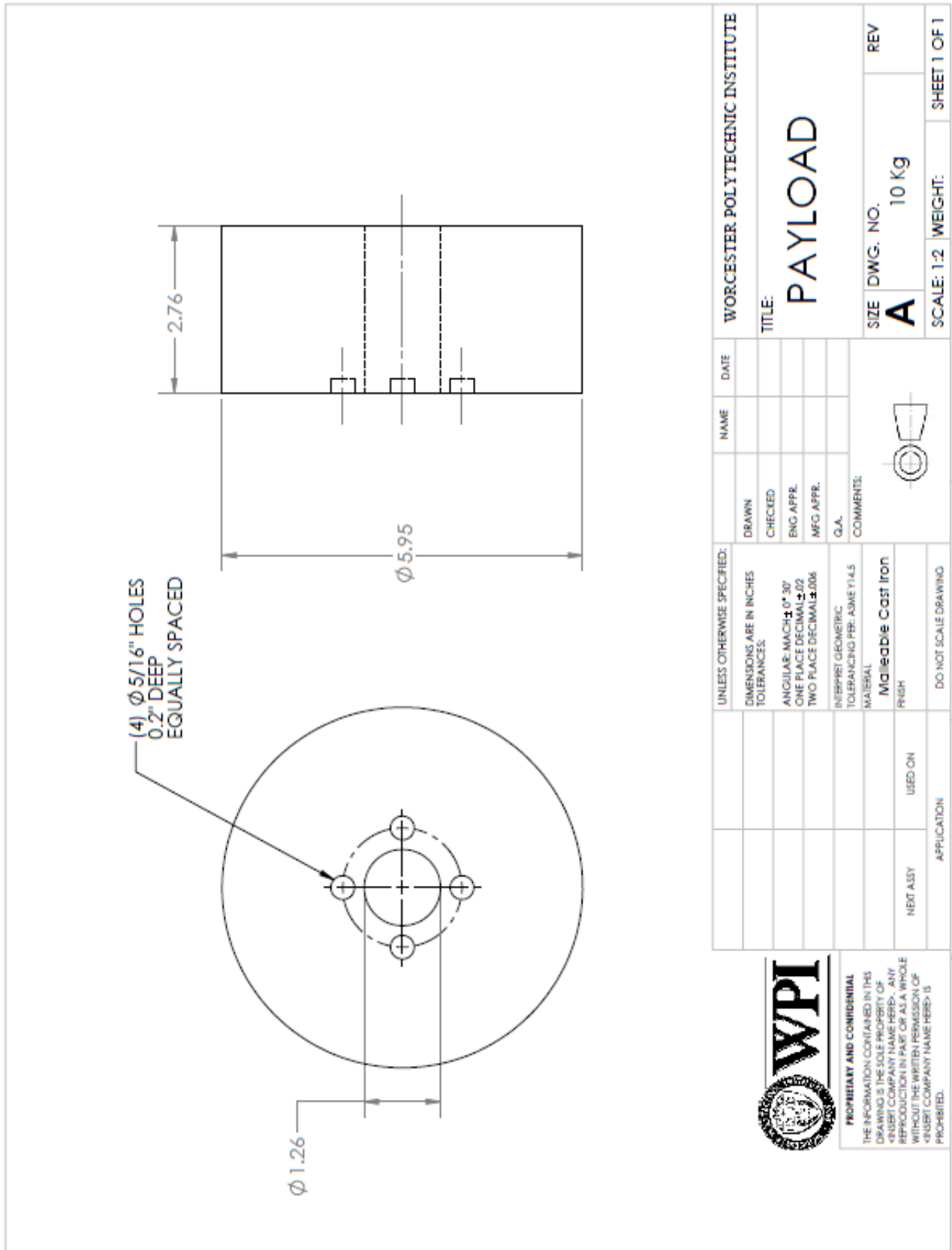


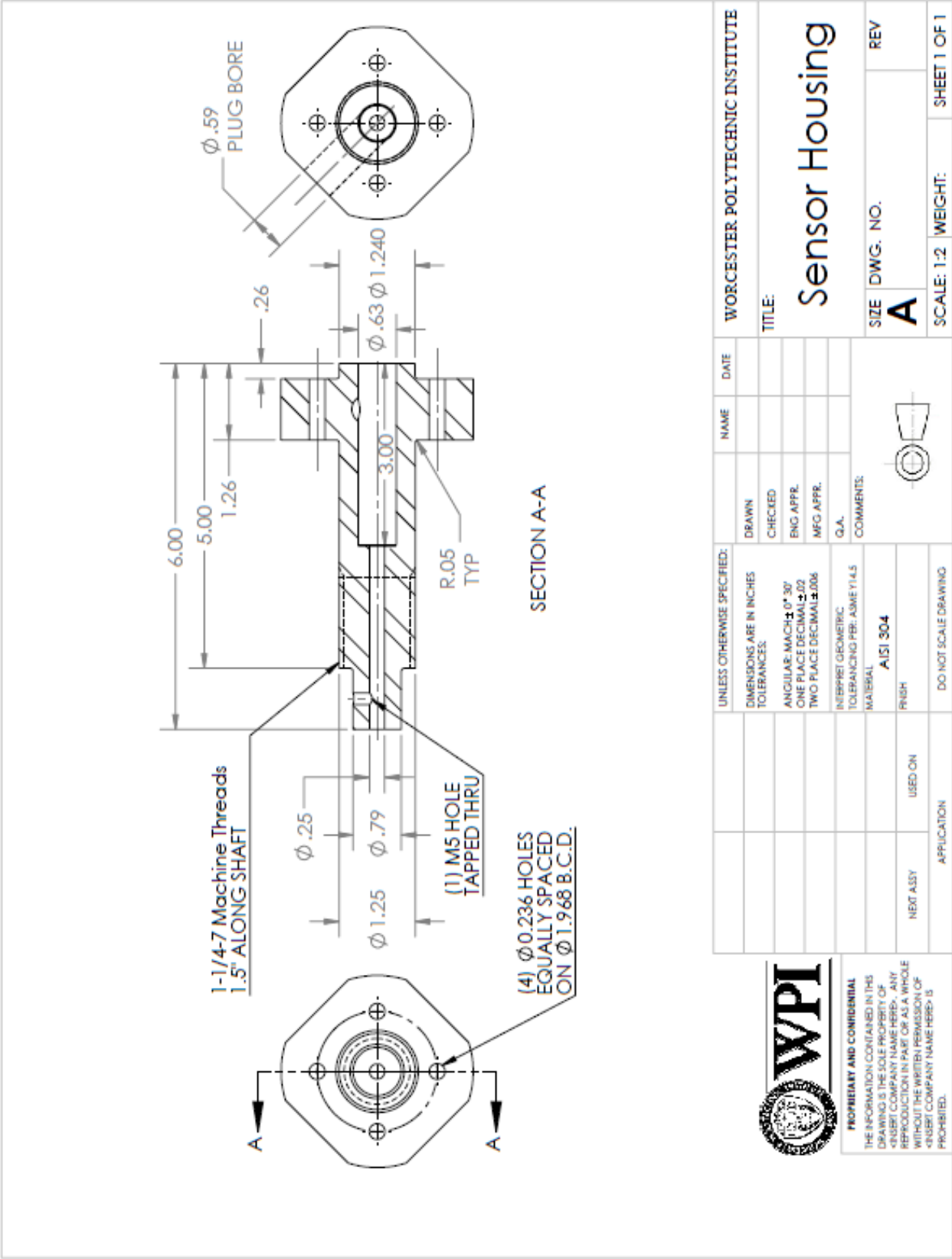


UNLESS OTHERWISE SPECIFIED:		NAME	DATE	WPI	
DIMENSIONS ARE IN INCHES		DRAWN		TITLE:	
TOLERANCES:		CHECKED		Gauge Plate	
FRACTIONAL: ±		ENG APPR.		SIZE	DWG. NO.
ANGULAR: MACH: ±		MFG APPR.		A	REV
TWO PLACE DECIMAL ±				SCALE: 1:2 WEIGHT: SHEET 1 OF 1	
THREE PLACE DECIMAL ±					
INTERPRET GEOMETRIC TOLERANCING PER:		COMMENTS:			
MATERIAL					
FINISH					
NEXT ASSY		USED ON			
APPLICATION					
DO NOT SCALE DRAWING					

PROPRIETARY AND CONFIDENTIAL
 THE INFORMATION CONTAINED IN THIS
 DRAWING IS THE SOLE PROPERTY OF
 WPI. ANY REPRODUCTION OR
 TRANSMISSION IN ANY FORM OR BY
 ANY MEANS, WITHOUT THE WRITTEN
 PERMISSION OF WPI, IS PROHIBITED.







Appendix H: UR10 Repeatability Polyscope Program

This is a representative program that is used to program the UR10 motion path for repeatability testing. The program specifies that the UR10 moves to 5 different positions on each face of the gauge block, touches each position 30 times and repeats the procedure for the remaining two faces.

Program

Robot Program

Loop 30 times

MoveL

Waypoint1

Waypoint2

Wait: 2.0

Set output_tri_1=5.0

Wait: 1.0

Set output_tri_1=1.0

Wait: 2.0

Waypoint1

Waypoint3

Waypoint4

Wait: 2.0

Set output_tri_1=5.0

Wait: 1.0

Set output_tri_1=1.0

Wait: 2.0

Waypoint3

Waypoint5

Waypoint6

Wait: 2.0

Set output_tri_1=5.0

Wait: 1.0
Set output_tri_1=1.0
Wait: 2.0
Waypoint5
Waypoint7
Waypoint8
Wait: 2.0
Set output_tri_1=5.0
Wait: 1.0
Set output_tri_1=1.0
Wait: 2.0
Waypoint7
Waypoint9
Waypoint10
Wait: 2.0
Set output_tri_1=5.0
Wait: 1.0
Set output_tri_1=1.0
Wait: 2.0
Waypoint9
MoveJ
Waypoint31
Waypoint11
Loop 30 times
MoveL
Waypoint12
Wait: 2.0
Set output_tri_1=5.0

Wait: 1.0
Set output_tri_1=1.0
Wait: 2.0
Waypoint11
Waypoint13
Waypoint14
Wait: 2.0
Set output_tri_1=5.0
Wait: 1.0
Set output_tri_1=1.0
Wait: 2.0
Waypoint13
Waypoint15
Waypoint16
Wait: 2.0
Set output_tri_1=5.0
Wait: 1.0
Set output_tri_1=1.0
Wait: 2.0
Waypoint15
Waypoint17
Waypoint18
Wait: 2.0
Set output_tri_1=5.0
Wait: 1.0
Set output_tri_1=1.0
Wait: 2.0
Waypoint17

Waypoint19

Waypoint20

Wait: 2.0

Set output_tri_1=5.0

Wait: 1.0

Set output_tri_1=1.0

Wait: 2.0

Waypoint19

Waypoint11

Appendix I: Repeatability Analysis MATLAB Script

The following MATLAB script is used to calculate the repeatability by using ISO 9283 equations in conjunction with recorded data along each axis.

```
close all; clear; clc;
rate = input('Enter sampling rate in Hz (default = 256 Hz) = '); % sampling rate
duration = input('Enter sampling duration in seconds (default = 2 s) = '); % duration of data per
sample
iteration = input('Enter iterations per test (default = 30) = '); % iteration per test
positions_to_test = input('Enter positions to test per test (default = 5) = ');
%% test parameters
% direction = [1 2 3] % stands for x, y, and z
direction = input('Enter directions to test in the form of [1, 2, 3] (stands for x y z)= ');
g = 9.81; % m/s^2
% acceleration = [0.2*g, 0.4*g, 0.6*g, 0.8*g, 1.0*g]
acceleration = input('Enter accelerations in m/s^2 to test in the form of [0.2*g, 0.4*g, 0.6*g,
0.8*g, 1.0*g] = ');
% payload = [1.1294, 5, 10] % kg
payload = input('Enter payloads in kg to test in the form of [1.1294, 5, 10] = ');
%%
number_of_tests = length(acceleration)*length(direction)*length(payload)
% test sequence: payload 1: acceleration 1: direction 1->3: -- test 1-3
%      payload 1: acceleration 2: direction 1->3: -- test 4-6
%      payload 1: acceleration 3: direction 1->3: -- test 7-9
%      payload 1: acceleration 4: direction 1->3: -- test 10-12
%      payload 1: acceleration 5: direction 1->3: -- test 13-15
%      payload 2: acceleration 1: direction 1->3: -- test 16-18
%      payload 2: acceleration 2: direction 1->3: -- test 19-21
%      payload 2: acceleration 3: direction 1->3: -- test 22-24
%      payload 2: acceleration 4: direction 1->3: -- test 25-27
%      payload 2: acceleration 5: direction 1->3: -- test 28-30
%      payload 3: acceleration 1: direction 1->3: -- test 31-33
%      payload 3: acceleration 2: direction 1->3: -- test 34-36
%      payload 3: acceleration 3: direction 1->3: -- test 37-39
%      payload 3: acceleration 4: direction 1->3: -- test 40-42
%      payload 3: acceleration 5: direction 1->3: -- test 43-45

% probe calibration: millimeter per volt
slope = 0.454;
offset = 2.97;

gauge_step = 0.25*1*2.54*10; % 0.25 inches in millimeters

%% calculation of repeatability
```

```

datalength = rate*duration; % length of data per sample
voltage = zeros(datalength,1,positions_to_test*iteration*number_of_tests); % pre-allocating
space for one sample data

for ii = 1:number_of_tests

    for i = 1:positions_to_test*iteration % counter for entire file; two position ("positions_to_test"
positions per iteration, one file per position)

        filenumb = (ii-1)*positions_to_test*iteration + i;

        numbering = sprintf('%04d',filenumb);

        fname = strcat('test_',numbering, '.lvm' );
        fileID = fopen(fname);
        C = textscan(fileID,'%f %f', datalength, 'delimiter','t','HeaderLines', 23 );
        fclose(fileID);
        voltage(:,:, (ii-1)*positions_to_test*iteration + i) = C{2};
    end
end
mean_vol = mean(voltage); % mean voltage in terms of 2 seconds of data per position,
2*iterations number of positions

allpositions = mean_vol.*slope+offset*ones(1,1,positions_to_test*iteration*number_of_tests);

poses_temp = zeros(positions_to_test,iteration*number_of_tests);
poses = zeros(positions_to_test*number_of_tests,iteration);
for kp = 1:positions_to_test*iteration*number_of_tests
    poses_temp(kp) = allpositions(kp);
end
for row_counter = 1:number_of_tests

    posesT((row_counter-
1)*positions_to_test+1:row_counter*positions_to_test,1:iteration)=poses_temp(1:positions_to_te
st,(row_counter-1)*iteration+1:row_counter*iteration);
end
poses = transpose(posesT);
l= zeros(1,iteration); % pre-allocating space
Sltop = zeros(1,iteration); % pre-allocating space
RP =zeros(1,positions_to_test*number_of_tests); % pre-allocating space

for pp = 1:positions_to_test*number_of_tests
    dist = poses(:,pp);
    dist_mean = mean(dist); % mean value of measured distance
    for kk = 1:iteration
        l(kk) = sqrt((dist(kk)-dist_mean)^2);
    end
end

```

```

end

l_mean = mean(l);
for kk = 1:iteration
    Sltop(kk) = (l(kk)-l_mean)^2;
end
Sl= sqrt((sum(Sltop))/(iteration-1));
RP(pp) = l_mean +3*Sl; % repeatability value on this test (after designated number of
iterations)
%    s(pp) = std(dist);
end
% RP is the repeatability for each position within this test
repeatability =zeros(1,number_of_tests); % pre-allocating space
for ii = 1:number_of_tests
    repeatability(ii) = mean(RP((ii-1)*positions_to_test+1:(ii)*positions_to_test)); % the
    repeatability for this test
end
repeatability

```


Appendix J: Denavit-Hartenberg Parameters

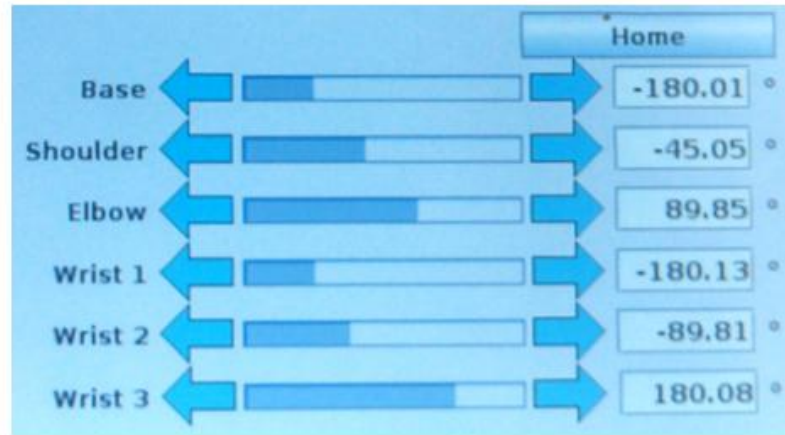
The following page contains the print out of the MathCAD file used to develop the UR10's DH parameter transform. The parameters themselves (shown in the first table) were taken from the UR10 Calibration Manual.

B.2 UR10

	θ [rad]	a [m]	d [m]	α [rad]
Joint 1:	0	0	0.118	$\frac{\pi}{2}$
Joint 2:	0	-0.6127	0	0
Joint 3:	0	-0.5716	0	0
Joint 4:	0	0	0.1639	$\frac{\pi}{2}$
Joint 5:	0	0	0.1157	$\frac{-\pi}{2}$
Joint 6:	0	0	0.0922	0

Table B.4: Denavit-Hartenberg parameters for the UR10 robot **serie 1**.

Establishing the inputs. Only theta values are variables - see figure below



$$\begin{array}{llll}
 \theta_1 := \frac{-180.01}{180} \cdot \pi & a_1 := 0 & d_1 := 0.1273 & \alpha_1 := \frac{\pi}{2} \\
 \theta_2 := \frac{-45.05}{180} \cdot \pi & a_2 := -0.612 & d_2 := 0 & \alpha_2 := 0 \\
 \theta_3 := \frac{89.85}{180} \cdot \pi & a_3 := -0.5723 & d_3 := 0 & \alpha_3 := 0 \\
 \theta_4 := \frac{-180.13}{180} \cdot \pi & a_4 := 0 & d_4 := 0.1639 & \alpha_4 := \frac{\pi}{2} \\
 \theta_5 := \frac{-89.81}{180} \cdot \pi & a_5 := 0 & d_5 := 0.1157 & \alpha_5 := \frac{-\pi}{2} \\
 \theta_6 := \frac{180.08}{180} \cdot \pi & a_6 := 0 & d_6 := 0.0922 & \alpha_6 := 0
 \end{array}$$

We know that the DH parameters can be used to make transforms based on the breakdown of the screw displacement into pure translation and pure rotation.

$$[Z_i] = \text{Trans}_{Z_i}(d_i) \text{Rot}_{Z_i}(\theta_i),$$

and

$$[X_i] = \text{Trans}_{X_i}(r_{i,i+1}) \text{Rot}_{X_i}(\alpha_{i,i+1}).$$

Then, each link must be described using the coordinate transform to the new coordinate system from the previous system according to:

$${}^{n-1}T_n = \text{Trans}_{z_{n-1}}(d_n) \cdot \text{Rot}_{z_{n-1}}(\theta_n) \cdot \text{Trans}_{x_n}(r_n) \cdot \text{Rot}_{x_n}(\alpha_n)$$

This product of two screw displacements can be accomplished using the following matrices:

$$\begin{aligned} \text{Trans}_{z_{n-1}}(d_n) &= \left[\begin{array}{ccc|c} 1 & 0 & 0 & 0 \\ 0 & 1 & 0 & 0 \\ 0 & 0 & 1 & d_n \\ \hline 0 & 0 & 0 & 1 \end{array} \right] \\ \text{Rot}_{z_{n-1}}(\theta_n) &= \left[\begin{array}{ccc|c} \cos \theta_n & -\sin \theta_n & 0 & 0 \\ \sin \theta_n & \cos \theta_n & 0 & 0 \\ 0 & 0 & 1 & 0 \\ \hline 0 & 0 & 0 & 1 \end{array} \right] \\ \text{Trans}_{x_n}(r_n) &= \left[\begin{array}{ccc|c} 1 & 0 & 0 & r_n \\ 0 & 1 & 0 & 0 \\ 0 & 0 & 1 & 0 \\ \hline 0 & 0 & 0 & 1 \end{array} \right] \\ \text{Rot}_{x_n}(\alpha_n) &= \left[\begin{array}{ccc|c} 1 & 0 & 0 & 0 \\ 0 & \cos \alpha_n & -\sin \alpha_n & 0 \\ 0 & \sin \alpha_n & \cos \alpha_n & 0 \\ \hline 0 & 0 & 0 & 1 \end{array} \right] \end{aligned}$$

These matrix transforms result in a [4x4] matrix transform given by:

$${}^{n-1}T_n = \left[\begin{array}{ccc|c} \cos \theta_n & -\sin \theta_n \cos \alpha_n & \sin \theta_n \sin \alpha_n & r_n \cos \theta_n \\ \sin \theta_n & \cos \theta_n \cos \alpha_n & -\cos \theta_n \sin \alpha_n & r_n \sin \theta_n \\ 0 & \sin \alpha_n & \cos \alpha_n & d_n \\ \hline 0 & 0 & 0 & 1 \end{array} \right]$$

The next step is to create the transforms from each link. The following is a list of the necessary transforms starting at link 1 (the base).

$$T_1 = \begin{pmatrix} \cos(\theta_1) & -\sin(\theta_1) \cdot \cos(\alpha_1) & \sin(\theta_1) \cdot \sin(\alpha_1) & a_1 \cdot \cos(\theta_1) \\ \sin(\theta_1) & \cos(\theta_1) \cdot \cos(\alpha_1) & -\cos(\theta_1) \cdot \sin(\alpha_1) & a_1 \cdot \sin(\theta_1) \\ 0 & \sin(\alpha_1) & \cos(\alpha_1) & d_1 \\ 0 & 0 & 0 & 1 \end{pmatrix}$$

$$T_2 = \begin{pmatrix} \cos(\theta_2) & -\sin(\theta_2) \cdot \cos(\alpha_2) & \sin(\theta_2) \cdot \sin(\alpha_2) & a_2 \cdot \cos(\theta_2) \\ \sin(\theta_2) & \cos(\theta_2) \cdot \cos(\alpha_2) & -\cos(\theta_2) \cdot \sin(\alpha_2) & a_2 \cdot \sin(\theta_2) \\ 0 & \sin(\alpha_2) & \cos(\alpha_2) & d_2 \\ 0 & 0 & 0 & 1 \end{pmatrix}$$

$$T_3 = \begin{pmatrix} \cos(\theta_3) & -\sin(\theta_3) \cdot \cos(\alpha_3) & \sin(\theta_3) \cdot \sin(\alpha_3) & a_3 \cdot \cos(\theta_3) \\ \sin(\theta_3) & \cos(\theta_3) \cdot \cos(\alpha_3) & -\cos(\theta_3) \cdot \sin(\alpha_3) & a_3 \cdot \sin(\theta_3) \\ 0 & \sin(\alpha_3) & \cos(\alpha_3) & d_3 \\ 0 & 0 & 0 & 1 \end{pmatrix}$$

$$T_4 = \begin{pmatrix} \cos(\theta_4) & -\sin(\theta_4) \cdot \cos(\alpha_4) & \sin(\theta_4) \cdot \sin(\alpha_4) & a_1 \cdot \cos(\theta_4) \\ \sin(\theta_4) & \cos(\theta_4) \cdot \cos(\alpha_4) & -\cos(\theta_4) \cdot \sin(\alpha_4) & a_1 \cdot \sin(\theta_4) \\ 0 & \sin(\alpha_4) & \cos(\alpha_4) & d_4 \\ 0 & 0 & 0 & 1 \end{pmatrix}$$

$$T_5 := \begin{pmatrix} \cos(\theta_5) & -\sin(\theta_5) \cdot \cos(\alpha_5) & \sin(\theta_5) \cdot \sin(\alpha_5) & a_5 \cdot \cos(\theta_5) \\ \sin(\theta_5) & \cos(\theta_5) \cdot \cos(\alpha_5) & -\cos(\theta_5) \cdot \sin(\alpha_5) & a_5 \cdot \sin(\theta_5) \\ 0 & \sin(\alpha_5) & \cos(\alpha_5) & d_5 \\ 0 & 0 & 0 & 1 \end{pmatrix}$$

$$T_6 := \begin{pmatrix} \cos(\theta_6) & -\sin(\theta_6) \cdot \cos(\alpha_6) & \sin(\theta_6) \cdot \sin(\alpha_6) & a_6 \cdot \cos(\theta_6) \\ \sin(\theta_6) & \cos(\theta_6) \cdot \cos(\alpha_6) & -\cos(\theta_6) \cdot \sin(\alpha_6) & a_6 \cdot \sin(\theta_6) \\ 0 & \sin(\alpha_6) & \cos(\alpha_6) & d_6 \\ 0 & 0 & 0 & 1 \end{pmatrix}$$

$$XYZ_6 := \begin{pmatrix} 0 \\ 0 \\ .135 \\ 1 \end{pmatrix}$$

Establishing tool tip coordinates
Note: We added an offset because the robot was calibrated to use its tool, but the tool was removed.
The Z-Direction offset is equal to the length of the 2-Finger Model - 85 Robotiq Adaptive Gripper.

The next step is to perform the backwards transfer starting from the tool tip to find the base coordinates. This step is accomplished by starting at the tool tip coordinates (XYZ.6) and performing the transforms starting with T.6 and working backwards to T.1. The last vector contains the coordinates of the base in the form of:

$$\begin{pmatrix} X \\ Y \\ Z \\ 1 \end{pmatrix}$$

Establishing the Matrix Transform using T1, T2, T3, T4, T5, T6

$$TT := T_1 \cdot T_2 \cdot T_3 \cdot T_4 \cdot T_5 \cdot T_6 = \begin{pmatrix} -1.202 \times 10^{-3} & 0.703 & 0.711 & 0.985 \\ 1 & -1.519 \times 10^{-3} & 3.192 \times 10^{-3} & 0.164 \\ 3.324 \times 10^{-3} & 0.711 & -0.703 & 0.175 \\ 0 & 0 & 0 & 1 \end{pmatrix}$$

$$TT\text{-}XYZ_6 = \begin{pmatrix} 1.081 \\ 0.164 \\ 0.08 \\ 1 \end{pmatrix}$$

$$XYZ_{\text{expected}} := \begin{pmatrix} 1.08 \\ .165 \\ .06 \\ 1 \end{pmatrix} \text{ m}$$

$$X_{\%Error} := \left| \frac{1.081 - 1.08}{1.08} \right| = 0.093\%$$

$$Y_{\%Error} := \left| \frac{.164 - .1651}{-.165} \right| = 0.667\%$$

$$Z_{\%Error} := \left| \frac{.071 - .06}{.06} \right| = 18.333\%$$

Tool Position		
X	1080.14	mm
Y	164.56	mm
Z	59.91	mm
RX	1.7575	
RY	1.7571	
RZ	0.7373	

The results show that the X and Y coordinates are both very close, with <5% error, but the Z location is very far from accurate as shown by the 18% error above. The Z-Direction error could be attributed to the aforementioned lack of recalibration after the gripper was removed, but we do not find this explanation satisfactory.

Appendix K: Repeatability Data Tables

Axis	Payload (kg)	Repeatability (mm)
X	1	0.059
		0.055
		0.047
		0.055
		0.059
	5	0.054
		0.052
		0.060
		0.045
		0.043
	10	0.065
		0.052
		0.051
		0.056
		0.041
acceleration=0.2g		

Axis	Payload (kg)	Repeatability (mm)
Y	1	0.043
		0.039
		0.045
		0.045
		0.033
	5	0.001
		0.056
		0.055
		0.001
		0.033
	10	0.041
		0.044
		0.030
		0.071
		0.032
acceleration=0.2g		

Axis	Payload (kg)	Repeatability (mm)
Z	1	0.070
		0.061
		0.079
		0.046
		0.049
	5	0.094
		0.054
		0.063
		0.057
		0.067
	10	0.205
		0.210
		0.302
		0.163
		0.301
acceleration=0.2g		

Axis	Payload (kg)	Repeatability (mm)
X	1	0.084
		0.076
		0.141
		0.118
		0.139
	5	0.059
		0.071
		0.065
		0.054
		0.043
	10	0.107
		0.131
		0.100
		0.079
		0.137
acceleration=0.5g		

Axis	Payload (kg)	Repeatability (mm)
Y	1	0.109
		0.090
		0.088
		0.093
		0.093
	5	0.003
		0.075
		0.109
		0.001
		0.073
	10	0.099
		0.057
		0.091
		0.083
		0.076
acceleration=0.5g		

Axis	Payload (kg)	Repeatability (mm)
Z	1	0.176
		0.164
		0.242
		0.122
		0.185
	5	0.176
		0.145
		0.181
		0.126
		0.177
	10	0.200
		0.163
		0.230
		0.141
		0.149
acceleration=0.5g		

Axis	Payload (kg)	Repeatability (mm)
X	1	0.181
		0.190
		0.204
		0.218
		0.212
	5	0.086
		0.108
		0.170
		0.081
		0.151
	10	0.194
		0.242
		0.249
		0.193
		0.268
acceleration=1g		

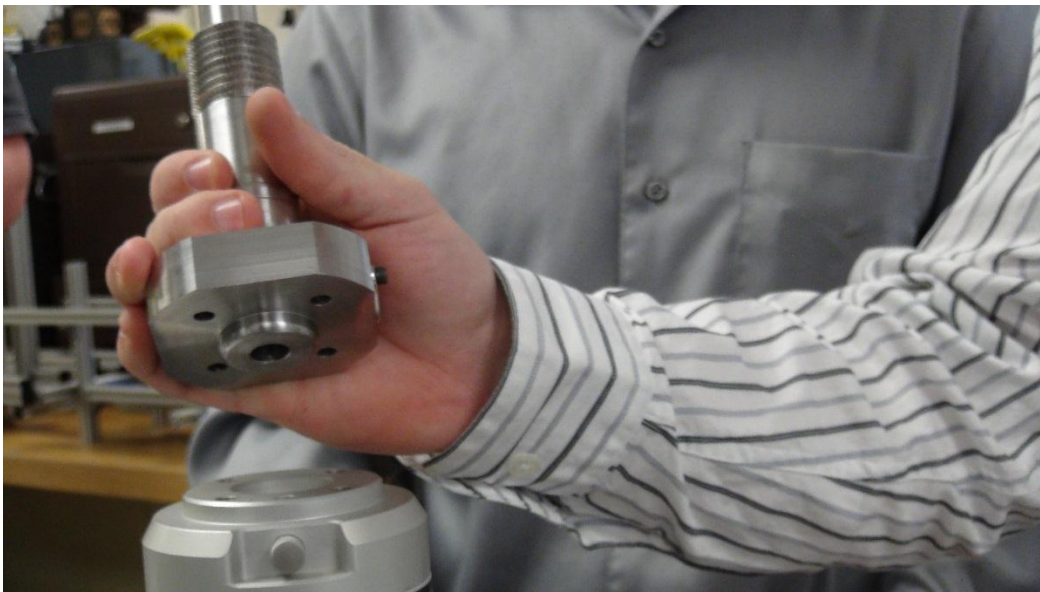
Axis	Payload (kg)	Repeatability (mm)
Y	1	0.060
		0.042
		0.099
		0.053
		0.060
	5	0.002
		0.139
		0.143
		0.001
		0.043
	10	0.284
		0.182
		0.246
		0.169
		0.287
acceleration=1g		

Axis	Payload (kg)	Repeatability (mm)
Z	1	0.174
		0.178
		0.079
		0.238
		0.140
	5	0.144
		0.161
		0.130
		0.281
		0.109
	10	0.206
		0.233
		0.243
		0.436
		0.308
acceleration=1g		

Appendix L: Instruction Manual for the DCM Repeatability Procedure

1. Hardware Setup

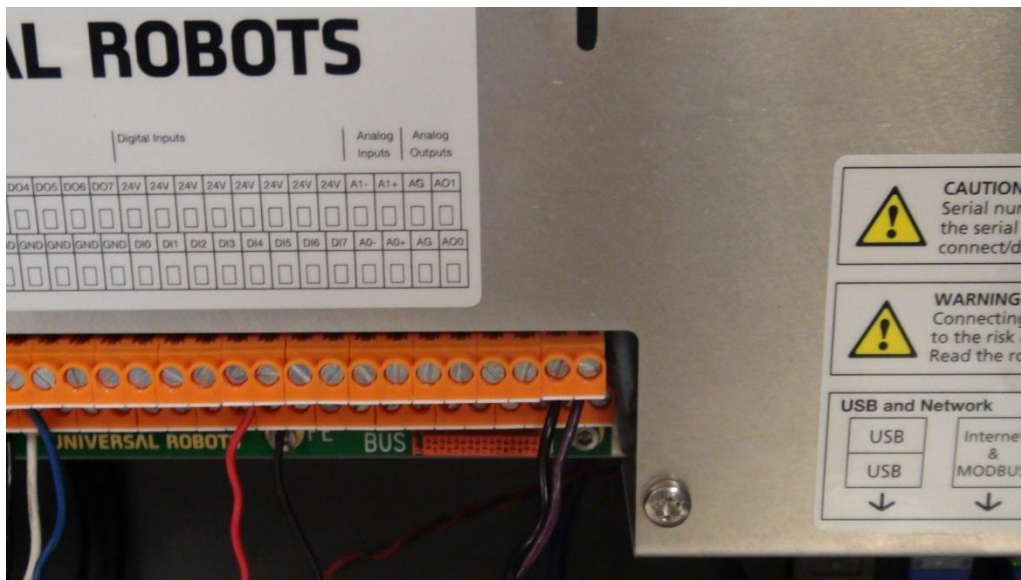
- a. Power on UR10
- b. Mount LVDT Fixture
 - i. Roughly Align UR10 vertically, tool plate facing upwards
 1. 1 Person Hold “teach” button on rear panel of controller
 2. Person #2 move the UR10 into upwards position
 3. After UR10 is moved into position release black button
 - a. Note: Whenever adding mass to the fixture change payload in controller panel: In order to do that, press “installation” tab, press “tcp position” in left panel, in white box insert corresponding mass after “The payload at the TCP is [mass here]” kg. TCP=Tool center point
 - ii. Align fixture mounting holes with tool plate mounting holes such that plug is rotated 90 degrees counter clockwise of tool tip power outlet when facing tool plate



Alignment of fixture mounting holes with tool plate mounting holes.

- iii. Fasten with 4 M6 x 25 socket cap screws
 1. Fig. X on hardware page
- c. LDX signal conditioner
 - i. Remove LDX top plate
 - ii. Locate black and red twisted and white and black twisted wire as well as black cord with 5 pin DIN connector (see hardware page)
 - iii. Loosen power terminal inside LDX conditioner. See Fig. x

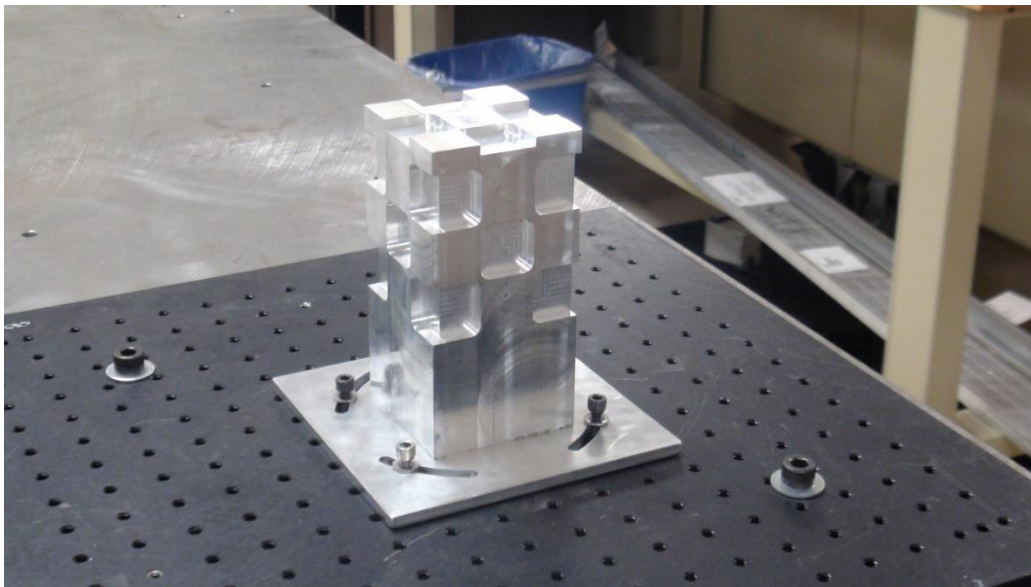
- iv. Feed black and red wire through hole nearest power terminal and lock rubber connector in place
- v. Insert red wire in positive terminal and black wire in negative ground terminal. Hand tighten screws
- vi. Locate UR10 computer box
- vii. open the door
- viii. locate the screw terminal panel
- ix. locate 24 volt power and ground screw terminals
- x. loosen power and ground screw terminal
- xi. insert black wire into ground terminal and tighten screw hand tight
- xii. insert red wire into +24 volt screw terminal and hand tighten
 1. Note: this may cause a spark
- xiii. Loosen analog output voltage terminal inside LDX conditioner. See Fig. x
- xiv. Feed black and white wire through hole nearest analog output voltage terminal and lock rubber connector in place
- xv. Insert white wire in positive voltage out terminal and black wire in negative ground terminal. Hand tighten screws



UR10 computer box wiring terminal.

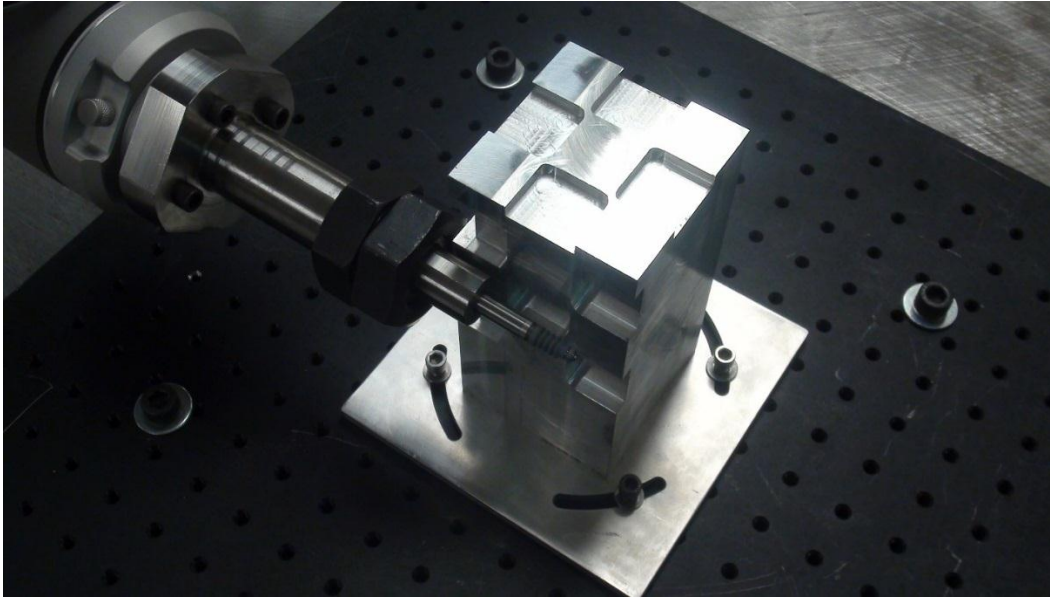
- d. DAQ box and laptop
 - i. Power on laptop
 - ii. Power DAQ box
 - iii. Connect DAQ box to computer using USB cable
 - iv. Turn on DAQ box
 - v. Attach two BNC cables to AI0 and AI1
 - vi. Locate black and purple twisted wire

- vii. Plug one BNC cable into one end of black and purple wire using screw terminal connector as seen in Fig. x
- viii. Locate loose end of purple black wire
- ix. Locate Analogue output 1 and ground screw terminal in UR10 computer
 - x. Insert black wire into ground and hand tighten
 - xi. Insert purple wire into analogue output 1 and hand tighten screw terminal
- xii. Locate loose end of black white twisted wire and connect to remaining BNC cable using screw terminal BNC connector
- e. Breadboard and Gauge block alignment
 - i. Mount breadboard in desired test position using 4 M10 socket cap screws
 - ii. Loosely mount gauge block onto the center of the breadboard using 4 1/4 20 screws



Gauge block mounted on an optical breadboard.

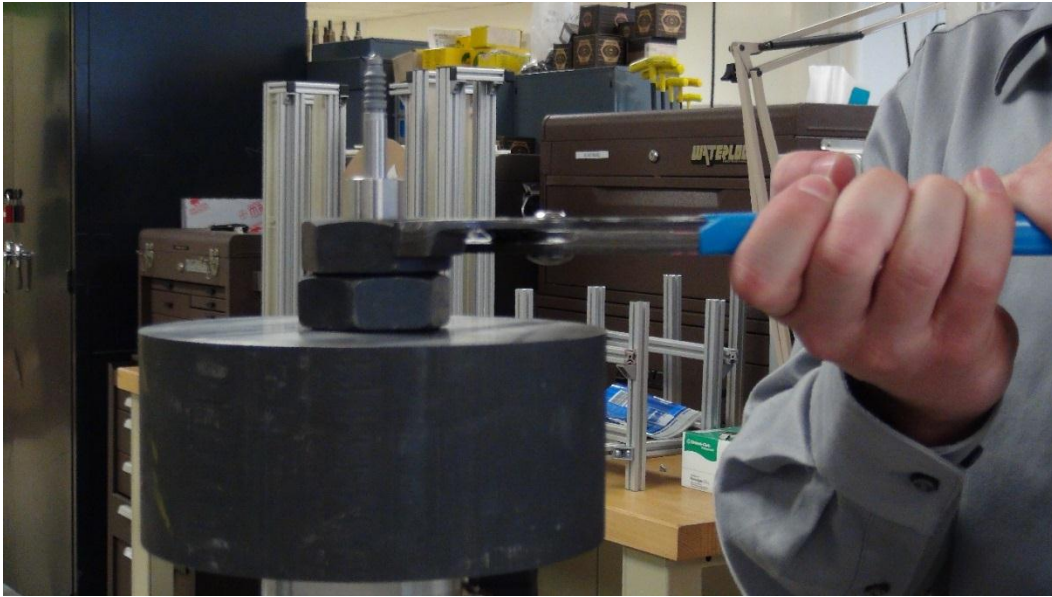
- iii. Screw lock nuts onto fixture
- iv. 1 Person Hold “teach” button on rear panel of controller
- v. Person #2 move the UR10 until face of nut and side of fixture are touching the gauge block



Alignment of gauge block to sensor fixture.

- vi. Screw the gauge block into place
 - 1. IMPORTANT! Be sure not move the UR10 out of this plane or you will have to re-align the gauge block
- 2. UR10 Programming and Running Tests
 - a. Start program by making the first loop
 - i. Click the program tab, structure sub tab, and then advanced
 - ii. Select loop. This will bring you to the command sub tab of the program tab
 - iii. Select “loop _ times using variable” and input 30 into the box
 - iv. Click on the structure tab again
 - v. Select Move and set to MoveL. This will let you change the speed and acceleration of the end effector in mm/s or mm/s²
 - vi. To set a waypoint, click structure then waypoint.
 - vii. Click set waypoint and jog the robot where you would like that position to be, then click ok
 - viii. To set a wait function click structure then wait
 - ix. Select the second bullet and enter the desired wait time
 - x. To output a trigger select set under the structure tab
 - xi. Select “set analog output”
 - xii. Select the output channel and desired voltage
 - xiii. To stop the robot entirely after running the program, insert a halt function at the end of the program. The halt function is located in the structure tab
- 3. Changing Payload
 - a. Click on “Move” tab
 - b. Use controls to jog UR10 away from gauge block
 - c. Jog UR10 with tool plate face facing upwards

- d. Remove outer jam nut by twisting counterclockwise
- e. Remove inner jam nut by twisting counterclockwise



Fixture with added payload.

- f. Lift existing payload off of mounting fixture, careful not to damage or scrape against lvdt
- g. 1 person hold arm of UR10 in place while second person adds payload
- h. 2nd person then grabs UR10 controller and changes payload in the “installation” tab as previously mentioned in step XXX
- i. Jog UR10 back into position and resume testing